Studies on the Eukaryotic Communities in Ticks

（マダニが保有する真核生物群に関する研究）

YURIE TAYA

Laboratory of Parasitology

Department of Disease Control

Graduate School of Infectious Diseases

Hokkaido University

2025

TABLE OF CONTENTS

ABBREVIATIONS

3’	3 prime
5’	5 prime
%	percentage
℃	degree Celsius
µl	microliter
µM	micromolar
bp	base pair
ASV	amplicon sequence valiant
cDNA	complementary deoxyribonucleic acid
COI	cytochrome oxidase subunit I gene
DNA	deoxyribonucleic acid
EDTA	ethylenediaminetetraacetic acid
min	minute(s)
ml	milliliter
mM	millimolar
NaOH	sodium hydroxide
nM	nanomolar
NGS	next-generation sequencing
NMDS	non-metric multidimensional scaling
NUMTs	nuclear mitochondrial DNA segments
PCoA	principal coordinates analysis
PCR	polymerase chain reaction
pH	potential of hydrogen
pmol	picomole
RNA	ribonucleic acid
rRNA	ribosomal RNA
rpm	revolutions per minute
sec	second(s)
sp.	species
TBP	tick-borne pathogen
Tris-HCl	tris (hydroxymethyl) aminomethane hydrochloride

List of Tables

Chapter I

Chapter II

Chapter III

List of Figures

Chapter I

Chapter II

Chapter III

GENERAL INTRODUCTION

1. Ticks, tick-borne pathogens, and current control measures

Ixodid ticks are significant vectors of pathogens to humans and animals (*1–3*). Ticks transmit a wide range of pathogenic microbes, including viruses, bacteria, and protozoans (*4*, *5*). Current tick management is commonly performed with acaricidal chemicals, however, their efficacy is increasingly compromised due to the development of acaricide resistance (*6*, *7*). Alternatively, integrated pest management programs offer a suitable approach by combining multiple countermeasures, such as chemicals, physical protection, and biological control agents (*8*). Among these, natural enemies have been successfully used as biological control agents in crop pest management. Commercially utilized biological agents include entomopathogenic microbes (e.g., nematodes, fungi, and bacteria) and predatory arthropods, such as parasitoid wasps (*9–11*). Despite their demonstrated utility in crop pest management, knowledge of natural enemies specific to ticks remains limited. To address this gap, systematic exploration and cataloging of potential tick antagonists are needed to identify candidates for biological control. This approach could provide a foundation for the development of sustainable tick management strategies.

2. Neglect of eukaryotes in tick - pathogen - microbiome interaction studies

Research into the tick microbiome has expanded our understanding of pathogen transmission and the interactions influencing tick physiology. For example, some non-pathogenic bacteria serve as endosymbionts which support the nutritional synthesis of ticks (*12*, *13*). In addition, it has been suggested that the pathogenic bacterial load in ticks is modulated by bacterial microbiome (*14*). However, such studies have primarily focused on bacterial and viral communities, and eukaryotes have been overlooked (*15–20*). In contrast, studies on other arthropods revealed the importance of symbiotic eukaryotes in microbiome interactions. For example, flagellates contribute to cellulose degradation in termite guts (*21–23*), and fungal symbionts in cicadas contribute to amino acid synthesis (*24*). These findings indicate the essential role of eukaryotic microorganisms in arthropod microbiomes. While some eukaryotic taxa such as Apicomplexa, trypanosomes, fungi, and nematodes have been observed in ticks (*25–29*), their roles in the tick microbiome remain unexplored. Without integrating data on eukaryotes, analyses of the tick microbiome remain incomplete.

3. Micro-eukaryotes associated with ticks

Ticks carry a diverse range of pathogenic and non-pathogenic eukaryotes. Among pathogenic eukaryotes, protozoan parasites, such as *Babesia*, *Colpodella*, *Hepatozoon*, and *Theileria* are known as tick-borne pathogens to vertebrates (*30–32*). *Trypanosoma* has been also detected in ticks, although the role of ticks in trypanosome transmission remains unclear (*25*, *27*, *33*). In addition, filarioid

nematodes of the Dipetalonema lineage were also indicated as potential tick-borne pathogens (*29*, *34*). Ticks also carry eukaryotes that are likely non-pathogenic to vertebrates. For instance, a yeast-like fungi, *Adlerocystis* spp., have been found in male spermatophores, although their function is yet to be elucidated (*35*). In addition, certain fungi, such as *Beauveria* and *Metarhizium*, and nematode, such as *Steinernema* and *Hetererhabditis*, have been reported to kill ticks, demonstrating their potential role as biological control agents (*28*, *34*, *36–38*). Despite sporadic reports on the presence of micro-eukaryotes in ticks, comprehensive studies on the diversity and natural eukaryotic microbiome of ticks are lacking. The ecological role of non-pathogenic eukaryotes in ticks remains poorly understood. Advancing our knowledge in this area could provide valuable insights for the development of improved biological control strategies targeting tick populations.

4. Macro-eukaryotes associated with ticks

Macro-eukaryotes visible to the naked eye include *Ixodiphagus* wasps (Encyrtidae), which are known to parasitize ticks. Various invertebrates prey on ticks. Generalist predators, such as ants, beetles, pseudoscorpions, spiders, mites, and crabs are known to eat ticks (*39–45*). Ants are considered significant predators (*46*). Fiddler crabs (*Uca rapax)* have been reported to reduce the tick population in coastal habitats by consuming the tick eggs (*43*). However, generalist predators often lack the specificity required for effective biological control. Specialized predators of ticks are relatively limited. Currently, parasitoid wasps, the genus *Ixodiphagus*, are the only known tick-specific predators (*47*). Despite their potential importance in controlling the tick population, knowledge about *Ixodiphagus* wasps remains limited, and their diversity is considered to be underestimated due to insufficient sampling efforts (*48*). In addition, the relationship between a parasitoid wasp and the symbiotic microbes of their host is also important. For example, *Drosophila* flies harbor defensive *Spiroplasma* bacteria that enhance their host survival against parasitoid wasp predation (*49*, *50*). This suggests that macro-eukaryotes including parasitoid wasps also need to be investigated as a member of communities carried by ticks. To extend the probability of parasitoid wasps as biological control agents against ticks, fundamental information on their taxonomy, distribution, and host preferences, is essential.

5. Aim of this dissertation

This dissertation aims to catalog and establish foundational knowledge about the micro- and macro-eukaryotes associated with ticks. To achieve this, the research is structured into three main chapters. Chapter I develops methods to detect eukaryotic microorganisms in ticks comprehensively. Chapter II characterizes eukaryotic communities in ticks and identifies keystone taxa within the tick microbiome network using the developed method. Chapter III isolates and investigates distribution of a macro-eukaryote, a parasitoid wasp, from ticks in Japan and characterizes them morphologically and molecularly.

Chapter I

Development of a high-throughput sequencing technique to investigate eukaryotic microbiome of ticks

1. Introduction

The bacterial microbiome in ticks has been investigated by deep-amplicon sequencing approaches. This approach consists of PCR amplifying the 16S rRNA gene with a universal primer set, followed by high-throughput sequencing with a next-generation sequencer (NGS) (*20*, *51*, *52*). However, the eukaryotic microbiome in ticks remains underexplored (*53*). A major obstacle to this approach is the over-amplification of host DNA. The commonly target gene for eukaryotic profiling, 18S rRNA gene, is highly conserved across eukaryotes. It leads to the unwanted amplification of host tick DNA upon using universal primers. Hence, it is necessary to develop a method to avoid the amplification from host ticks upon the amplification form target micro-eukaryotes.

One possible solution is the use of a universal primer set in combination with blocking oligonucleotides to suppress amplification from tick DNA. Artificial nucleic acid molecules, which mimic DNA, are commonly used to suppress dominant sequences from non-target organisms. For instance, peptide nucleic acid (PNA) is a synthetic molecule with a peptide backbone and nucleobases, that bind strongly and specifically to complementary DNA strands. PNA has been used to inhibit the amplification of plant and coral organellar DNA (mitochondria and plastid) in bacterial 16S rRNA studies, as well as to block mosquito DNA in eukaryotic 18S rRNA gene amplification (*54–58*).

Another artificial nucleic acid with blocking potential is locked nucleic acid (LNA). LNA has a bridged backbone that restricts rotation and results in stronger binding affinity than conventional DNA (*59*). LNA-based blockers have been applied in PCR protocols, such as denaturing gradient gel electrophoresis, to inhibit plant ribosomal RNA amplification and detect plant-associated bacterial communities simultaneously (*60*). Given these successful applications, artificial nucleic acids such as PNA and LNA hold potential for eukaryotic microbiome studies in ticks.

Alternatively, universal primers specifically designed for non-metazoan eukaryotes could be employed. The UNonMet-PCR method, for example, targets the 18S rRNA gene of non-metazoan organisms, facilitating the detection of protists in various host-associated environments, such as oysters, ctenophores, corals, and human samples (*61–64*). Since ticks are also metazoans, UNonMet-PCR could be applied to identify eukaryotic taxa within tick samples without amplifying host DNA.

In this chapter, several approaches to investigating the eukaryotic microbiome in ticks were assessed. Blocking oligonucleotides, PNA and LNA, were designed to inhibit tick DNA amplification during universal PCR. Library preparation methods were also optimized to enhance the effectiveness of these blockers. Additionally, the performance of the UNonMet-PCR method was compared with that of blocker nucleic acids to evaluate their relative effectiveness in eukaryotic microbiome profiling in ticks.

2. Material and Methods

2.1. Study design

Five approaches to generate the PCR amplicon libraries were assessed to investigating the eukaryotic microbiome in ticks (Table I - 1). As the control, the universal primer set, TAReuk454FWD1 and TAReukREV3, was used. Two artificial oligonucleotides, PNA and LNA, were assessed their efficacies as blockers to inhibit amplification from tick DNA. The sequences of PNA and LNA were designed in this study. The same primer set as the control was also used for the amplification with the blocking oligonucleotides. To improve the resulting microbiome data with the blockers, two library purification methods, AMPure and SizeSelect were assessed. The other nested primer sets, EUK581F and EUK1134R for the first PCR followed by E572F and E1009R for the second PCR, were used as UNonMet-PCR. The details of each information are described in the following sections. The libraries were prepared from each PCR amplification method and sequenced with NGS. The PCR methods were compared based on the sequencing results.

2.2. Design of the blocker nucleic acids

Blockers sequences were designed to bind ticks based on tick sequences obtained from NCBI. A total of 250 sequences of the V4 hypervariable region of the 18S rRNA gene of ixodid ticks, argasid ticks, and mites were obtained from NCBI GenBank. The sequences were aligned with the universal primer binding sites (primers TAReuk454FWD1 and TAReukREV3; Figure I - 1 and Table I - 2) using MEGA7 (*65*) and PROSEQ (*66*). Based on the alignments, a median-joining network was constructed using Network ver. 4.6.1.6 (*67*) for each primer binding site. The blocker site was selected based on the following criteria: (1) no mismatches among tick sequences, (2) at least one mismatches with apicomplexan parasite sequences, (3) Tm value of >70 °C, and (4) low self-complementarity. PNA (TickB_PNA) and LNA (TickB_LNA) were synthesized by PANAGENE (Daejeon, Korea) and GeneDesign Inc. (Osaka, Japan), respectively.

2.3. Ticks and DNA extraction

A total of 17 adult ticks of three species, *Amblyomma testudinarium* (n = 5), *Haemaphysalis longicornis* (n = 6), and *Ixodes persulcatus* (n = 6), were used to compare the PCR approaches (Table I - 3). The ticks were collected from vegetation by flagging and identified based on the morphological key (*68*). The ticks were individually washed once with 1 mL of 10% sodium hypochlorite, twice with 1 mL of 70% ethanol, and once with 1 mL of sterile phosphate-buffered saline (pH7.0 – 7.6) to decontaminate the surfaces. The ticks were then homogenized with 4.8 mm stainless steel beads (TOMY, Tokyo, Japan) using the Micro Smash MS-100R (TOMY) in 100 µl of Dulbecco's Modified Eagle Medium (Gibco, Life Technologies, Gland Island, NY, USA). DNA was extracted from 50 µl

of the tick homogenates using the blackPREP Tick DNA/RNA Kit (Analytik Jena, Jena, Germany), following the manufacturer's protocol.

2.4. PCR amplification with the TickB_PNA or the TickB_LNA

Either of TickB_PNA or TickB_LNA blocker molecules were added to the PCR mixture prior to the amplification (Table I - 1, Figure I - 1, Table I - 2). Each PCR was performed in a 25.0 µl reaction mixture containing 12.5 µl of 2 × KAPA HiFi HotStart ReadyMix (KAPA Biosystems, Wilmington, MA, USA), 200 nM of each primer (TAReuk454FWD1 and TAReuREV3, Figure I - 1, Table I - 2), 2.5 µl of template DNA, and 50 pmol of either TickB_PNA or TickB_LNA. The reaction conditions were 95 °C for 3 min, followed by 35 cycles of 98 °C for 30 sec, 50 °C for 30 sec, 72 °C for 30 sec, and 72°C for 10 min.

2.5. UNonMet-PCR amplification

The UNonMet-PCR was performed as previously described [30]. The first PCR was performed in a total reaction volume of 25.0 µl, containing 12.5 µl of 2 × KAPA HiFi HotStart ReadyMix, 200 nM of each primer (EUK581F and EUK1134R; Figure I - 1, Table I - 2), and 2.5 µl of template DNA (Table I - 3), with the remaining volume adjusted with molecular-grade water. The first PCR conditions were 95 °C for 3 min, followed by 35 cycles of 95 °C for 30 s, 51.1 °C for 30 s, and 72 °C for 1 min, and 72 °C for 5 min. The first PCR products were purified using the NucleoSpin Gel and PCR Clean-Up Kit (Takara Bio Inc.). To avoid cross-sample contamination, the purification was performed directly on the first PCR product without electrophoresis. The second PCR mixtures were identical to the first PCR, except the primers were replaced with EUK572F and EUK1009R, and 1.0 µl of the purified first PCR products were used as the DNA template. The reaction was performed at 95 °C for 3 min, followed by 25 cycles of 95 °C for 30 sec, 55 °C for 30 sec, and 72 °C for 1 min and 72 °C for 5 min.

2.6. Library preparation

The libraries were prepared using the Nextera XT Kit (Illumina, San Diego, CA, USA). The PCR products were purified using the Agencourt AMPure XP Kit (AMPure; Beckman Coulter Inc., Brea, CA, USA). The index PCR was performed according to the manufacturer's protocol. The index PCR products were purified using AMPure or NucleoMag NGS Clean-up and Size Select (SizeSelect; Macherey-Nagel, Düren, Germany) as specified in Table I - 1. The AMPure was used to purify >100 bp DNA fragments as the manufacturer's protocol. The SizeSelect was used to enrich DNA fragments between 150 and 800 bp according to the manufacturer's protocol. The length of the final products was analyzed using the Agilent 2100 Bioanalyzer System (Agilent, Santa Clara, CA, USA).

Table I - 1: The PCR primer sets, blockers and library purification methods of the library preparation protocols assessed in this study.

Protocol name (Abbreviation)	Primer set(s)	Blocker	Library purification
Control (C)	TAReuk454FWD1 and TAReukREV3	No	AMPure
PNA-AMPure (PA)	TAReuk454FWD1 and TAReukREV3	TickB_PNA	AMPure
PNA-SizeSelect (PS)	TAReuk454FWD1 and TAReukREV3	TickB_PNA	SizeSelect
LNA-AMPure (LA)	TAReuk454FWD1 and TAReukREV3	TickB_LNA	AMPure
LNA-SizeSelect (LS)	TAReuk454FWD1 and TAReukREV3	TickB_LNA	SizeSelet
UNonMet (U)	EUK581F and EUK1134R for the first PCR / E572F and E1009R for the second PCR	No	AMPure

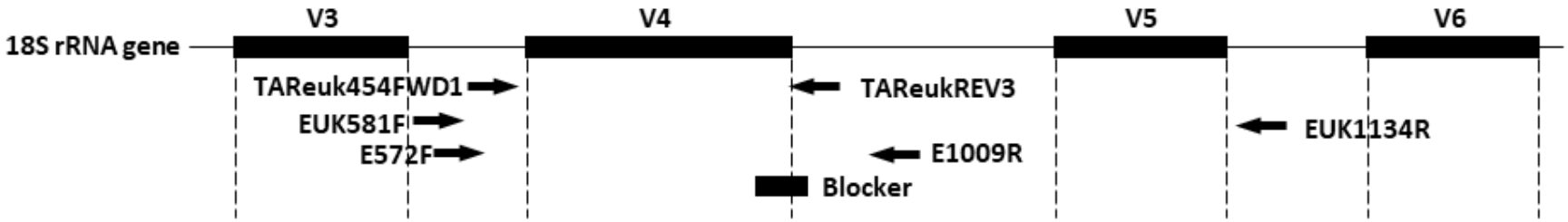

Figure I - 1: Locations of the primers and blockers on the 18S rRNA **gene.**

The upper horizontal bars indicate the hypervariable regions (V3, V4, V5, and V6) of 18S rRNA gene. Each arrow indicates the position and orientation of the primer. A box represents the position of the blockers.

Table I - 2: Primers and blockers used for amplification.

Name	Application	Sequence (5′→3′)	Reference
TAReuk454FWD1	Eukaryote V4 region of 18S rRNA	CCAGCASCYGCGGTAATTCC	(*69*)
TAReukREV3		ACTTTCGTTCTTGATYRA	
EUK581F	UNonMet-PCR (first PCR)	GTGCCAGCAGCCGCG	(*64*)
EUK1134R		TTTAAGTTTCAGCCTTGCG	
E572F	UNonMet-PCR (second PCR)	CCATCTCATCCCTGCGTGTCTCCGACTCAG	(*63*)
E1009R		CCTATCCCCTGTGTGCCTTGGCAGTCTCAG	
TickB_PNA	Blocking the amplification of tick 18S rRNA	GATCAAWGAAAACATT	This study
TickB_LNA	Blocking the amplification of tick 18S rRNA	GATCAAWGAAAACATT[*1]	This study

[*1] Underlined bases are LNA replacements.

2.7. Sequencing and data processing

The libraries were pooled and sequenced on an Illumina MiSeq system using the MiSeq Reagent Kit v3 (600 cycles). The FASTQ data were deposited in the DNA Data Bank of Japan (DDBJ) Sequence Read Archive (*https://www.ddbj.nig.ac.jp/index.html*) under an accession number of DRA011889. The raw data was processed using the QIIME2 (version 2019.10.0) (*70*). The fastq files were demultiplexed and merged. The merged sequences were analyzed by the The DADA2 plugin (*71*) in the QIIME2 to generate the amplicon sequence variants (ASVs). The potential contaminants were identified using the Decontam package in R with a threshold of 0.1 (*72*). Taxonomic information was assigned using the SILVA classifier (release 138). The ASVs identified as contaminant, archaea, bacteria, or unidentified to the supergroup level were removed.

2.8. Statistical Analysis

The PCR methods were evaluated based on the enrichment of non-tick reads and microbial composition. Non-tick read enrichment values were calculated by dividing proportion of non-tick reads (each method) by proportion of non-tick reads (control). The proportions of non-tick reads (eukaryote reads excluding tick reads) were calculated and compared using the pairwise.prop.test function with Bonferroni correction in R. The alpha diversity indices, including the number of observed sequence variants (ASVs), Shannon diversity, and Faith's phylogenetic diversity (PD), were calculated using QIIME2. The obtained indices were visualized in R using the qiime2R (*73*) and the phyloseq (*74*) packages.

Significant differences in alpha diversity were determined using restricted maximum likelihood (REML) estimates in linear mixed-effects models with the lmer function in the lme4 package (*75*). The response variable was log-transformed alpha diversity, with collection site as a random effect and blocking methods, including PCR and purification techniques, as fixed effects. Linear discriminant analysis effect size (LEfSe) (*76*) was applied to compare the relative abundances of microbial genera across different PCR methods (alpha values <0.05, logarithmic LDA score threshold = 2.0).

3. Results

3.1. Designing of TickB_PNA and TickB_LNA

On the forward primer franking region, the network analysis showed that ixodid tick sequences were separated into multiple haplotypes, with no conserved region identified across the reference (Figure I - 2ab). On the other hand, on the reverse primer franking region, the network analysis showed that the ixodid tick sequences were clustered into two haplotypes (Figure I - 2cd). To identify a suitable blocking site, the region spanning 27 bp upstream to 1 bp downstream of the reverse primer's 3′ end in ticks was subjected to BLAST searching against known apicomplexan protozoan sequences.

Table I - 3: Tick samples used to compare the different PCR methods.

Tick ID	Tick species	Sex	Prefecture	Location	Year
66	*I. persulcatus*	F	Hokkaido	42.61, 141.95	2013
210	*I. persulcatus*	F	Hokkaido	42.98, 142.80	2013
258	*I. persulcatus*	F	Hokkaido	43.08, 142.01	2013
467	*I. persulcatus*	M	Hokkaido	43.36, 142.61	2013
932	*I. persulcatus*	M	Hokkaido	43.92, 142.86	2014
933	*I. persulcatus*	M	Hokkaido	43.92, 142.86	2014
2592	*A. testudinarium*	M	Shimane	35.04, 132.68	2016
2874	*A. testudinarium*	F	Ehime	33.35, 132.02	2017
2876	*A. testudinarium*	F	Kochi	33.27, 132.99	2017
3148	*A. testudinarium*	F	Ehime	33.63, 132.56	2017
3149	*A. testudinarium*	F	Ehime	33.63, 132.56	2017
3332	*H. longicornis*	F	Hiroshima	34.49, 132.45	2017
3611	*H. longicornis*	F	Chiba	35.19, 140.25	2018
3620	*H. longicornis*	M	Chiba	35.19, 140.25	2018
3631	*H. longicornis*	M	Wakayama	33.83, 135.30	2018
3643	*H. longicornis*	F	Wakayama	34.37, 135.64	2018
3648	*H. longicornis*	M	Kochi	33.29, 134.17	2018

F, female; M, male.

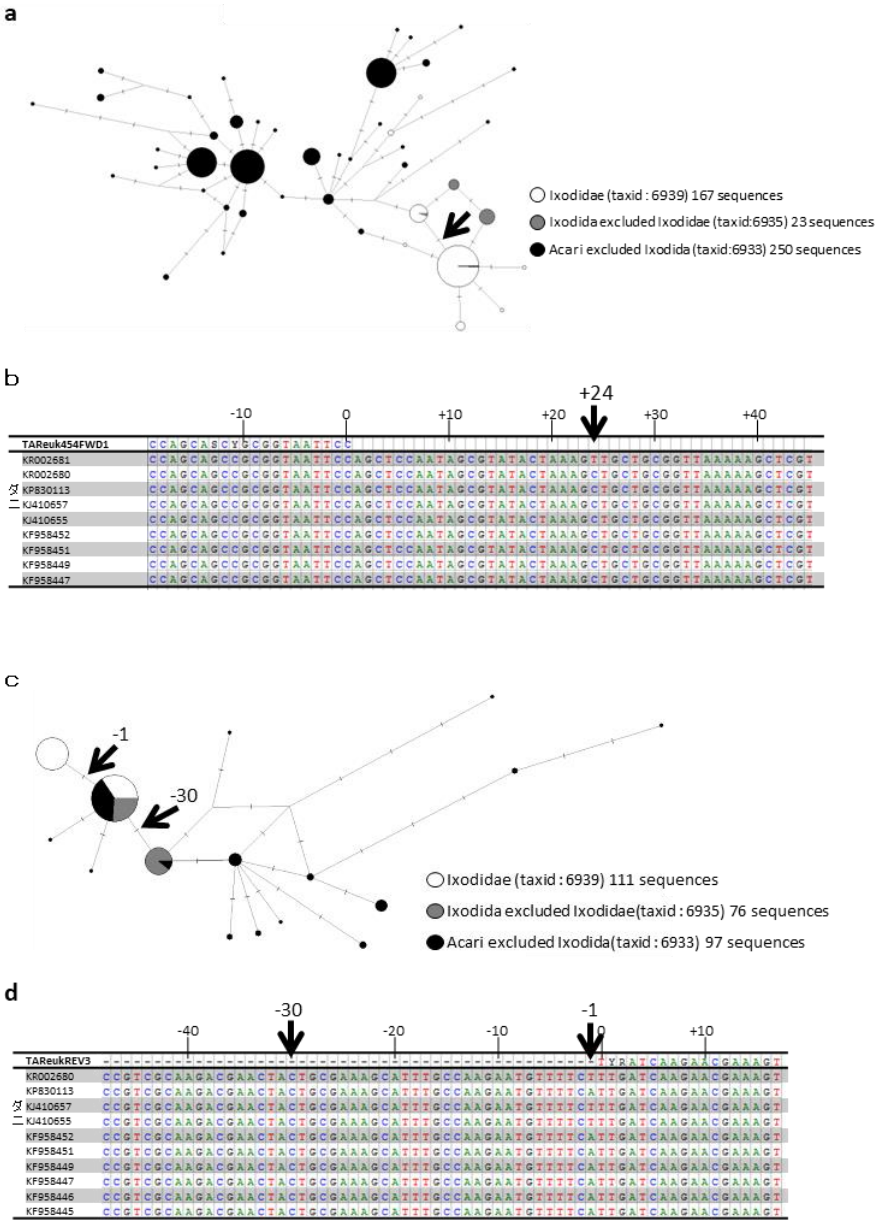

Figure I - 2: Median-joining network and the reference sequence alignments to design blocker sequence.

Median-joining network based on the region near the forward (a) or reverse (c) primer binding site. The arrow indicates the single nucleotide mismatch identical to the position in the alignment. Alignment of the forward (b) or reverse (d) primer and the reference sequences. The left column shows the primer name or the accession number of the sequences. The numbers at the top indicate the nucleotide positions relative to the 3' end.

A region between 11 bp upstream and 6 bp downstream of the 3′ end of the reverse primer, including 3 bp mismatches between ticks and apicomplexan parasites, was selected as the blocking site (Figure I - 1). The artificial nucleic acids were synthesized as follows: tick blocker PNA (TickB_PNA), 5′-GAT*C*AAWGAAAACATT*-3′ (* indicates nucleotide mismatch) and tick blocker LNA (TickB_LNA), 5′- GAT*C*AAWGAAAACATT*-3′ (* indicates nucleotide mismatch; underline indicates LNA replacement) (Table I - 1).

3.2. Comparison of purification methods by a fragment length analysis

To optimize performance of PCR amplicon library preparation with the blockers, AMPure and SizeSelect were validated by the fragment length analysis of the purified amplicon products (Figure I - 3). Without the blockers, the PCR products purified with AMPure indicated nearly single peaks. However, with blockers, the AMPure-purified products showed multiple peaks, with additional long off-target fragments. In contrast, the SizeSelect-purified products showed the reduced frequency of long off-target fragments.

3.3. Comparison of non-tick read enrichment

To evaluate the performance of the five PCR approaches (Table I - 3), the amplicon libraries were generated with the sample set of 17 adult ticks using each approach, and sequenced with MiSeq. After formal data processing, a total of 6,724,825 reads and 18,901 ASVs were generated. Following the removal of ASVs identified as contaminants, archaea, bacteria, or unclassified at the kingdom level, 6,163,967 reads (averaging 385,248 per sample, with a range of 13 to 253,437 reads) represented with 2,510 ASVs, were retained for further analysis.

The proportion of non-tick reads among all eukaryotic reads was significantly higher in PCRs with blockers and in UNonMet than in the control ($p < 0.01$) (Figure I - 4). The median proportion of non-tick reads in eukaryote reads was 0.03% for the control method, whereas other methods PNA-AMPure, PNA-SizeSelect, LNA-AMPure, LNA-SizeSelect, and UNonMet showed higher medians of 3.24%, 5.75%, 1.53%, 3.18%, and 1.37%, respectively.

The median non-tick read enrichment values for PNA-AMPure, PNA-SizeSelect, LNA-AMPure, LNA-SizeSelect, and UNonMet were 60.3, 103.8, 19.6, 32.9, and 35.2-fold, respectively (Figure I - 4). PNA-based methods, including PNA-AMPure and PNA-SizeSelect, showed over 12.8-fold enrichment in all samples except for tick ID 467, with values ranging from 12.8 to 705.0-fold. Decreased proportions of non-tick reads relative to the control were observed only in tick IDs 66 and 2876 upon UNonMet method.

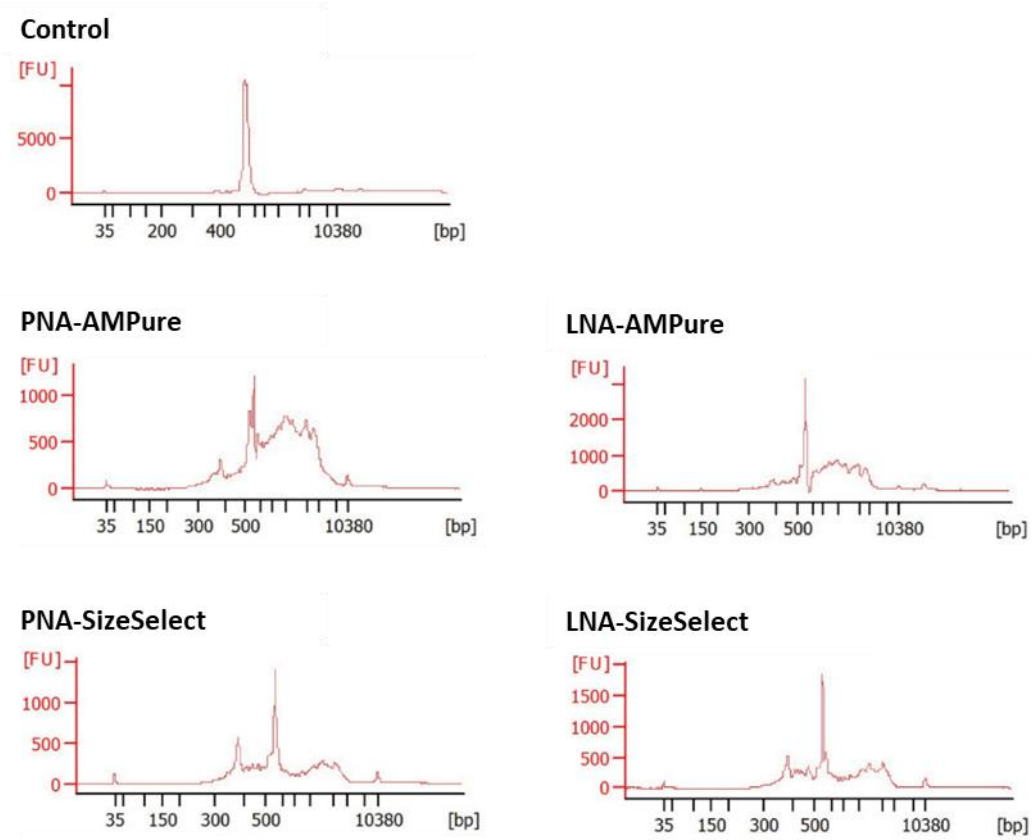

Figure I - 3: The fragment length distribution of the amplicon libraries generated by different library preparation protocols.

Haemaphysalis longicornis (tick ID 3631) DNA was used as the template DNA. The x- and y-axes show fragment size and fluorescent units, respectively.

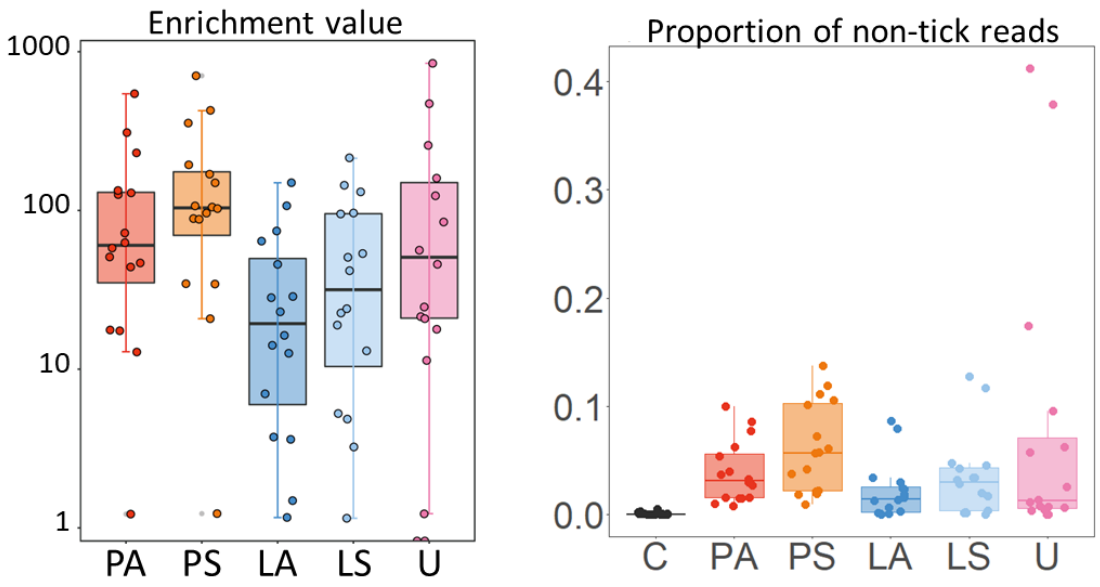

Figure I - 4:. Enrichment values and proportions of non-tick reads observed in the different library preparation protocols.

a) Non-tick read enrichment value and b) proportion of non-tick reads were indicated. The values were obtained from the amplification protocols, PNA-AMPure (PA), PNA-SizeSelect (PS), LNA-AMPure (LA), LNA-SizeSelect (LS), and UNonMet (U). Each dot represents a sample. Non-tick read enrichment values = proportion of non-tick reads (each method) / proportion of non-tick reads (control). Tick ID 3611 was filtered out from a) because only tick reads were detected in the control method. Tick ID 3148 was filtered out from b) due to higher proportion of non-tick reads, 0.0031, 0.086, 0.13, 0.054, 0.11, 0.38 from C, PA, PS, LA, LS, and U, respectively.

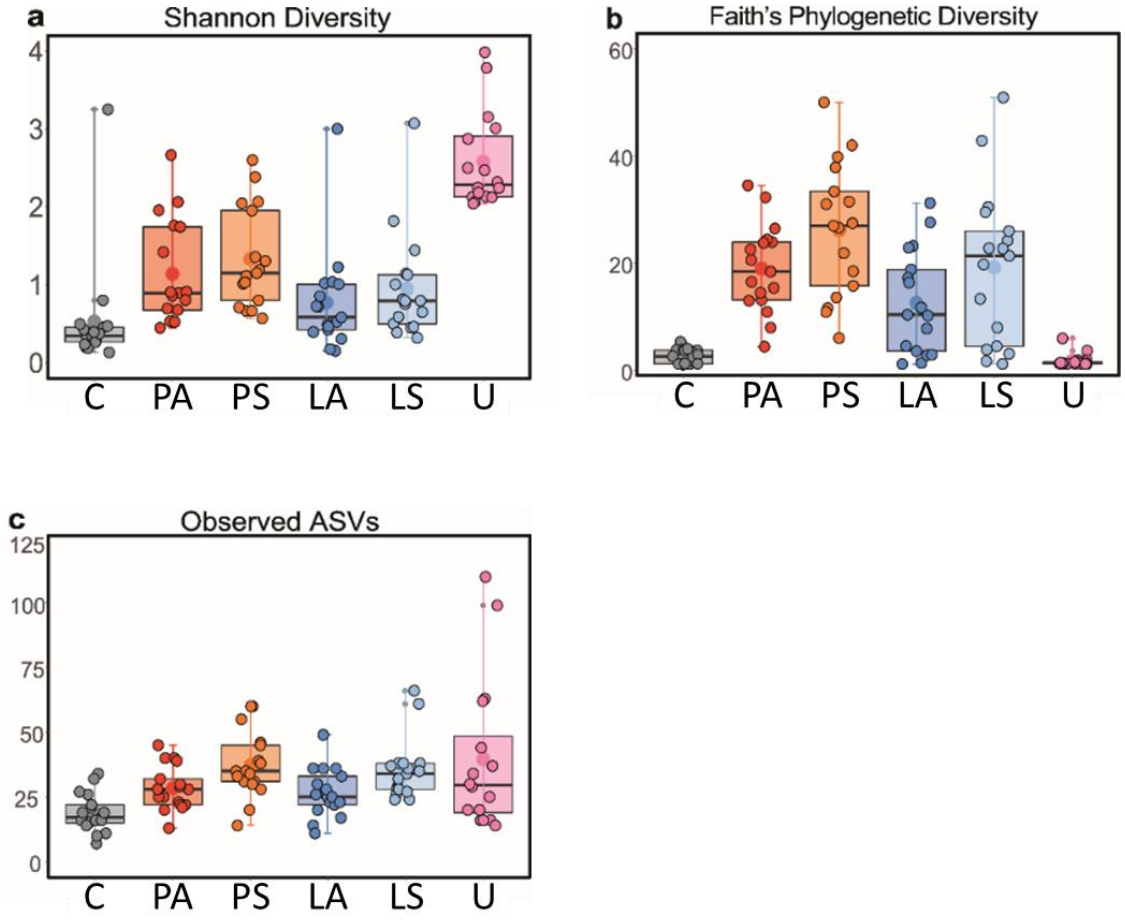

Figure I - 5: Comparison of the library preparation methods based on alpha diversity indices. The alpha diversity indices were calculated to compare the library preparation protocols, PNA-AMPure (PA), PNA-SizeSelect (PS), LNA-AMPure (LA), LNA-SizeSelect (LS), and UNonMet (U). The diversity indices were calculated based on (a) Shannon diversity, (b) Faith's phylogenetic diversity, and (c) the number of observed amplicon sequence variants (ASVs). Outlier plots are indicated by additional dots in gray.

Table I - 4: Statistical significances of alpha diversity metric differences among library preparation methods.

Comparison	Shannon diversity				Faith's phylogenetic diversity				Observed ASVs			
	Estimate	Standard Error	t-value	p-value	Estimate	Standard Error	t-value	p-value	Estimate	Standard Error	t-value	p-value
Control vs LNA-AMPure	-0.47	0.16	-2.90	0.05	-1.30	0.21	-6.24	2.21×10^{-7}	-0.36	0.12	-2.86	0.06
Control vs LNA-SizeSelect	-0.76	0.16	-4.63	1.78×10^{-4}	-1.67	0.21	-8.06	4.07×10^{-10}	-0.66	0.12	-5.27	1.42×10^{-5}
Control vs PNA-AMPure	-0.97	0.16	-5.93	8.54×10^{-7}	-2.00	0.21	-9.66	3.56×10^{-10}	-0.43	0.12	-3.48	0.01
Control vs PNA-SizeSelect	-1.16	0.16	-7.14	4.23×10^{-9}	-2.30	0.21	-11.10	3.56×10^{-10}	-0.69	0.12	-5.55	4.33×10^{-6}
Control vs UNonMet	-1.89	0.17	-11.41	3.56×10^{-10}	0.35	0.21	1.65	0.57	-0.59	0.13	-4.63	0.00
LNA-AMPure vs LNA-SizeSelect	-0.28	0.16	-1.73	0.51	-0.38	0.21	-1.82	0.46	-0.30	0.12	-2.40	0.17
LNA-AMPure vs PNA-AMPure	-0.50	0.16	-3.04	0.04	-0.71	0.21	-3.42	0.01	-0.08	0.12	-0.62	0.99
LNA-AMPure vs PNA-SizeSelect	-0.69	0.16	-4.24	7.65×10^{-4}	-1.01	0.21	-4.86	7.36×10^{-5}	-0.34	0.12	-2.69	0.09
LNA-AMPure vs UNonMet	-1.42	0.17	-8.56	3.61×10^{-10}	1.64	0.21	7.79	5.41×10^{-10}	-0.23	0.13	-1.82	0.46
LNA-SizeSelect vs PNA-AMPure	-0.21	0.16	-1.30	0.78	-0.33	0.21	-1.59	0.60	0.22	0.12	1.79	0.48
LNA-SizeSelect vs PNA-SizeSelect	-0.41	0.16	-2.51	0.13	-0.63	0.21	-3.03	0.04	-0.04	0.12	-0.29	1.00
LNA-SizeSelect vs UNonMet	-1.14	0.17	-6.86	1.44×10^{-8}	2.02	0.21	9.58	3.56×10^{-10}	0.07	0.13	0.55	0.99
PNA-AMPure vs PNA-SizeSelect	-0.20	0.16	-1.20	0.83	-0.30	0.21	-1.44	0.70	-0.26	0.12	-2.07	0.31
PNA-AMPure vs UNonMet	-0.92	0.17	-5.57	3.94×10^{-6}	2.35	0.21	11.15	3.56×10^{-10}	-0.15	0.13	-1.21	0.83
PNA-SizeSelect vs UNonMet	-0.73	0.17	-4.39	4.39×10^{-4}	2.65	0.21	12.57	3.56×10^{-10}	0.11	0.13	0.83	0.96

3.4. Comparison of alpha-diversity indices

Linear mixed models were used to assess differences in alpha diversity metrics across the library preparation methods (Figure I - 5, Table I - 4). For Shannon diversity, significant differences were observed for PNA-AMPure, PNA-SizeSelect, LNA-SizeSelect, and UNonMet compared to the control (p-values ranging from 3.56×10^{-10} to 1.78×10^{-4}), while LNA-AMPure did not show a significant difference ($p = 0.052$). For Faith's phylogenetic diversity (PD), the PNA-AMPure, PNA-SizeSelect, LNA-SizeSelect, and LNA-AMPure methods showed significant differences compared to the control (p-values ranging from 4.07×10^{-10} to 2.21×10^{-7}), while UNonMet was not significantly different from the control ($p = 0.57$). For the number of observed ASVs, only PNA-SizeSelect and LNA-SizeSelect showed significant increases relative to the control ($p = 4.33 \times 10^{-6}$ and $p = 1.42 \times 10^{-5}$, respectively). Comparing the blocking methods to the UNonMet, UNonMet had significantly higher Shannon diversity than all the four blocking methods (p-values ranging from 3.61×10^{-10} to 4.39×10^{-4}). In contrast, the blocking methods displayed significantly higher Faith's PD compared to UNonMet (p-values ranging from 5.41×10^{-10} to 3.56×10^{-10}). There were no significant differences in the number of observed ASVs between the blocking methods and UNonMet-PCR ($p > 0.09$). When comparing the two purification methods, AMPure and SizeSelect, no significant differences were observed across the three alpha diversity metrics ($p > 0.17$).

3.5. Comparison of the detected taxonomic groups

Fungi, Charophyta, Ciliophora, Apicomplexa, Cercozoa, and Retaria were detected at high abundances (Figure I - 6). The relative abundances of detected taxa across the library preparation methods were compared based on LEfSe (Figure I - 7). Compared to the control, PNA-SizeSelect and LNA-SizeSelect showed significantly higher abundances of Fungi, Archaeplastida, Alveolata, and Rhizaria. For UNonMet, Fungi and Alveolata were significantly more abundant than in the control. In addition, compared PNA-SizeSelect and LNA-SizeSelect to UNonMet, UNonMet showed significantly higher abundances of Nucletmycea, while PNA-SizeSelect and LNA-SizeSelect showed higher relative abundances of Alveolata, Chloroplastida, and unclassified eukaryotes. Between PNA-SizeSelect and LNA-SizeSelect, unclassified eukaryotes were significantly more abundant in PNA-SizeSelect.

4. Discussion

This study aimed to develop methods to analyze the eukaryotic microbiome in ticks. This is also the first comprehensive analysis of eukaryotes carried by ticks. The library preparation methods in this study effectively detected both pathogenic protozoa, such as Apicomplexa, and a broad range of microeukaryotes in ticks (Figure I - 6, Figure I - 7). Compared to the control, all the tested methods

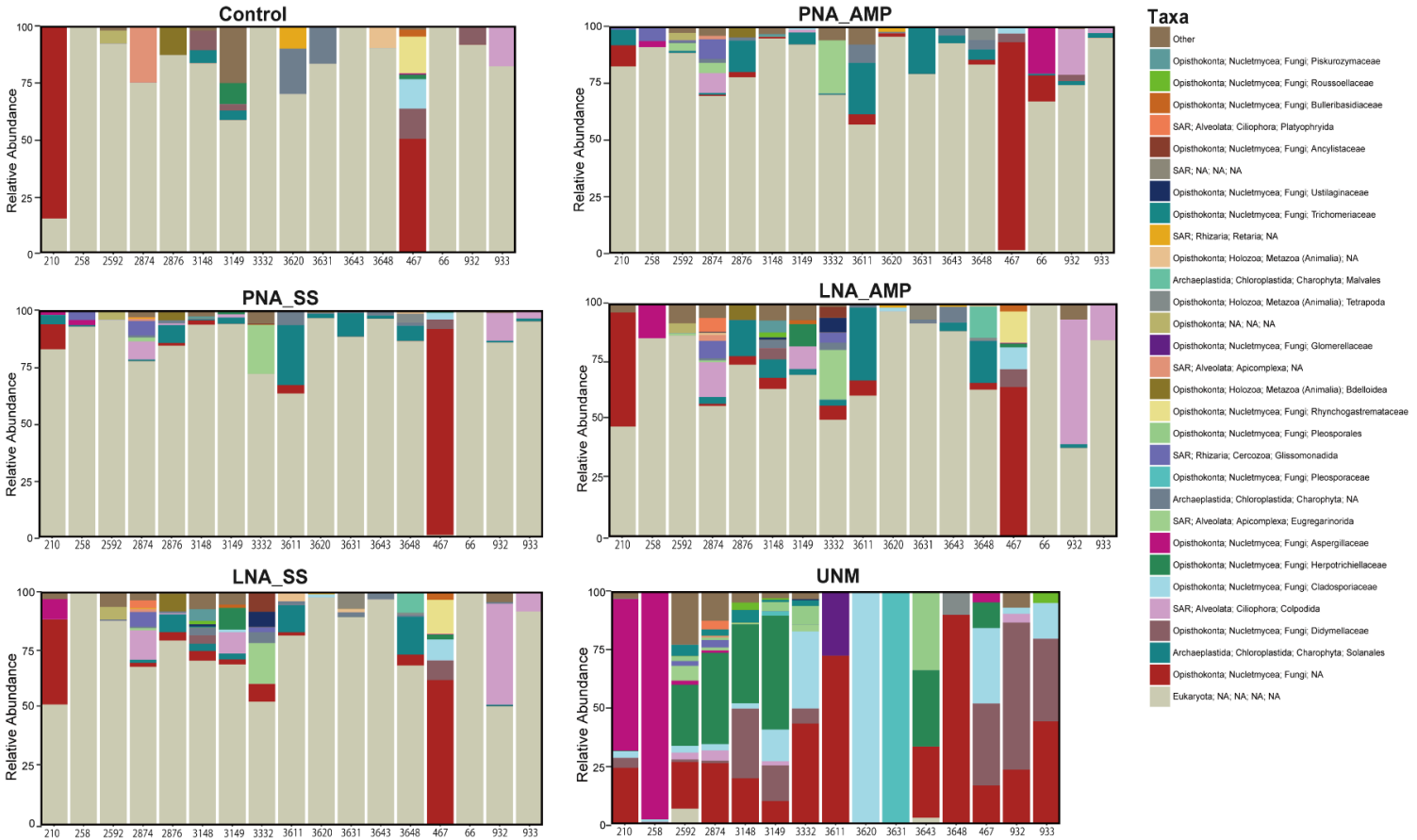

Figure I - 6: Relative abundance of the eukaryotic taxa detected by the different library preparation methods.

Each bar represents the eukaryotic taxa detected in one tick sample. Each color represents the eukaryotic as shown in the right panel. The sample ID is provided on the bottom of each bar. Tick ID 3631 of the control and tick IDs 66 and 2876 of UNM were excluded because no non-tick read was obtained.

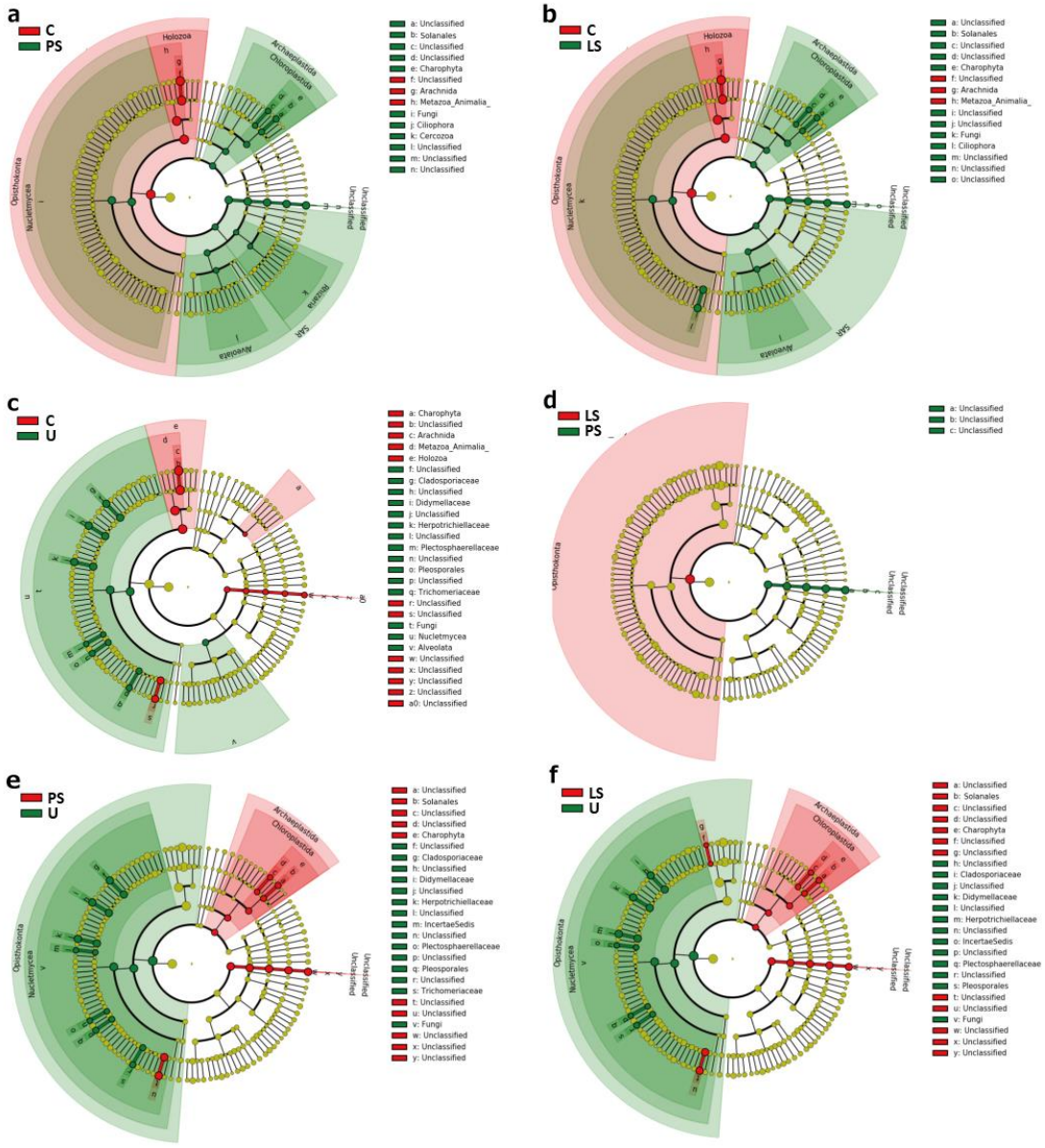

Figure I - 7: Cladograms showing differential abundant taxa among the library preparation protocols.

The LefSe analysis was performed to compare the library preparation methods, PNA-AMPure (PA), PNA-SizeSelect (PS), LNA-AMPure (LA), LNA-SizeSelect (LS), and UNonMet (U). The results were shown by (a) control vs PNA-SizeSelect, (b) control vs LNA-SizeSelect, (c) control vs UNonMet, (d) LNA-SizeSelect vs PNA-SizeSelect, (e) PNA-SizeSelect vs UNonMet, and (f) LNA-SizeSelect and UNonMet.

increased the proportion of non-tick reads and the alpha diversity indices (Figure I - 4, Figure I - 5, Table I - 4). PNA-SizeSelect and UNonMet were especially effective in increasing the proportion of non-tick reads. These findings suggest that these methods are suitable for sequencing tick-associated eukaryotes. Additionally, these methods are applicable to other ixodid tick species.

The PNA-SizeSelect, LNA-AMPure, LNA-SizeSelect, and UNonMet methods demonstrated significantly higher Shannon diversity and observed ASVs than the control (Figure I - 5). These observations indicate that these methods detected a wider range of microbial diversity. Blocker-based methods increased the abundance of the non-tick eukaryote compared to both the control and the UNonMet. While the UNonMet showed comparable Shannon diversity and ASV count to the blocker-based methods, it showed significantly lower Faith's PD (Figure I - 5). In addition, UNonMet detected significantly more fungi and Alveolata taxa (Figure I - 7). In contrast, PNA-SizeSelect and LNA-SizeSelect detected taxa from wider groups, including fungi, Alveolata, Archaeplastida, Rhizaria, Chloroplastida, and unclassified eukaryotes (Figure I - 7). These findings suggest that PNA-SizeSelect is suitable for pan-eukaryotic analyses, while UNonMet is more suitable for targeted analysis of fungi and Alveolata.

PNA-SizeSelect showed higher enrichment value, proportion of non-tick reads, and alpha-diversity indices than LNA-SizeSelect (Figure I - 4, Figure I - 5). This suggests that PNA inhibited off-target amplification more efficiently than LNA. However, it is worth noting that only 11 of the 16 bases in TickB_LNA were synthesized with LNAs in this study. LNA-SizeSelect could potentially be improved by replacing more bases of the blocker with LNAs. While the use of PNAs as blockers in library preparation has been widely documented (*54–56*, *58*), there are no reports of LNAs applied as blockers in comprehensive analyses with NGS. Additional trials are needed to optimize artificial nucleic acids for blocking purposes.

The use of blockers in PCRs increased nonspecific amplification of long sequences (Figure I - 3). Such nonspecific amplification potentially affects the pooling process, cluster formation, and data yield. In this study, these off-target sequences were reduced by using SizeSelect instead of AMPure (Figure I - 5). The source of this off-target amplification remains unknown. It is recommended to evaluate library size upon using TickB_PNA and TickB_LNA to manage this issue.

Amplicon analyses using blockers detected a substantial proportion of unclassified eukaryote sequences (Figure I - 6). Such sequences were also observed in other studies using blocker PNAs for 18S rRNA analysis (*56*, *77*). These sequences could represent either unregistered rRNA gene sequences or off-target amplifications. With the increasing use of high-throughput environmental DNA sequencing, there is a growing need for more comprehensive eukaryotic reference databases (*77–80*). Expanding these databases with proper classification will improve the accuracy of taxonomic assignments in high-throughput sequencing.

This study successfully detected the eukaryotic microbiome in ticks, particularly with the PNA-SizeSelect and UNonMet methods. In addition to known tick-borne protozoa, a diversity of micro-eukaryotes was detected in ticks. These methods are applicable to explore the eukaryotic microbiome in ticks and may enhance our understanding of ticks and tick-borne pathogen dynamics.

5. Summary

This study introduces novel methods to analyze the eukaryotic microbiome in ticks using high-throughput sequencing. The methods were designed to selectively amplify microeukaryote genes in tick-derived DNA by suppressing the amplification of the tick DNA. Two types of artificial nucleic acids, PNAs and LNAs, were assessed. In addition, a PCR approach using UNonMet was also evaluated. A set of tick DNA samples was used to evaluate the methods. While the conventional method primarily yielded tick-derived sequences, the use of blocker-based and UNonMet methods significantly increased the proportion of micro eukaryotic reads and increased alpha diversity indices. Additionally, UNonMet detected fungi and Alveolata, while the PNA-based method detected a wider range of taxa, including fungi, Alveolata, Archaeplastida, Rhizaria, Chloroplastida, and unclassified eukaryotes. The PNA-based method was considered to be suitable for pan-eukaryotic analyses, while UNonMet was suitable for targeted studies of fungi and Alveolata. This approach provides valuable tools to understand tick microbiome and tick-borne pathogen ecology.

Chapter II

Detection of potential entomopathogenic taxa and keystone taxa in ticks by cross-domain microbiome analysis

1. Introduction

Microorganisms interact through a wide range of relationships, from cooperative relationships, such as the exchange of metabolic products, to antagonistic interactions, such as a competition for limited resources or direct interference (*81–83*). To gain a comprehensive insight into the structure and dynamics of microbial communities in ticks, it is essential to explore interactions across diverse microbial domains, including bacteria, archaea, viruses, and eukaryotes (*84*, *85*). In the previous chapter, a novel method to detect eukaryotic microbiome in ticks was developed using artificial nucleic acids. The developed method provides a valuable opportunity to investigate interactions between eukaryotes and other microbial domains.

Network-based analysis offers a useful approach to uncover the complex interactions within microbial communities (*86*). Co-occurrence networks are suitable approach to analyze microbiome data (*87*, *88*). The co-occurrence network is constructed based on pairwise correlations among microbes. A key advantage of network analysis lies in its ability to determine keystone taxa (*89*). Keystone taxa are a microorganism or a group of microorganisms those are highly connected with other taxa (*90*). Keystone taxa play crucial roles in the stability of microbiome, and serve as functional drivers within the community (*91*).

Ticks are known to harbor bacterial endosymbionts, such as *Coxiella*-like endosymbionts or *Francisella*-like endosymbionts, which provide essential nutrients to their host ticks (*92*, *93*). Studies of the bacterial microbiome in ticks have shown that endosymbionts often dominate in the relative abundances (*20*, *94*). However, even taxa with low abundance can act as keystone taxa, and significantly influence microbial community stability (*95*). Previous studies suggested that the pathogenic microorganism invasion by *Anaplasma*, *Rickettsia*, or *Babesia* affect the bacterial microbiome network in ticks (*84*, *85*, *96*). Therefore, comprehensive analyses that incorporate pathogens, endosymbionts, and other taxa are crucial to understand pathogen transmission mechanism. Furthermore, eukaryotic communities have not been previously included in microbial network studies. Including these communities may offer new insights into the dynamics of complex microbiome systems.

In this chapter, the keystone eukaryotic taxa in ticks were aimed to be determined using network analyses. Four species of ticks were collected from four distinct geographic regions in Japan. The bacterial and eukaryotic tick microbiomes were characterized based on the 16S and 18S rRNA gene amplicon sequencing strategies, respectively. The abundant eukaryotic taxa in the tested ticks were identified. Diversity analysis was performed to assess the contribution of species, sex, and sampling region. Cross-domain co-occurrence networks were constructed to detect microbial interactions and to determine the keystone taxa.

2. Material and Methods

2.1. Ticks

A total of 184 questing ticks were collected by flagging between 2013 and 2019 from four different geographic blocks (Hokkaido, Tohoku, Kinki, and Kyushu) (Figure II - 1, Table I - 1). The collected ticks were morphologically identified based on the morphological key (*68*). The females and males of four tick species, *Haemaphysalis flava* (n = 56), *Haemaphysalis longicornis* (n = 47), *Ixodes ovatus* (n = 41), and *Ixodes persulcatus* (n = 40) were included in this study (Table I - 2). The ticks were reared under 16℃ until the DNA extraction.

2.2. DNA extraction

The ticks were individually washed once with 1 ml of 10% sodium hypochlorite, twice with 1 ml of 70% ethanol, and once with 1 ml of sterile phosphate-buffered saline (pH7.0 – 7.6) to decontaminate the tick surface. The ticks were then homogenized with 4.8 mm stainless steel beads (TOMY, Tokyo, Japan) using the Micro Smash MS-100R (TOMY) in 100 µl of Dulbecco's Modified Eagle Medium (Gibco, Life Technologies, Gland Island, NY, USA). DNA was extracted from 50 µl of the tick homogenates using the blackPREP Tick DNA/RNA Kit (Analytik Jena, Jena, Germany), following the manufacturer's protocol.

2.3. 16S rRNA gene amplicon sequencing

The sequencing library was generated for a total of 184 tick samples as mentioned above (Table II - **1**). The Initial PCRs were performed using the KAPA HiFi HotStart ReadyMix (KAPA Biosystems, Wilmington, MA, USA) to amplify bacterial 16S rRNA gene with a set of universal primers Illumina_16S_341F and Illumina_16S_805R (Table II - 3). The libraries were prepared using the Nextera XT Kit (Illumina, San Diego, CA, USA) according to the manufacturer's protocol. The PCR products were purified using the Agencourt AMPure XP Kit (Beckman Coulter Inc., Brea, CA, USA). The length of the final products was analyzed using the Agilent 2100 Bioanalyzer System (Agilent, Santa Clara, CA, USA). The libraries were pooled and sequenced on the Illumina MiSeq system using the MiSeq Reagent Kit v3 (600 cycles).

2.4. 18S rRNA gene amplicon sequencing

The sequencing library of 18S rRNA gene amplicon was generated with the same set of samples as the 16S rRNA gene amplicon sequencing analysis (Table II - 1). The library preparation was based on the PNA-SizeSelect protocol described in the Chapter I. Briefly, PCR was performed using a universal primer set (TAReuk454FWD1 and TAReuREV3, Table II - 3) with TickB_PNA to inhibit amplification of the host tick gene. The reaction mixture was in 25.0 µl containing 12.5 µl of 2 × KAPA HiFi HotStart ReadyMix, 200 nM of each prime, 2.5 µl of template DNA, and 50 pmol of

Figure II - 1: Sampling regions of the ticks used for the 18S rRNA gene amplicon sequencing.

Table II - 1: Sampling metadata, and total number of obtained reads and total number of observed ASVs after filtering of each sample.

Sample ID	Species	Sex	Region	Sampling site GPS	Sampling year	Sampling month	16S total number of obtained reads	16S total number of observed ASVs	18S total number of obtained reads	18S total number of observed ASVs
2281	*H. flava*	F	Kinki	34.35, 136.70	2016	3	56,461	50	454	19
2282	*H. flava*	F	Kinki	34.35, 136.70	2016	3	61,680	92	896	19
2283	*H. flava*	F	Kinki	34.35, 136.70	2016	3	54,497	38	6,013	13
2284	*H. flava*	F	Kinki	34.35, 136.70	2016	3	30,368	31	412	13
2285	*H. flava*	F	Kinki	34.35, 136.70	2016	3	57,852	32	23,231	8
2286	*H. flava*	F	Kinki	34.35, 136.70	2016	3	47,280	28	505	15
2322	*H. flava*	F	Kinki	34.45, 136.78	2016	3	61,625	22	164	5
2323	*H. flava*	F	Kinki	34.45, 136.78	2016	3	55,592	26	511	19
2324	*H. flava*	F	Kinki	34.45, 136.78	2016	3	25,909	21	213	17
2275	*H. flava*	M	Kinki	34.35, 136.70	2016	3	50,990	83	684	17
2276	*H. flava*	M	Kinki	34.35, 136.70	2016	3	47,380	49	269	9
2277	*H. flava*	M	Kinki	34.35, 136.70	2016	3	51,212	108	1,324	15
2278	*H. flava*	M	Kinki	34.35, 136.70	2016	3	39,529	66	558	12
2279	*H. flava*	M	Kinki	34.35, 136.70	2016	3	37,100	64	2,459	18
2280	*H. flava*	M	Kinki	34.35, 136.70	2016	3	72,287	50	1,116	10
2325	*H. flava*	M	Kinki	34.45, 136.78	2016	3	62,995	28	80	3
2326	*H. flava*	M	Kinki	34.45, 136.78	2016	3	54,725	42	2,596	11
2327	*H. flava*	M	Kinki	34.45, 136.78	2016	3	52,730	32	1,159	2
2328	*H. flava*	M	Kinki	34.45, 136.78	2016	3	34,045	27	683	9
2329	*H. flava*	M	Kinki	34.45, 136.78	2017	3	60,650	75	10,372	10
2330	*H. flava*	M	Kinki	34.45, 136.78	2017	3	55,030	15	36	2
1708	*H. flava*	F	Kyushu	31.93, 130.79	2015	5	59,143	125	365	17
1764	*H. flava*	F	Kyushu	31.75, 130.57	2015	5	56,893	92	1,415	23
1765	*H. flava*	F	Kyushu	31.75, 130.57	2015	5	44,603	37	993	23
1766	*H. flava*	F	Kyushu	31.75, 130.57	2015	5	60,016	99	4,362	20
1767	*H. flava*	F	Kyushu	31.75, 130.57	2015	5	66,850	66	1,750	29
1768	*H. flava*	F	Kyushu	31.75, 130.57	2016	5	59,040	126	6,562	47
2750	*H. flava*	F	Kyushu	31.75, 130.57	2017	3	75,567	81	4,795	46
2751	*H. flava*	F	Kyushu	31.75, 130.57	2017	3	55,150	27	584	19
2752	*H. flava*	F	Kyushu	31.75, 130.57	2017	3	67,120	53	2,816	33
2753	*H. flava*	F	Kyushu	31.75, 130.57	2017	3	53,518	40	456	19
2754	*H. flava*	F	Kyushu	31.75, 130.57	2017	3	57,322	106	16,396	66
2755	*H. flava*	M	Kyushu	31.75, 130.57	2017	3	40,006	77	9,994	30
2756	*H. flava*	M	Kyushu	31.75, 130.57	2017	3	42,951	57	2,198	26
2757	*H. flava*	M	Kyushu	31.75, 130.57	2017	3	36,023	48	1,537	10
2758	*H. flava*	M	Kyushu	31.75, 130.57	2017	3	42,811	23	10,128	14
2759	*H. flava*	M	Kyushu	31.75, 130.57	2018	3	40,872	46	3,539	22
2760	*H. flava*	M	Kyushu	31.75, 130.57	2018	3	42,105	71	1,523	18
2761	*H. flava*	M	Kyushu	31.75, 130.57	2018	3	36,868	80	856	12
2762	*H. flava*	M	Kyushu	31.75, 130.57	2018	3	43,250	51	2,344	9
1156	*H. flava*	F	Tohoku	37.47, 139.98	2014	6	61,578	94	2,700	45
1157	*H. flava*	F	Tohoku	37.47, 139.98	2014	6	61,155	91	6,124	60
1158	*H. flava*	F	Tohoku	37.47, 139.98	2014	6	62,271	50	2,820	33
800	*H. flava*	F	Tohoku	37.73, 140.48	2013	10	35,562	22	544	20
801	*H. flava*	F	Tohoku	37.73, 140.48	2013	10	39,320	60	2,039	26

Table II – 1 continued

892	*H. flava*	F	Tohoku	37.73, 140.48	2014	5	52,607	26	1,193	33
893	*H. flava*	F	Tohoku	37.73, 140.48	2014	5	47,592	20	592	23
896	*H. flava*	F	Tohoku	37.77, 140.38	2014	5	42,440	25	301	19
1153	*H. flava*	M	Tohoku	37.47, 139.98	2014	6	93,416	114	2,018	26
1154	*H. flava*	M	Tohoku	37.47, 139.98	2014	6	57,472	145	1,554	37
1155	*H. flava*	M	Tohoku	37.47, 139.98	2014	6	43,710	132	2,377	30
795	*H. flava*	M	Tohoku	37.73, 140.48	2013	10	43,386	97	2,475	17
796	*H. flava*	M	Tohoku	37.77, 140.30	2013	10	43,438	94	2,455	22
797	*H. flava*	M	Tohoku	37.13, 140.94	2013	10	47,597	163	2,448	22
798	*H. flava*	M	Tohoku	37.13, 140.94	2013	10	31,148	60	1,280	20
799	*H. flava*	M	Tohoku	37.13, 140.94	2013	10	30,833	201	359	12
3981	*H. longicornis*	F	Hokkaido	42.79, 141.70	2020	5	57,226	21	1,267	7
510	*H. longicornis*	F	Hokkaido	42.87, 142.12	2013	7	40,259	30	77	6
511	*H. longicornis*	F	Hokkaido	42.87, 142.12	2013	7	37,933	78	479	17
512	*H. longicornis*	F	Hokkaido	42.87, 142.12	2013	7	55,640	74	318	8
513	*H. longicornis*	F	Hokkaido	42.87, 142.12	2013	7	49,077	60	297	7
2271	*H. longicornis*	F	Kinki	34.35, 136.70	2016	3	55,013	36	0	0
2272	*H. longicornis*	F	Kinki	34.35, 136.70	2016	3	55,290	35	347	16
2273	*H. longicornis*	F	Kinki	34.35, 136.70	2016	3	50,809	29	112	11
2274	*H. longicornis*	F	Kinki	34.35, 136.70	2016	3	52,280	61	60,353	19
2310	*H. longicornis*	F	Kinki	34.45, 136.78	2016	3	29,567	123	4,298	24
3623	*H. longicornis*	F	Kinki	33.83, 135.30	2018	6	58,946	15	8,018	17
3624	*H. longicornis*	F	Kinki	33.83, 135.30	2018	6	57,453	20	9,209	5
3625	*H. longicornis*	F	Kinki	33.83, 135.30	2018	6	46,341	14	44	4
3626	*H. longicornis*	F	Kinki	33.83, 135.30	2018	6	126,727	13	129	5
3627	*H. longicornis*	F	Kinki	33.83, 135.30	2018	6	121,470	25	49	4
3836	*H. longicornis*	F	Kinki	34.35, 136.70	2019	7	38,644	12	0	0
3838	*H. longicornis*	F	Kinki	34.29, 136.58	2019	7	48,237	11	8,702	10
3839	*H. longicornis*	F	Kinki	34.29, 136.58	2019	7	59,957	10	54	2
2268	*H. longicornis*	M	Kinki	34.35, 136.70	2016	3	43,743	172	39,978	16
2269	*H. longicornis*	M	Kinki	34.35, 136.70	2016	3	45,199	70	788	18
2270	*H. longicornis*	M	Kinki	34.35, 136.70	2016	3	48,632	52	136	7
2288	*H. longicornis*	M	Kinki	34.35, 136.70	2016	3	27,312	34	5	1
2289	*H. longicornis*	M	Kinki	34.35, 136.70	2016	3	42,037	67	1,431	11
2309	*H. longicornis*	M	Kinki	34.45, 136.78	2016	3	33,588	73	3,664	13
2311	*H. longicornis*	M	Kinki	34.45, 136.78	2016	3	41,061	52	598	19
2312	*H. longicornis*	M	Kinki	34.45, 136.78	2016	3	36,878	62	1,337	10
3628	*H. longicornis*	M	Kinki	33.83, 135.30	2018	6	71,917	29	26	3
3629	*H. longicornis*	M	Kinki	33.83, 135.30	2019	6	54,555	13	186	8
3630	*H. longicornis*	M	Kinki	33.83, 135.30	2019	6	55,281	16	8,141	10
3631	*H. longicornis*	M	Kinki	33.83, 135.30	2019	6	49,061	14	214	9
3632	*H. longicornis*	M	Kinki	33.83, 135.30	2019	6	50,731	16	60	5
3837	*H. longicornis*	M	Kinki	34.35, 136.70	2019	7	33,924	13	8,779	34
3840	*H. longicornis*	M	Kinki	34.29, 136.58	2019	7	29,662	19	68	3
1653	*H. longicornis*	F	Kyushu	31.48, 130.34	2015	5	50,385	88	4,336	40
1654	*H. longicornis*	F	Kyushu	31.48, 130.34	2015	5	120,260	103	3,961	40
1655	*H. longicornis*	F	Kyushu	31.48, 130.34	2015	5	148,104	111	3,023	26
1728	*H. longicornis*	F	Kyushu	32.12, 130.52	2015	5	52,829	88	137	12
1729	*H. longicornis*	F	Kyushu	32.12, 130.52	2015	5	55,244	59	839	14
1730	*H. longicornis*	F	Kyushu	32.12, 130.52	2015	5	52,202	115	398	23

Table II – 1 continued

1731	*H. longicornis*	F	Kyushu	32.12, 130.52	2015	5	49,269	40	463	10
1758	*H. longicornis*	F	Kyushu	31.75, 130.57	2015	5	56,424	213	3,992	33
1759	*H. longicornis*	F	Kyushu	31.75, 130.57	2015	5	127,586	223	2,299	24
1760	*H. longicornis*	F	Kyushu	31.75, 130.57	2015	5	64,086	102	0	0
1761	*H. longicornis*	F	Kyushu	31.75, 130.57	2015	5	56,812	203	376	13
1762	*H. longicornis*	F	Kyushu	31.75, 130.57	2015	5	58,327	112	4,181	29
1763	*H. longicornis*	F	Kyushu	31.75, 130.57	2015	5	58,985	152	1,369	30
1693	*H. longicornis*	M	Kyushu	31.93, 130.79	2015	5	79,811	50	395	18
3684	*I. ovatus*	F	Hokkaido	42.90, 141.11	2019	7	54,520	38	277	7
3685	*I. ovatus*	F	Hokkaido	42.90, 141.11	2019	7	61,284	39	123	6
3686	*I. ovatus*	F	Hokkaido	42.90, 141.11	2019	7	63,216	45	583	13
3687	*I. ovatus*	F	Hokkaido	42.90, 141.11	2019	7	72,866	34	1,243	1
3688	*I. ovatus*	F	Hokkaido	42.90, 141.11	2019	7	54,310	33	5,532	11
3689	*I. ovatus*	F	Hokkaido	42.90, 141.11	2019	7	57,164	35	253	8
3690	*I. ovatus*	F	Hokkaido	42.90, 141.11	2019	7	57,752	27	2,496	6
3691	*I. ovatus*	F	Hokkaido	42.90, 141.11	2019	7	60,093	33	88	4
3704	*I. ovatus*	M	Hokkaido	42.90, 141.11	2019	7	53,078	31	9,406	6
3705	*I. ovatus*	M	Hokkaido	42.90, 141.11	2019	7	65,866	33	887	12
3706	*I. ovatus*	M	Hokkaido	42.90, 141.11	2019	7	61,404	27	842	10
3707	*I. ovatus*	M	Hokkaido	42.90, 141.11	2019	7	55,282	39	168	8
3708	*I. ovatus*	M	Hokkaido	42.90, 141.11	2019	7	47,167	30	1,081	14
3709	*I. ovatus*	M	Hokkaido	42.90, 141.11	2019	7	50,501	28	855	15
3710	*I. ovatus*	M	Hokkaido	42.90, 141.11	2019	7	50,939	34	140	6
3711	*I. ovatus*	M	Hokkaido	42.90, 141.11	2019	7	48,022	33	7,557	12
868	*I. ovatus*	F	Kinki	34.18, 136.10	2014	5	27,728	28	293	12
869	*I. ovatus*	F	Kinki	34.18, 136.10	2014	5	50,431	34	633	12
870	*I. ovatus*	F	Kinki	34.18, 136.10	2014	5	53,851	32	331	17
871	*I. ovatus*	F	Kinki	34.18, 136.10	2014	5	63,510	30	241	7
872	*I. ovatus*	F	Kinki	34.18, 136.10	2014	5	52,655	38	2,815	15
873	*I. ovatus*	F	Kinki	34.18, 136.10	2014	5	52,172	33	2,248	13
865	*I. ovatus*	M	Kinki	34.18, 136.10	2014	5	27,797	25	371	11
866	*I. ovatus*	M	Kinki	34.18, 136.10	2014	5	34,396	25	174	10
867	*I. ovatus*	M	Kinki	34.18, 136.10	2014	5	31,061	29	2,419	15
764	*I. ovatus*	F	Kyushu	32.03, 131.19	2013	10	47,928	46	514	13
2717	*I. ovatus*	M	Kyushu	31.75, 130.57	2017	3	55,848	25	298	12
2725	*I. ovatus*	M	Kyushu	31.70, 130.50	2017	3	46,117	36	1,708	12
1087	*I. ovatus*	F	Tohoku	37.03, 139.38	2014	6	29,283	40	4,971	8
1088	*I. ovatus*	F	Tohoku	37.03, 139.38	2014	6	30,644	54	594	14
1089	*I. ovatus*	F	Tohoku	37.03, 139.38	2014	6	45,907	49	441	15
1090	*I. ovatus*	F	Tohoku	37.03, 139.38	2014	6	126,198	61	398	11
1091	*I. ovatus*	F	Tohoku	37.03, 139.38	2014	6	64,851	71	322	16
1092	*I. ovatus*	F	Tohoku	37.03, 139.38	2014	6	85,152	61	897	13
1080	*I. ovatus*	M	Tohoku	37.03, 139.38	2014	6	27,142	28	95	6
1081	*I. ovatus*	M	Tohoku	37.03, 139.38	2014	6	29,366	36	731	18
1082	*I. ovatus*	M	Tohoku	37.03, 139.38	2014	6	42,812	34	392	16
1083	*I. ovatus*	M	Tohoku	37.03, 139.38	2014	6	38,027	46	577	19
1084	*I. ovatus*	M	Tohoku	37.03, 139.38	2014	6	42,480	35	791	9
1085	*I. ovatus*	M	Tohoku	37.03, 139.38	2014	6	27,699	54	1,357	17
1086	*I. ovatus*	M	Tohoku	37.03, 139.38	2014	6	40,562	39	539	10
3649	*I. persulcatus*	F	Hokkaido	42.90, 141.11	2019	7	45,436	13	189	6

Table II – 1 continued

3650	*I. persulcatus*	F	Hokkaido	42.90, 141.11	2019	7	83,376	10	301	14
3651	*I. persulcatus*	F	Hokkaido	42.90, 141.11	2019	7	93,012	19	6,031	7
3652	*I. persulcatus*	F	Hokkaido	42.90, 141.11	2019	7	139,501	25	42	6
3653	*I. persulcatus*	F	Hokkaido	42.90, 141.11	2019	7	57,174	13	21	5
3654	*I. persulcatus*	F	Hokkaido	42.90, 141.11	2019	7	45,023	11	137	5
3655	*I. persulcatus*	F	Hokkaido	42.90, 141.11	2019	7	46,574	14	348	10
3656	*I. persulcatus*	F	Hokkaido	42.90, 141.11	2019	7	56,468	9	666	10
3664	*I. persulcatus*	M	Hokkaido	42.90, 141.11	2019	7	3,067	9	148	6
3665	*I. persulcatus*	M	Hokkaido	42.90, 141.11	2019	7	2,714	13	22,235	13
3666	*I. persulcatus*	M	Hokkaido	42.90, 141.11	2019	7	49,685	14	184	10
3667	*I. persulcatus*	M	Hokkaido	42.90, 141.11	2019	7	4,713	15	152	8
3668	*I. persulcatus*	M	Hokkaido	42.90, 141.11	2019	7	6,246	17	1,641	10
3669	*I. persulcatus*	M	Hokkaido	42.90, 141.11	2019	7	20,586	14	120	7
3670	*I. persulcatus*	M	Hokkaido	42.90, 141.11	2019	7	9,695	12	601	4
3671	*I. persulcatus*	M	Hokkaido	42.90, 141.11	2019	7	44,869	23	440	8
880	*I. persulcatus*	F	Kinki	34.18, 136.10	2014	5	30,716	13	426	11
881	*I. persulcatus*	F	Kinki	34.18, 136.10	2014	5	44,164	24	12	1
874	*I. persulcatus*	M	Kinki	34.18, 136.10	2014	5	24,507	18	274	8
875	*I. persulcatus*	M	Kinki	34.18, 136.10	2014	5	30,764	151	224	9
876	*I. persulcatus*	M	Kinki	34.18, 136.10	2014	5	25,197	29	62	6
877	*I. persulcatus*	M	Kinki	34.18, 136.10	2014	5	10,180	17	261	7
878	*I. persulcatus*	M	Kinki	34.18, 136.10	2014	5	11,399	20	192	12
879	*I. persulcatus*	M	Kinki	34.18, 136.10	2014	5	17,611	15	121	7
1101	*I. persulcatus*	F	Tohoku	37.03, 139.38	2014	6	59,937	30	920	7
1102	*I. persulcatus*	F	Tohoku	37.03, 139.38	2014	6	44,960	60	360	11
1103	*I. persulcatus*	F	Tohoku	37.03, 139.38	2014	6	28,262	33	1,973	17
1104	*I. persulcatus*	F	Tohoku	37.03, 139.38	2014	6	26,817	49	683	9
1105	*I. persulcatus*	F	Tohoku	37.03, 139.38	2014	6	22,764	58	300	18
1106	*I. persulcatus*	F	Tohoku	37.03, 139.38	2014	6	8,107	29	199	9
1107	*I. persulcatus*	F	Tohoku	37.03, 139.38	2014	6	28,707	39	286	13
1108	*I. persulcatus*	F	Tohoku	37.03, 139.38	2014	6	26,527	79	870	20
1093	*I. persulcatus*	M	Tohoku	37.03, 139.38	2014	6	23,758	24	246	9
1094	*I. persulcatus*	M	Tohoku	37.03, 139.38	2014	6	13,513	25	38	5
1095	*I. persulcatus*	M	Tohoku	37.03, 139.38	2014	6	48,364	33	147	8
1096	*I. persulcatus*	M	Tohoku	37.03, 139.38	2014	6	10,605	30	104	9
1097	*I. persulcatus*	M	Tohoku	37.03, 139.38	2014	6	38,110	28	479	13
1098	*I. persulcatus*	M	Tohoku	37.03, 139.38	2014	6	13,481	49	290	11
1099	*I. persulcatus*	M	Tohoku	37.03, 139.38	2014	6	12,933	32	228	15
1100	*I. persulcatus*	M	Tohoku	37.03, 139.38	2014	6	22,748	47	201	10

Table II - 2: Species, sex, and sampling regions of the tick samples.

Species	Sex	Hokkaido	Tohoku	Kinki	Kyushu	Total
H. flava	F	0	8	9	11	28
	M	0	8	12	8	28
H. longicornis	F	5	0	13	13	31
	M	0	0	15	1	16
I. ovatus	F	8	6	6	1	21
	M	8	7	3	2	20
I. persulcatus	F	8	8	2	0	18
	M	8	8	6	0	22
Total		37	45	66	36	184

F, female. M, male.

Table II - 3: Origo nucleotides and PCR information used to generate 16S and 18S rRNA gene amplicon libraries.

Origo nucleotide name	Target gene	Primer sequence (5' → 3')	Cycling conditions	Reference(s)
Illumina_16S_341F	16S rRNA	CCTACGGGNGGCWGCAG	95℃ for 3 min, 35 cycles of 95℃ for 30 sec, 55℃ for 30 sec, 72℃ for 30 sec, and 72℃ for 5 min	(*97*, *98*)
Illumina_16S_805R		GACTACHVGGGTATCTAATCC		
TAReuk454FWD1	18S rRNA	CCAGCASCYGCGGTAATTCC	95 °C for 3 min, 35 cycles of 98 °C for 30 sec, 50 °C for 30 sec, 72 °C for 30 sec, and 72°C for 10 min	(*69*)
TAReukREV3		ACTTTCGTTCTTGATYRA		
TickB_PNA	18S rRNA	GATCAAWGAAAACATT	NA	This study

NA, not applicable.

TickB_PNA. The PCR products were purified with the Agencourt AMPure XP Kit. The purified products were indexed with the Nextera XT Kit. The index PCR products were purified with NucleoMag NGS Clean-up and Size Select to extract the DNA fragments between 150 bp and 800 bp. The length of the final products was analyzed using the Agilent 2100 Bioanalyzer System. The libraries were pooled and sequenced on the Illumina MiSeq system using the MiSeq Reagent Kit v3 (600 cycles).

2.5. Data processing, taxonomy annotation, and diversity analyses

The raw fastq data were obtained through BaseSpace system (Illumina). The data was processed using the QIIME2 (version 2024.5) (*70*). The raw reads were demultiplexed and quality-checked, and denoised with the DADA2 plugin (*71*) to generate the amplicon sequence variants (ASVs). The potential contaminants were identified in R (version 4.4.1) using the package Decontam (*72*) with a threshold of 0.1. The ASVs determined as contaminants were removed from the downstream analyses. The ASVs were annotated with taxonomic information using q2-feature-classifier plugin with Naive Bayes classifier trained on the SILVA database at 99% sequence similarity in QIIME2. From the 16S rRNA gene amplicon sequencing data, ASVs classified as archaea, eukaryote, unassigned, and unassigned bacterial sequences were removed. From the 18S rRNA gene amplicon sequencing data, ASVs classified as archaea, bacteria, vertebrata, unassigned, and unassigned eukaryotic sequences were removed. The composition of microbial taxa was visualized in R with the package fantaxtic (*99*). The alpha-diversity and beta-diversity analyses were performed and visualized in R using the packages qiime2r (*73*), phyloseq (*74*), and vegan (*100*). Shannon indices were calculated to evaluate the alpha-diversity, reflecting species richness within the samples. The beta-diversity analyses were performed based on the Bray-Curtis distance at the ASV level to determine the differences and similarities among samples. The beta-diversity results were visualized using Principal Coordinates Analysis (PCoA) and Non-Metric Multidimensional Scaling (NMDS).

2.6. Co-occurrence analysis

Co-occurrence analysis was performed in R with the package SPIEC-EASI (*101*). The SPIEC-EASI is suitable to determine co-occurring taxa in compositional data, and applicable for multiple domain analysis. The network analyses were performed based only on bacterial composition, and based on both bacterial and eukaryotic compositions. The network analyses were performed independently for each tick species. The samples and ASVs were filtered based on the previously proposed guidelines (*102*). In brief, the samples without saturation on the rarefaction curve were removed. The ASVs were combined at the genus level with tax_glom function in the package phyloseq to avoid false-positive due to intra-species variations. The ASVs appear only in one sample is removed. The co-occurrence analysis was performed using the spiec.easi function with the Meinshausen and Bühlmann (mb)

method with nlamda = 20, lambda.min.ratio = 1e-2, pulsar.params = list(rep.num = 50). The co-occurrence network was visualized using the package igraph (*103*) and the software Cytoscape version 3.10.3 (*104*). To determine the keystone taxa in the cross-domain network, the eigenvector centrality scores were calculated in Cytoscape. Eigenvector centrality is based on the principle that a node in a network is more central if it is connected to other important nodes. It is calculated as the weighted sum of the centralities of the correlated nodes.

3. Results

3.1. The result of the data filtering

For the 16S amplicon sequencing, a total of 8,997,695 reads (48,900 for average, 48,498 for median, and ranging from 2,714 to 148,104) belonged to 3,207 ASVs were obtained after the filtering (Table I - 1). The sampling depth of all the samples were determined to be saturated based on the alpha-rarefaction analysis.

For the 18S rRNA gene amplicon sequencing, a total of 440,393 reads ranging from 0 to 60,353 per sample (average = 2433; median = 592) were obtained after quality filtering, resulting in 1,699 ASVs (Table I - 1). Based on the sampling depth evaluated by alpha-rarefaction analysis, the 17 samples determined to not be saturated were excluded from the downstream analysis. Finally, a total of 167 samples were included in the following analysis.

3.2. Composition of detected bacterial microorganisms in the tested ticks

In all the samples, 3,207 ASVs belonging to 20 phyla, 44 classes, 108 orders, 174 families, and 361 genera were detected. The most abundant taxa were *Coxiella* (Coxiellales) in *H. flava, H. longicornis* and *I. ovatus,* and *Candidatus* Lariskella (Rickettsiales) in *I. persulcatus* (Table II - 4, Figure II - 3, and Figure II - 4). The genera known to include the endosymbionts of the ticks were detected at high relative abundance, including *Coxiella*, *Rickettsia*, and *Spiroplasma*. Several genera known to include tick-borne pathogens were also detected. *Anaplasma* was detected in two *H. flava* and one *H. longicornis*. *Borreliela* (*Borrelia*) was detected in 13 *I. ovatus* and 11 *I. persulcatus. Rickettsia* was detected in seven *H. flava*, 25 *H. longicornis*, three *I. ovatus*, and 11 *I. persulcatus*. *Ehrlichia* was detected in four *I. ovatus* and one *H. longicornis.*

Beta-diversity analyses were performed by applying the Bray-Curtis metrics (Figure II - 5). Based on NMDS and PCoA, 16S rRNA data showed that microbiome of ticks clustered based on the tick species instead of the tick sex or the sampling region

.

3.3. Composition of detected eukaryotic microorganisms in the tested ticks

In all the samples, 1,699 ASVs belonging to 26 phyla, 48 classes, 91 orders, 125 families, and 145

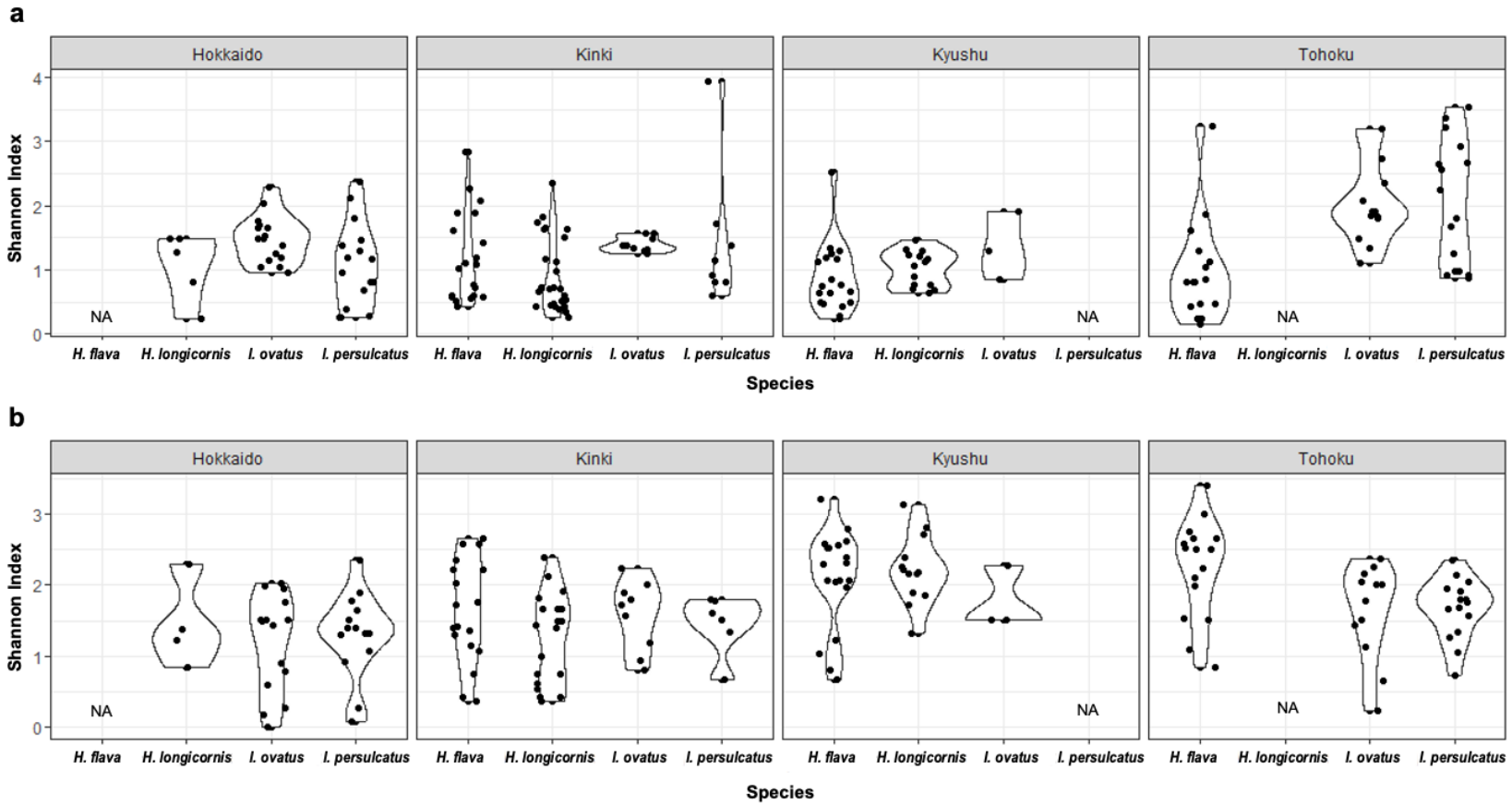

Figure II - 2: Alpha-diversity metrices of the 16S and 18S rRNA gene amplicon sequencing obtained in each species and region.

Shannon index was calculated based on the 16S (a) and 18S (b) rRNA gene amplicon sequencing. NA indicates no samples were included in the analysis.

Table II - 4: The top 10 most abundant bacterial taxa at the genus level detected in the each tick species.

Rank	*H. flava*	*H. longicornis*	*I. ovatus*	*I. persulcatus*
1	*Coxiella* (Proteobacteria, 84.47%)	*Coxiella* (Proteobacteria, 84.6%)	*Coxiella* (Proteobacteria, 63.56%)	Candidatus *Lariskella* (Proteobacteria, 35.43%)
2	*Methylobacterium-Methylorubrum* (Proteobacteria, 4.51%)	*Rickettsia* (Proteobacteria, 4.44%)	*Spiroplasma* (Firmicutes, 28.83%)	*Spiroplasma* (Firmicutes, 11.34%)
3	*Mycobacterium* (Actinobacteriota, 3.26%)	*Methylobacterium-Methylorubrum* (Proteobacteria, 4.14%)	*Rickettsiella* (Proteobacteria, 1.93%)	*Rickettsia* (Proteobacteria, 10.22%)
4	*Williamsia* (Actinobacteriota, 1.45%)	*Mycobacterium* (Actinobacteriota, 1.95%)	*Rickettsia* (Proteobacteria, 1.79%)	*Bosea* (Proteobacteria, 6.41%)
5	*Sphingomonas* (Proteobacteria, 0.82%)	*Burkholderia-Caballeronia-Paraburkholderia* (Proteobacteria, 0.74%)	*Ehrlichia* (Proteobacteria, 0.92%)	*Borreliella* (Spirochaetota, 5.61%)
6	*Burkholderia-Caballeronia-Paraburkholderia* (Proteobacteria, 0.76%)	*Pseudomonas* (Proteobacteria, 0.61%)	*Pseudomonas* (Proteobacteria, 0.92%)	*Methylobacterium-Methylorubrum* (Proteobacteria, 4.79%)
7	*Pseudomonas* (Proteobacteria, 0.72%)	*Williamsia* (Actinobacteriota, 0.55%)	*Bosea* (Proteobacteria, 0.49%)	*Pseudomonas* (Proteobacteria, 3.97%)
8	*Anaplasma* (Proteobacteria, 0.51%)	*Luteibacter* (Proteobacteria, 0.29%)	*Rhodococcus* (Actinobacteriota, 0.32%)	*Mycobacterium* (Actinobacteriota, 2.91%)
9	*Stenotrophomonas* (Proteobacteria, 0.49%)	*Ehrlichia* (Proteobacteria, 0.28%)	*Borreliella* (Spirochaetota, 0.2%)	*Aquabacterium* (Proteobacteria, 1.58%)
10	*Pseudonocardia* (Actinobacteriota, 0.24%)	*Sphingomonas* (Proteobacteria, 0.24%)	*Mycobacterium* (Actinobacteriota, 0.16%)	*Staphylococcus* (Firmicutes, 1.35%)

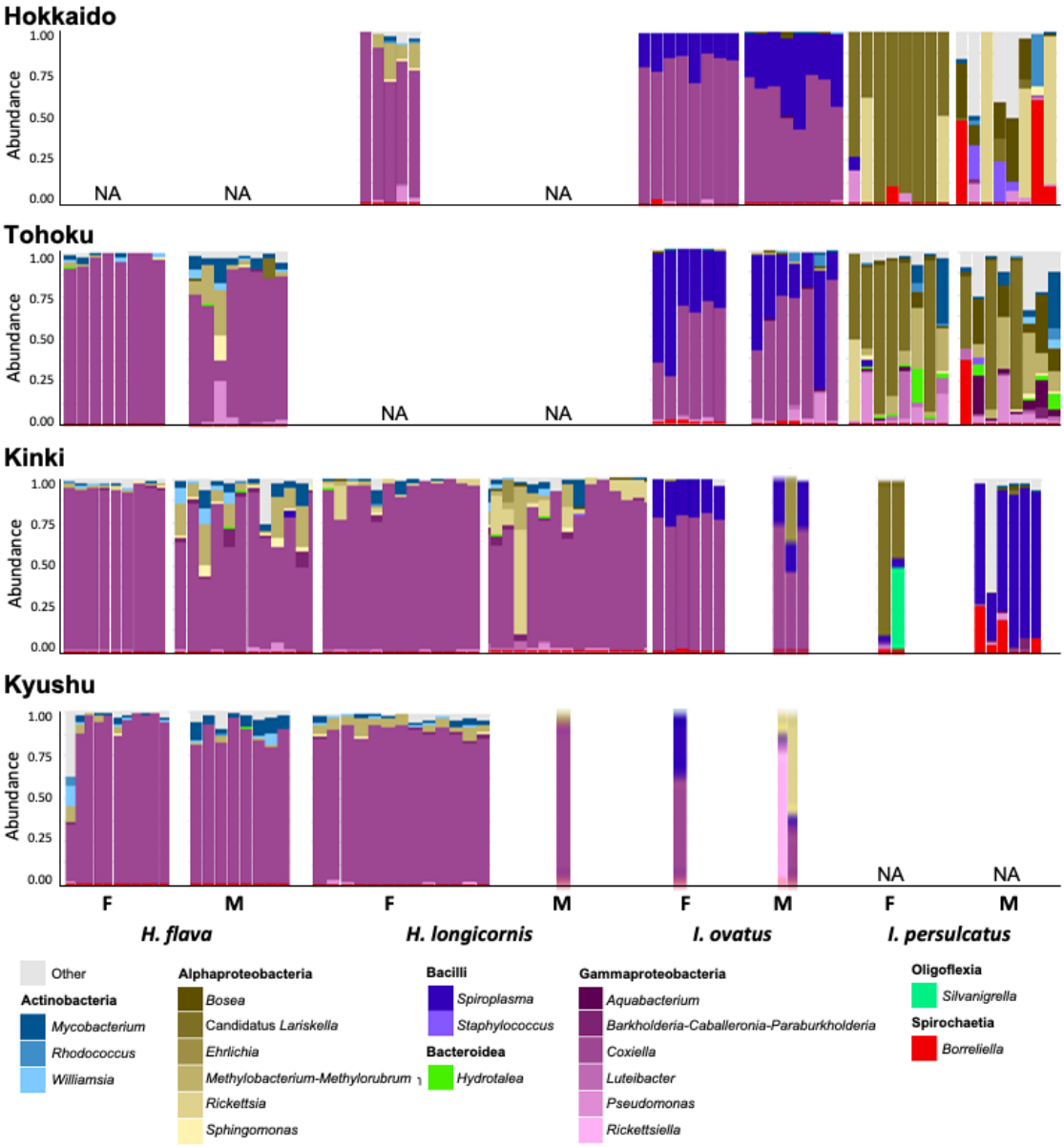

Figure II - 3: Relative abundances of the bacterial taxa detected by the 16S rRNA gene amplicon sequencing.

Each bar represents the relative abundances of the detected taxa in each tick sample. Each color represents the genus of the detected bacterial taxa.

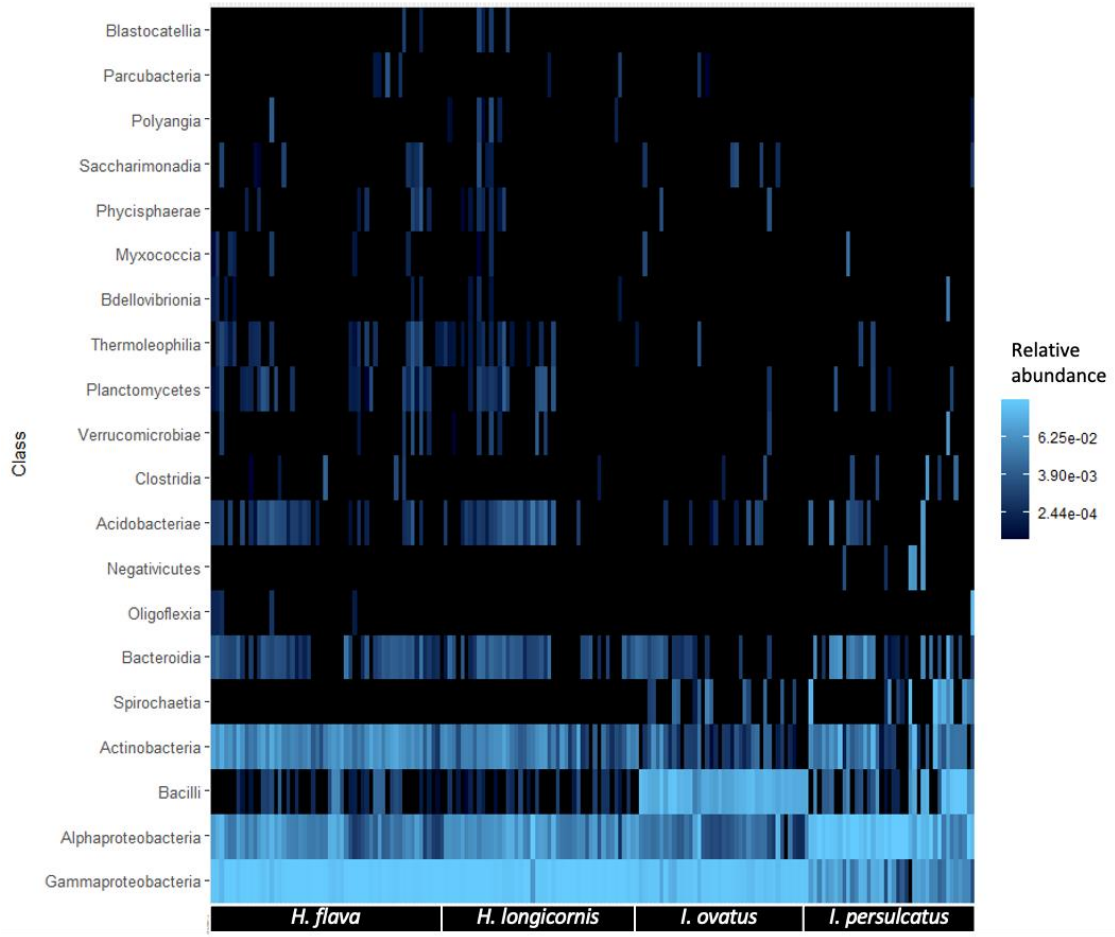

Figure II - 4: A heat map of the 20 most abundant bacterial taxa at the class level by the 16S rRNA gene amplicon sequencing.

Tiles indicate the detected taxa in a sample. Tile color represents the relative abundances. The tick species are represented below the panel. The detected bacterial taxa are indicated on the left at the class level.

genera were detected. The most abundant taxa and their average relative abundances were represented in Table II - 4. At the phylum level, Cnidaria, Ascomycota, Apicomplexa, Basidiomycota, Chlorophyta, Cercozoa, Phragmoplastophyta, Ochrophyta, Ciliophora, and Nematozoa were the most abundant (Figure II - 7). At the genus level, the most abundant taxa were unclassified Bivalvulida (Cnidaria) in all the tick species, *H. flava*, *H. longicornis*, *I. ovatus*, and *I. persulcatus* (Figure II - 6, Table II - 5). The potential insect parasites, Gregarina, D3P05A02, and Stenophora (Eugregarinorida, Apicomplexa) were detected in all the tick species. Several genera known to include tick-borne pathogens were also detected (Figure II - 6). *Babesia* were detected in a *H. longicornis*, six *I. ovatus*, and a *I. persulcatus*. *Hepatozoon* was detected in a *H. longicornis*. *Theileria* were detected in a *H. flava*, and five *H. longicornis*.

Based on the beta-diversity analysis by PCoA, 18S rRNA data did not show clear clustering neither based on species, sex, and regions (Figure II - 5). In addition, it was not possible to perform NMDS on 18S rRNA gene amplicon data due to insufficient number of ASVs.

3.4. Cross-domain network analysis and determination of keystone taxa

The co-occurrence networks were analyzed based on only 16S amplicon sequencing data (bacterial microbiome network) and based on both 16S and 18S amplicon sequencing data (cross-domain microbiome network). Since the beta-diversity analysis showed that the bacterial microbiome clustered by species (Figure II - 5), the network analyses were performed by each species separately to reduce the bias of habitat filtering. After the ASV and the sample filtering, a total of 36 *H. longicornis* samples with 33 eukaryotic and 133 bacterial taxa and, 54 *H. flava* samples with 57 eukaryotic and 152 bacterial taxa were finally included in the analysis (Table II - 6). *Ixodes ovatus* and *I. persulcatus* were not included for the network analysis due to only small number of the ASVs (8 and 24, respectively) were kept after quality filtering.

In the microbiome networks in *H. flava*, a total of 136 or 207 nodes were included in bacterial and cross-domain networks, respectively (Table II - 6). Fourteen components of the networks were detected in the bacterial network, while the cross-domain network was constructed as a single component (Table II - 6, Figure II - 8, and Figure II - 9). The six bacterial taxa, *Ferruginibacter*, Uncultured *Gammataceae*, *Parafilimonas*, *Aquispfaera*, *Noyosphingobium*, and *Tepidisphaera* were detected within the 10 taxa with the highest eigenvector centrality ins both bacterial and cross-domain network (Table II - 7 and Table II - 8). In the cross-domain network, *Bromeliothrix* (Family Colpodea; Phylum Ciliophora) was indicated as one of the highest 10 eigenvector centrality nodes.

In the microbiome networks in *H. longicornis*, a total of 137 or 165 nodes were included in bacterial and cross-domain networks, respectively (Table II - 6). Two network components were detected in the bacterial network, while the cross-domain network was constructed as a single component. Regarding the 10 taxa with the highest eigenvector centrality, none of the bacterial taxa were common between

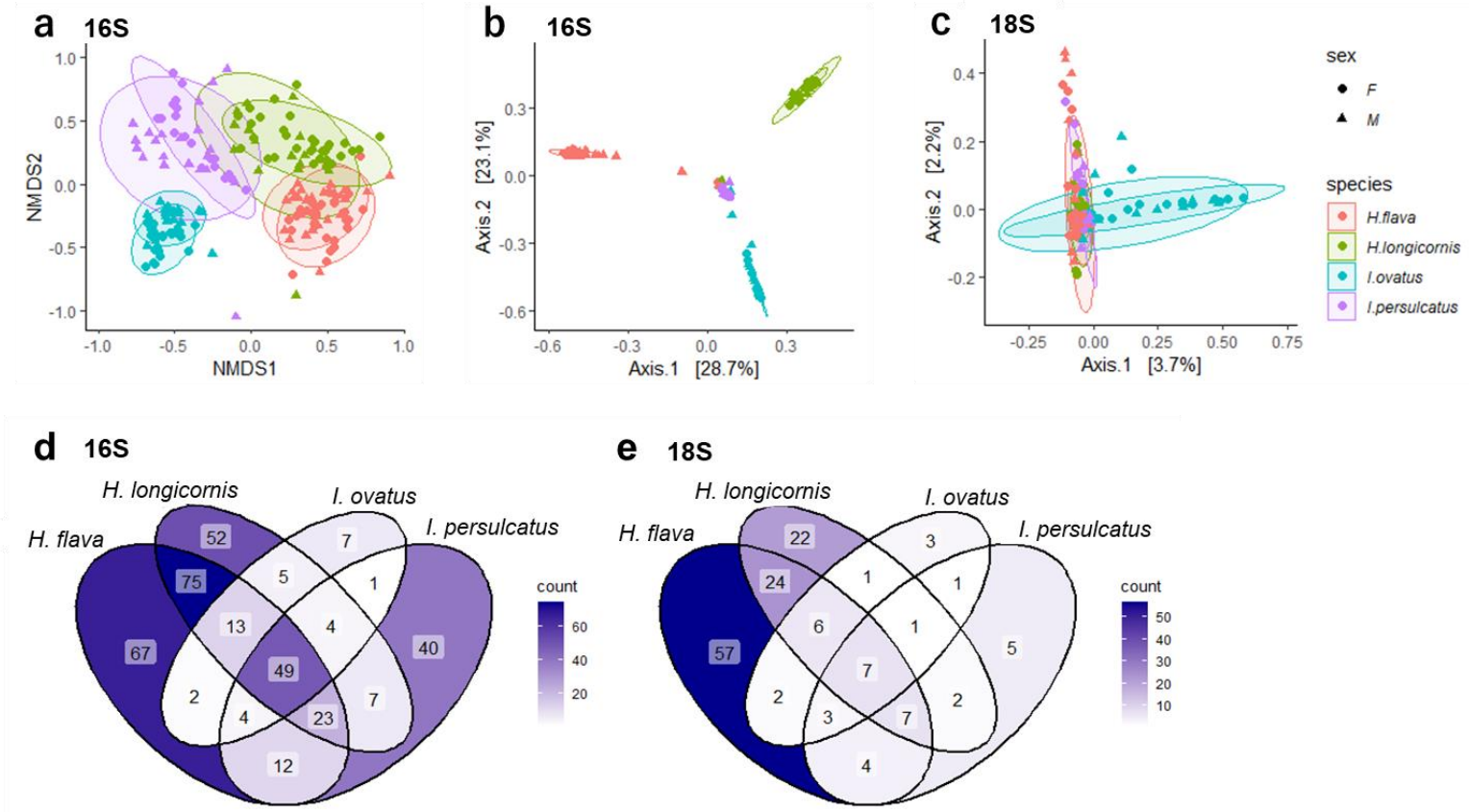

Figure II - 5: Beta diversity analyses based on the 16S and 18S rRNA gene amplicon sequencing.

NMDS based on the 16S amplicon sequencing (a), PCoA based on the 16S (b) or 18S (c) amplicon sequencing, Venn diagrams representing the shared bacterial (d) or eukaryotic (e) genus among the species observed in the amplicon sequencing.

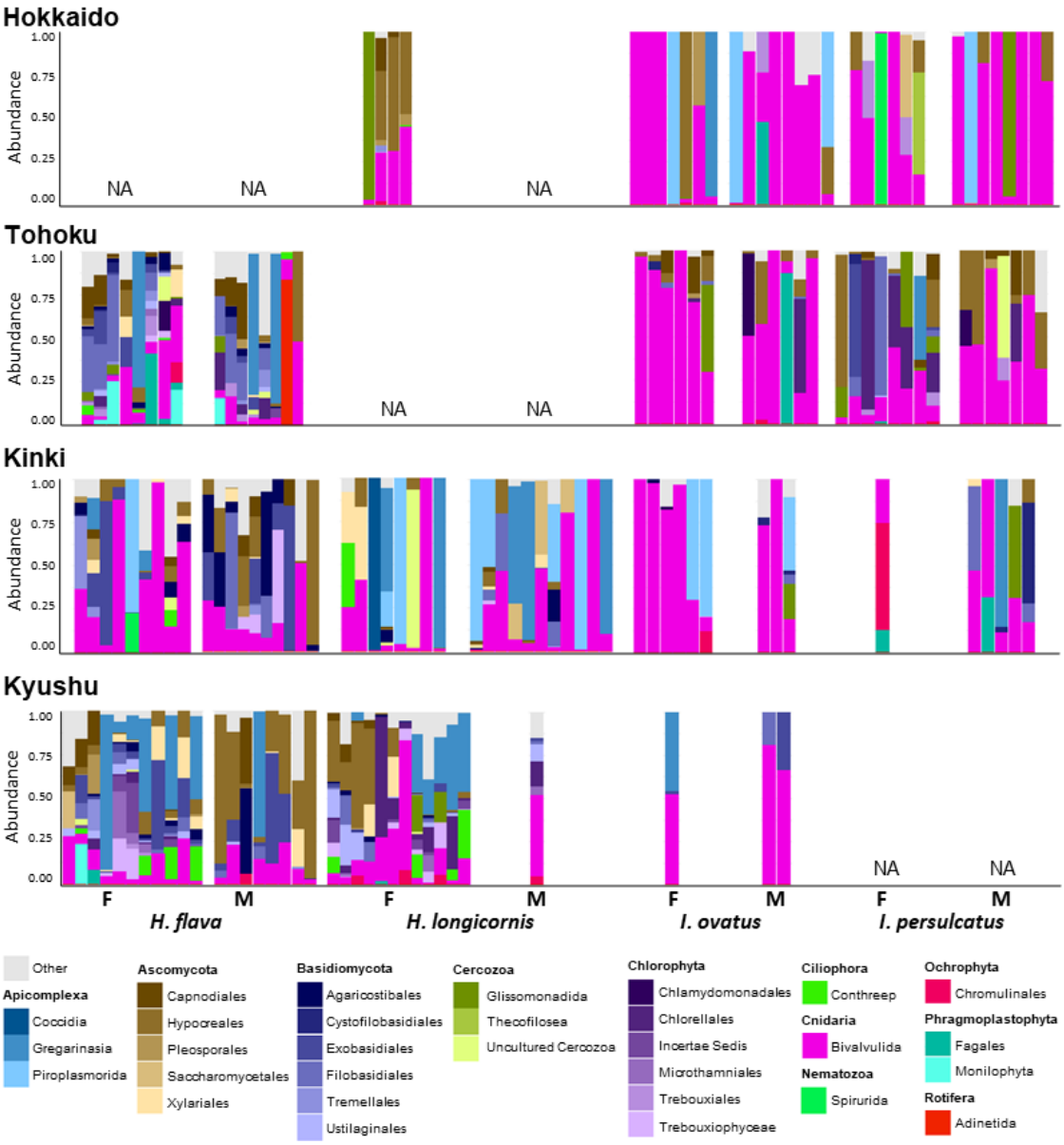

Figure II - 6: Relative abundances of the eukaryotic tasxa detected by the 18S rRNA gene amplicon sequencing.

Each bar represents the relative abundances of the detected taxa in each tick sample. Each color represents the order of the detected eukaryotic taxa.

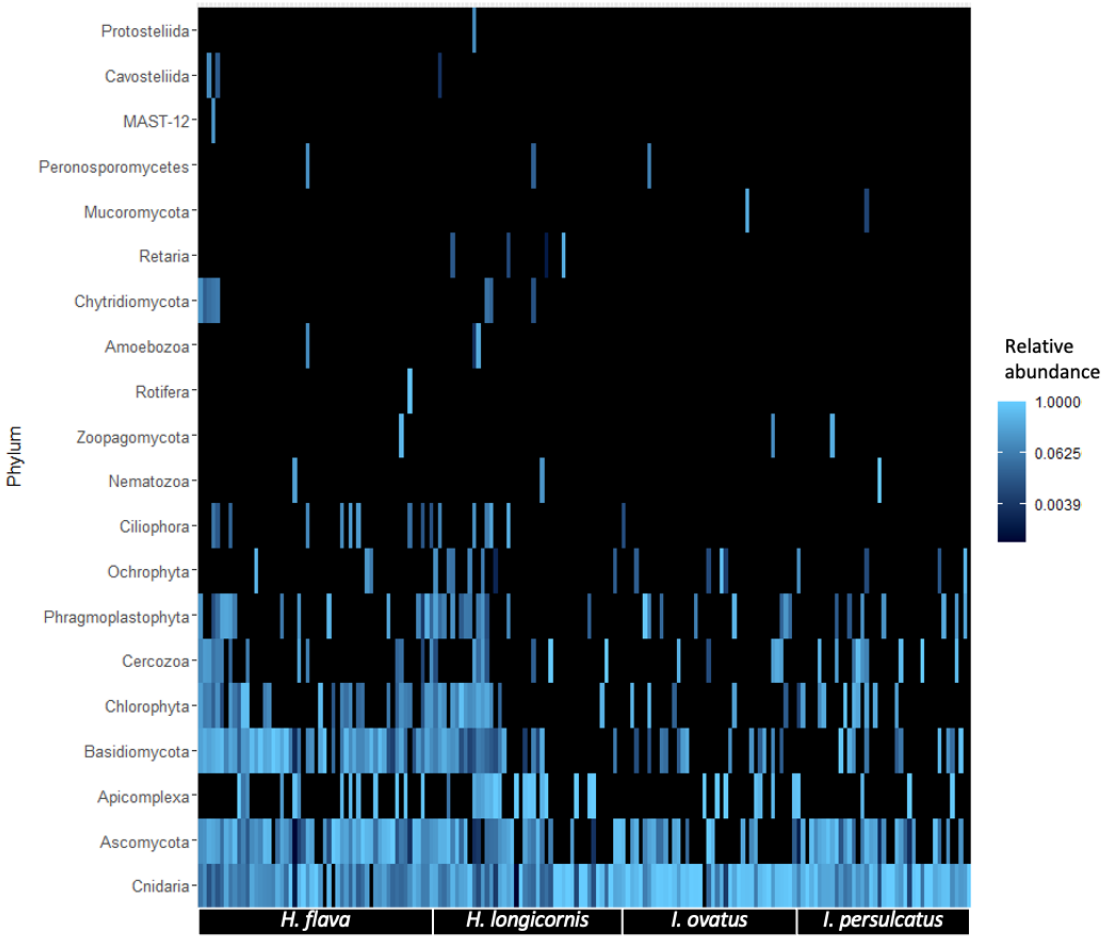

Figure II - 7: A heat map of the 20 most abundant eukaryotic taxa at the phylum level by the 18S rRNA gene amplicon sequencing.

Tiles indicate the detected taxa in a sample. Tile color represents the relative abundances. The tick species are represented below the panel. The detected eukaryotic taxa are indicated on the left at the phylum level.

Table II - 5: The top 10 most abundant eukaryotic taxa at the genus level detected in each tick species.

Rank	*H. flava*	*H. longicornis*	*I. ovatus*	*I. persulcatus*
1	Bivalvulida (Cnidaria, 24.52%)	Bivalvulida (Cnidaria, 32.57%)	Bivalvulida (Cnidaria, 69.87%)	Bivalvulida (Cnidaria, 52.45%)
2	*Gregarina* (Apicomplexa, 7.75%)	*Gregarina* (Apicomplexa, 13.58%)	*Babesia* (Apicomplexa, 12.36%)	*Heteromita* (Cercozoa, 8.47%)
3	Piskurozyma (Basidiomycota, 5.16%)	*Theileria* (Apicomplexa, 8.86%)	*Paraschneideria* (Apicomplexa, 2.44%)	*Chloroidium* (Chlorophyta, 6.71%)
4	*Exobasidiales* (Basidiomycota, 5.14%)	*Chloroidium* (Chlorophyta, 5%)	*Heteromita* (Cercozoa, 2.07%)	*Babesia* (Apicomplexa, 2.83%)
5	*Exobasidium* (Basidiomycota, 3.77%)	*Heteromita* (Cercozoa, 3.3%)	*Chloroidium* (Chlorophyta, 1.59%)	Spirurida (Nematozoa, 2.83%)
6	Brachybasidiaceae (Basidiomycota, 3.29%)	uncultured* (Cercozoa, 2.85%)	*Acremonium* (Ascomycota, 1.29%)	*Piskurozyma* (Basidiomycota, 2.72%)
7	Trebouxiophyceae (Chlorophyta, 2.62%)	*Hepatozoon* (Apicomplexa, 2.78%)	Chloromonas (Chlorophyta, 1.28%)	*Trebouxia* (Chlorophyta, 2.56%)
8	*Fusarium* (Ascomycota, 2.11%)	*Babesia* (Apicomplexa, 2.76%)	*Gregarina* (Apicomplexa, 1.18%)	*Mrakia* (Basidiomycota, 2.49%)
9	*Pestalotiopsis* (Ascomycota, 2.09%)	D3P05A02 (Apicomplexa, 2.51%)	*Trebouxia* (Chlorophyta, 1.17%)	Eugregarinorida (Apicomplexa, 2.44%)
10	*Kurtzmanomyces* (Basidiomycota, 2.03%)	*Stenophora* (Apicomplexa, 1.87%)	*Arthopyrenia* (Ascomycota, 1.09%)	*Exobasidium* (Basidiomycota, 2.13%)

In case of the ASVs which were not identified at genus level, the lowest taxon name was presented (e.g. Bivalvulida).

* "uncultured" indicates that the reference sequences were derived from uncultured samples and the taxonomy placement of that is undefined.

Table II - 6: The topologies of the bacterial and cross-domain microbiome networks of *Haemaphysalis flava* and *Haemaphysalis longicornis.*

	H. flava		***H. longicornis***	
	Bacterial network	**Cross domain network**	**Bacterial network**	**Cross domain network**
Number of analyzed bacterial taxa	152	152	137	133
Number of analyzed eukaryotic taxa	0	57	0	33
Number of included tick samples	54	54	36	36
Number of nodes	136	207	137	165
Number of edges	150	404	185	230
Average number of neighbors	2.568	3.903	2.726	2.788
Network diameter	16	10	17	16
Network radius	8	6	9	8
Characteristic path length	5.985	4.446	6.641	6.021
Clustering coefficient	0.126	0.116	0.092	0.077
Network density	0.032	0.019	0.02	0.017
Network heterogeity	0.547	0.479	0.476	0.482
Network centralization	0.07	0.03	0.04	0.032
Connected components	14	1	2	1

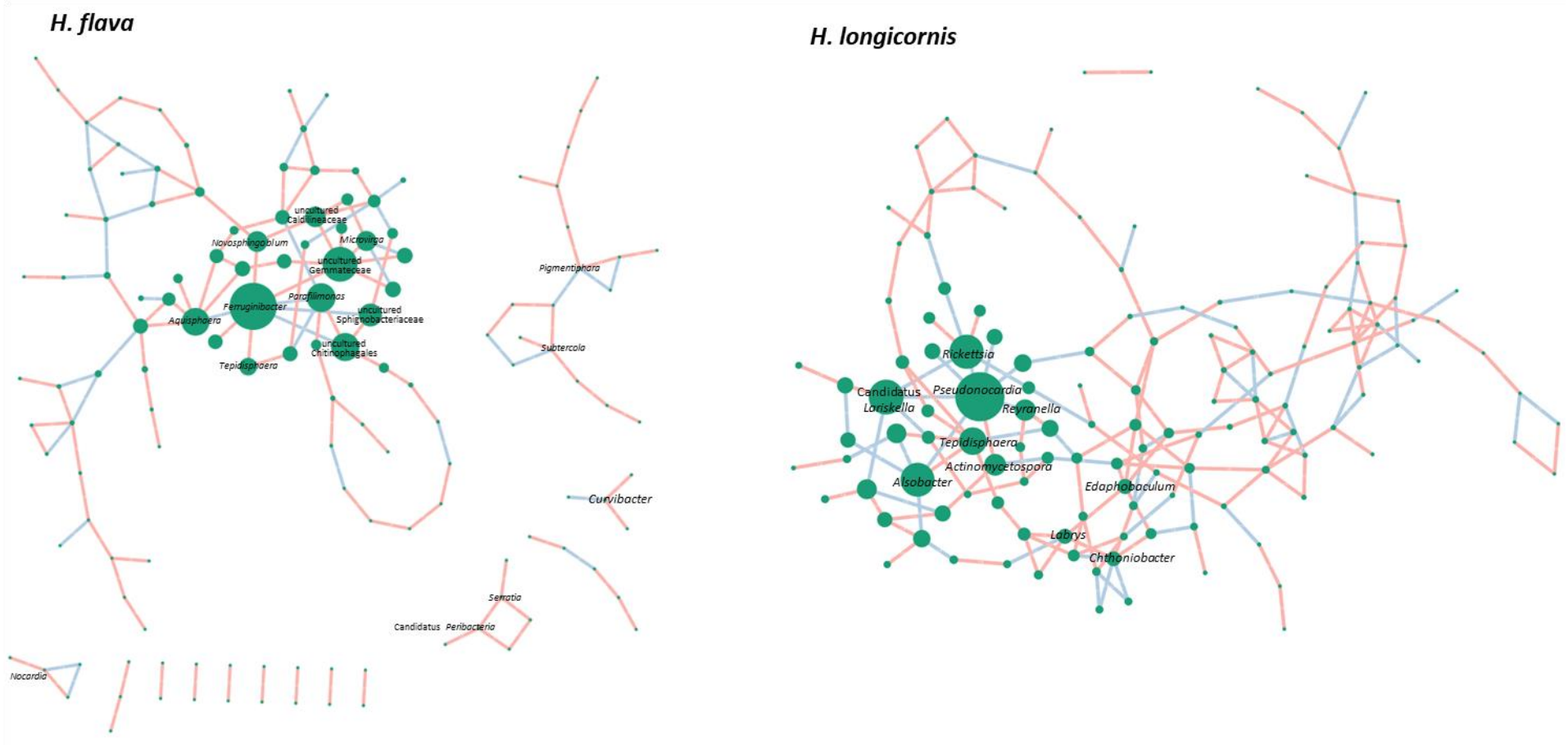

Figure II - 8: The bacterial microbiome networks of *Haemaphysalis flava* and *Haemaphysalis longicornis* based on the 16S amplicon sequencing.

Node size represents its eigenvector centrality. The node colors, purple and green, represent eukaryotic and bacterial taxa, respectively. The red and blue edges represent positive and negative interaction, respectively.

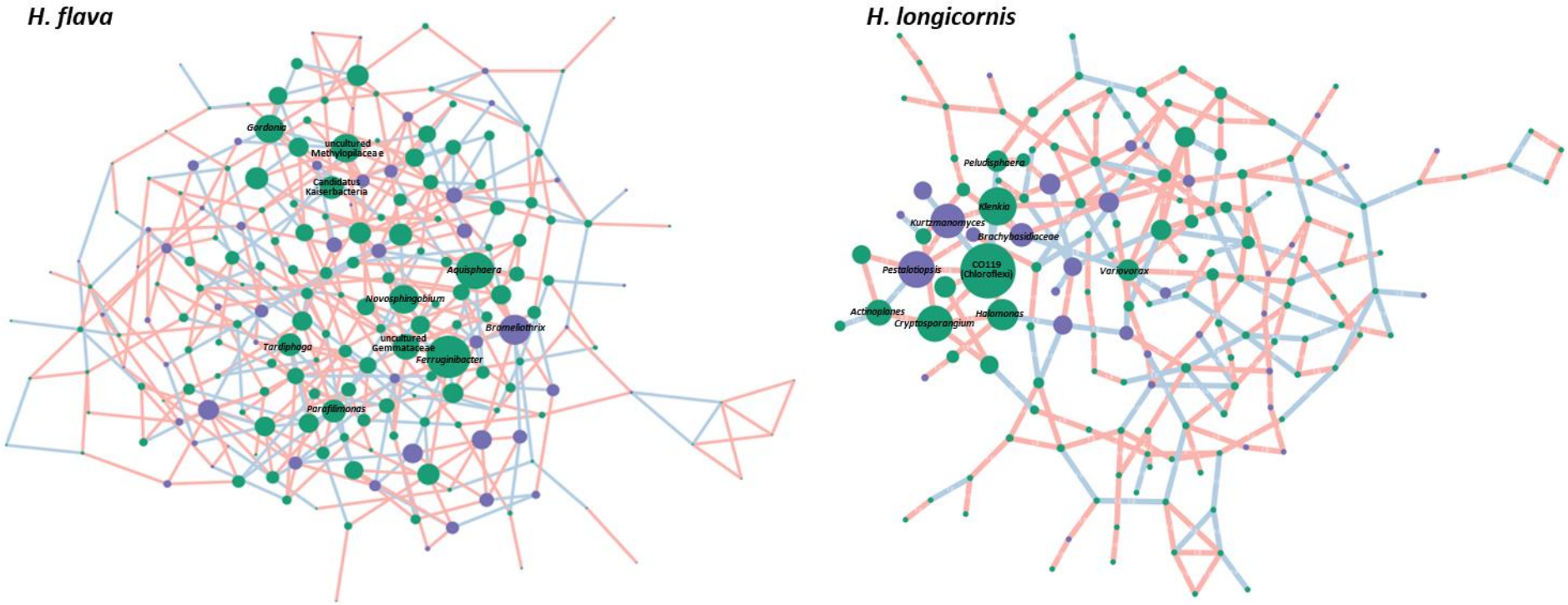

Figure II - 9: The cross-domain microbiome networks of *Haemaphysalis flava* and *Haemaphysalis longicornis* based on the 16S and 18S amplicon sequencing.

The node size represents its eigenvector centrality. The node colors, purple and green, represent eukaryotic and bacterial taxa, respectively. The red and blue edges represent positive and negative interaction, respectively.

Table II - 7: The taxa determined with the highest eigenvector centrality indices in the bacterial microbiome network in *Haemaphysalis flava.*

Rank	Phylum	Class	Order	Family	Genus	Eigenvector centrality	Degree	Betweenness centrality
1	Bacteroidota	Bacteroidia	Chitinophagales	Chitinophagaceae	*Ferruginibacter*	0.478	8	0.500
2	Planctomycetota	Planctomycetes	Gemmatales	Gemmataceae	uncultured*	0.348	7	0.132
3	Bacteroidota	Bacteroidia	Chitinophagales	Chitinophagaceae	*Parafilimonas*	0.277	5	0.262
4	Bacteroidota	Bacteroidia	Chitinophagales	Chitinophagaceae	Uncultured*	0.270	4	0.124
5	Planctomycetota	Planctomycetes	Isosphaerales	Isosphaeraceae	*Aquisphaera*	0.269	6	0.375
6	Bacteroidota	Bacteroidia	Sphingobacteriales	Sphingobacteriaceae	Uncultured*	0.215	3	0.030
7	Proteobacteria	Alphaproteobacteria	Sphingomonadales	Sphingomonadaceae	*Novosphingobium*	0.192	3	0.198
8	Chloroflexi	Anaerolineae	Caldilineales	Caldilineaceae	Uncultured*	0.191	4	0.087
9	Proteobacteria	Alphaproteobacteria	Rhizobiales	Beijerinckiaceae	*Microvirga*	0.186	4	0.006
10	Planctomycetota	Phycisphaerae	Tepidisphaerales	Tepidisphaeraceae	*Tepidisphaera*	0.156	2	0.012

* "Uncultured" indicates that the reference sequences were derived from uncultured samples and the taxonomy placement of that is undefined.

Table II - 8: The taxa determined with the highest eigenvector centrality indices in the cross-domain microbial network in *Haemaphysalis flava.*

Rank	Kingdom	Phylum	Class	Order	Family	Genus	Eigenvector centrality	Degree	Betweenness centrality
1	Bacteria	Bacteroidota	Bacteroidia	Chitinophagales	Chitinophagaceae	*Ferruginibacter*	0.265	10	0.099
2	Bacteria	Planctomycetota	Planctomycetes	Isosphaerales	Isosphaeraceae	*Aquisphaera*	0.229	10	0.093
3	Eukaryota	Ciliophora	Intramacronucleata	Conthreep	Colpodea	*Bromeliothrix*	0.185	8	0.051
4	Bacteria	Proteobacteria	Alphaproteobacteria	Sphingomonadales	Sphingomonadaceae	*Novosphingobium*	0.176	6	0.051
5	Bacteria	Proteobacteria	Alphaproteobacteria	Rhizobiales	Methylopilaceae	Uncultured*	0.175	9	0.051
6	Bacteria	Actinobacteriota	Actinobacteria	Corynebacteriales	Nocardiaceae	*Gordonia*	0.173	8	0.036
7	Bacteria	Planctomycetota	Planctomycetes	Gemmatales	Gemmataceae	Uncultured*	0.156	9	0.058
8	Bacteria	Patescibacteria	Parcubacteria	Candidatus Kaiserbacteria	Candidatus Kaiserbacteria	Candidatus *Kaiserbacteria*	0.139	6	0.071
9	Bacteria	Bacteroidota	Bacteroidia	Chitinophagales	Chitinophagaceae	*Parafilimonas*	0.139	6	0.025
10	Bacteria	Proteobacteria	Alphaproteobacteria	Rhizobiales	Xanthobacteraceae	*Tardiphaga*	0.138	9	0.058

* "Uncultured" indicates that the reference sequences were derived from uncultured samples and the taxonomy placement of that is undefined.

the bacterial and cross-domain networks (Table II - 9, Table II - 10). In the cross-domain network, three taxa, *Pastalotiopsis* (Family Sporocadaceae; Phylum Ascomycota), *Kutzmanomyces* (Family Chionosphaeraceae; Phylum Basidiomycota), and unclassified Brachybasidiaceae (Phylum Basidicomycota), were included in the highest 10 eigenvector centrality nodes (Table II - 10).

4. Discussion

This study presents the first comprehensive catalog of the eukaryotic composition of the tick microbiome. In addition, this is the first microbiome network analyses incorporating eukaryotic communities in ticks. In the cross-domain networks, eukaryotic microbes with high eigenvector centrality were identified in both *H. flava* and *H. longicornis*. A comparison between the bacterial and cross-domain networks determined distinct keystone taxa for *H. flava* and *H. longicornis*. Additionally, in *H. flava*, 14 components of the bacterial microbiome network were integrated into a single component in the cross-domain network. The identification of eukaryotic taxa as keystone members highlights the importance of including multiple domains in microbiome network analyses of ticks.

Among the keystone eukaryotic taxa, *Kurtzmanomyces* (Agaricostilbomycetes: Basidiomycota) and unclassified Brachybasidiaceae (Basidiomycota) were relatively abundant, while *Pestalotiopsis* (Sordariomycetes: Ascomycota), *Bromeliothrix* (Intramacronucleata, Conthreep, Colpodea, and Ciliophora), were not included. These observations indicate that the low abundant taxa in the microbiome potentially act as keystone. Sordariomycetes species distribute to the environment and also act as insect pathogens. A report presented that *Metarhizium flavoviride* (Sordariomycetes: Hypocreales) exposure changed the midgut microbiome of *Nilaparvata lugens* (Hemiptera: Delphacidae) (*105*). The unclassified Trebouxiophyceae (Chlorophyta) and *Trebouxia* (Trebouxyophyceae: Chlorophyta) were also detected at relatively high abundance. The class Trebouxiophyceae includes free-living group, plant-symbiotic group, fungi-symbiotic group and arthropod parasitic group (*106*, *107*). These two taxa, Hypocreales and Trebouxiophyceae need to be investigated from the point of view of tick-pathogen or tick-symbiotic microbes. Other taxa determined as keystone, *Bromeliothrix* have been reported to be free-living (*108*), and *Pestalotiopsis*, *Kutzmanomyces*, and Brachybasidiaceae have been reported to be plant-pathogen (*109*). These observations also need to be clarified with other molecular and isolation techniques.

Among the detected taxa, Nematozoa and Hypocreales (phylum Ascomycota) were previously found from ticks. Filarial parasites have been detected molecularly and under microscope from ticks (*34*, *110*, *111*). For Hypocreales, *Metarhizium* sp. was reported to kill *Argas persicus*, and Hypocreales fungi are known to infect other insect as well (*112*, *113*). These microeukaryote groups seem to be ubiquitous even in healthy questing ticks, because this study was performed with the ticks collected by flagging. Fundamental research about classification, distribution, and host range are needed to

Table II - 9: The taxa determined with the highest eigenvector centrality indices in the bacterial microbiome network in *Haemaphysalis longicornis.*

Rank	Phylum	Class	Order	Family	Genus	Eigenvector centrality	Degree	Betweenness centrality
1	Actinobacteriota	Actinobacteria	Pseudonocardiales	Pseudonocardiaceae	*Pseudonocardia*	0.374	8	0.166
2	Proteobacteria	Alphaproteobacteria	Rhizobiales	Rhizobiales Incertae Sedis*	*Alsobacter*	0.256	5	0.074
3	Proteobacteria	Alphaproteobacteria	Rickettsiales	Fokiniaceae	Candidatus *Lariskella*	0.253	5	0.054
4	Proteobacteria	Alphaproteobacteria	Rickettsiales	Rickettsiaceae	*Rickettsia*	0.247	6	0.124
5	Planctomycetota	Phycisphaerae	Tepidisphaerales	Tepidisphaeraceae	*Tepidisphaera*	0.216	6	0.104
6	Verrucomicrobiota	Verrucomicrobiae	Chthoniobacterales	Chthoniobacteraceae	*Chthoniobacter*	0.202	6	0.047
7	Proteobacteria	Alphaproteobacteria	Rhizobiales	Labraceae	*Labrys*	0.197	5	0.068
8	Bacteroidota	Bacteroidia	Chitinophagales	Chitinophagaceae	*Edaphobaculum*	0.192	5	0.095
9	Actinobacteriota	Actinobacteria	Pseudonocardiales	Pseudonocardiaceae	*Actinomycetospora*	0.154	3	0.092
10	Proteobacteria	Alphaproteobacteria	Reyranellales	Reyranellaceae	*Reyranella*	0.150	3	0.022

* Incertae_Sedis indicates that the taxonomy placement of the reference sequences is undefined.

Table II - 10: The taxa determined with the highest eigenvector centrality indices in the cross-domain microbial network in *Haemaphysalis longicornis.*

Rank	Kingdom	Phylum	Class	Order	Family	Genus	Eigenvector centrality	Degree	Betweenness centrality
1	Bacteria	Chloroflexi	Ktedonobacteria	C0119	NA*	NA*	0.460	8	0.076
2	Bacteria	Actinobacteriota	Actinobacteria	Frankiales	Geodermatophilaceae	*Klenkia*	0.301	5	0.054
3	Eukaryota	Ascomycota	Sordariomycetes	Xylariales	Sporocadaceae	*Pestalotiopsis*	0.288	5	0.034
4	Bacteria	Actinobacteriota	Actinobacteria	Frankiales	Cryptosporangiaceae	*Cryptosporangium*	0.283	5	0.059
5	Eukaryota	Basidiomycota	Agaricostilbomycetes	Agaricostilbales	Chionosphaeraceae	*Kurtzmanomyces*	0.269	3	0.007
6	Bacteria	Proteobacteria	Gammaproteobacteria	Pseudomonadales	Halomonadaceae	*Halomonas*	0.239	4	0.084
7	Bacteria	Actinobacteriota	Actinobacteria	Micromonosporales	Micromonosporaceae	*Actinoplanes*	0.190	4	0.017
8	Eukaryota	Basidiomycota	Exobasidiomycetes	Exobasidiales	Brachybasidiaceae	NA*	0.169	4	0.071
9	Bacteria	Proteobacteria	Gammaproteobacteria	Burkholderiales	Comamonadaceae	*Variovorax*	0.149	6	0.117
10	Bacteria	Planctomycetota	Planctomycetes	Isosphaerales	Isosphaeraceae	*Paludisphaera*	0.148	3	0.015

* NA indicates that the classifier could not determine the ASVs at low level due to insufficient similarity to reference sequences.

investigate their role in microbiome of ticks.

Bivalvulida and Eugregarinorida were detected at high abundances, while there is no record of this group detected in ticks. Bivalvulida (Class Myxozoa; Phylum Cnidaria) was detected from most of the samples. Myxozoa is a group of obligate parasite of vertebrates, while there are no record of myxozoan species detected in arthropods (*114–116*). The family Eugregarinorida (phylum Apicomplexa) was detected from many of the tick samples. Eugregarinorida protozoan has been detected in a wide range of arthropods (*117*). There are also reports of symbiotic Eugregarinorida in arachnids (*118*), as well as in blood-sucking insects such as sand flies and mosquitoes (*119–121*). Further studies are needed to determine the effects of Eugregarinorida in ticks.

Detection of some taxon was potentially from the environment. Spore of fungi, Ciliophora , and Cercozoa are ubiquitous in soil and freshwater (*122–124*). Chalophyta is also likely from the environment. Although the possibility of contamination from the body surface of ticks with these microbial DNA cannot be completely excluded, it is likely that the origin of the detected protists was mostly from internal (*125*). Ticks obtain water transdermally from water vapor when not attached to a host (*126*), but *Amblyomma americanum* is known to take water also from liquid water and takes up water in its salivary glands and intestinal tract (*127*). The frequent detections of taxa that are likely to be from the environment may indicate that other ticks also consume liquid water. The potential for the uptake of microorganisms from the environment is an important consideration, as it may disrupt the tick microbiome.

This study has some limitations. The relative abundance and network analysis might have been affected with temporal patterns in this study. Bacterial microbiome of ticks was suggested to change depend on the season (*128*), which is also potentially similar to the eukaryotic microbiome. Some samples had a very low proportion of non-tick reads even with the high number of host tick reads. Eukaryotic microbes in ticks might be intaken sporadically, unlike endosymbiotic bacteria such as *Coxiella* and *Rickettsia*. For annotation of eukaryotic taxa with the naïve bayes classifier, a lot of the annotation of ASVs limited only at high level. This was due to the use of highly conserved genes, and due to the shortage of the database. Alternatively, the evolutionally placement algorithm (EPA) could be applied to improve the annotation (*129*). The EPA uses a reference tree based on a sequence database with long sequence fragments, and place targeted query short reads on the reference tree to annotate the query reads. These limitations need to be improved in the future.

In this chapter, major groups of microeukaryotes in microbiome of ticks are catalogued. Potential pathogens against ticks and keystone taxa of the microbiome in ticks were detected. Since these findings are not more than hypothesis, the determined taxa need to be characterized with multiple approaches including phylogeny, morphology, isolation, and culture in the future.

5. Summary

The potential predominant eukaryotic taxon was determined based on the sequencing data using the developed method in the chapter I. Important taxa of eukaryotes for the ticks and the microbial network were determined. The criteria for important taxon were, abundant, close to arthropod pathogenic group, or determined as keystone taxa. The sample ticks were collected from four species, females and males, four regions. The bacterial and eukaryotic microbiome were simultaneously investigated from the sample set. First, ASVs classified as Bivalvulida or Eugregarinorida were detected as the abundant taxa. Second, ASVs classified as Nematozoa and Hypocreales were close groups as the entomopathogenic organisms. Finally, the keystone taxa in the cross-domain network in the ticks were detemined. As a result, *Bromeliothrix* (Ciliophora) in *Haemaphysalis flava*, and *Kurtzmanomyces* (Basidiomycota), unclassified Brachybasidiaceae (Basidiomycota), and *Pestalotiopsis* (Sordariomycetes: Ascomycota) in *Haemaphysalis longicornis*, were determined as keystone taxa. These findings propose valuable hypothesis, which need to be clarified with specific techniques, including phylogeny, morphology, isolation, and culture.

Chapter III

Isolation and characterization of a macro-eukaryote, a parasitoid wasp

1. Introduction

Encyrtid (Hymenoptera: Chalcidoidea) wasps are a species-rich family of arthropod parasitoids (*130–132*). Parasitoid wasps play an essential role in the control of host populations, as they kill their hosts in a species-specific manner (*9*, *133*). For this reason, Encyrtid wasps and other members of the Chalcidoidea are recognized as an important groups as biological control agents against arthropod pests (*9–11*).

Female *Ixodiphagus* wasps lay their eggs inside the body of ticks by inserting their ovipositor through the host exoskeleton (*134*). These eggs then remain dormant until the tick feeds on a host (*135*). As with other parasitoids, the wasp larvae kill the host tick during the development and later emerge as adult. To date, at least 16 species of *Ixodiphagus* wasps have been described, and they are known to parasitize at least 15 species of Ixodid ticks across six genera (*135–137*). *Ixodiphagus* wasps have been recorded around the world including in Asia, Europe, Africa, North America, South America, and Oceania (*137*). In Asia, these wasps have been recorded from South Asia, Southeast Asia, and Far Eastern Siberia, while there is no documented record from Eastern Asia aside from an incidental record from Japan (*136*). The diversity of *Ixodiphagus* wasps is considered to be underestimated due to lack of sampling (*48*). Therefore, investigation in the Eastern Asia region is valuable for addressing this knowledge gap.

Molecular techniques have been useful for systematics and evolutionary studies of arthropods (*138*, *139*). These techniques are also applicable for species-specific detection and barcoding (*140*). Mitochondrial genes are widely used for these purposes and are well-represented in genetic databases (*141*, *142*). Several characteristics make mitochondrial genes useful for such studies: their high copy number within cells, conserved gene catalogs across species, and moderate mutation rates between species. However, there are several difficulties in the use of mitochondrial genes for Hymenoptera characterization. Intra-individual variations on mitochondrial gene have been reported in a range of wasps and bees (*143–146*). This phenomenon is caused by heteroplasmy, where individuals possess multiple sets of mitochondrial genes, and nuclear mitochondrial DNA segments (NUMTs), where fragments of mitochondrial DNA are inserted into the nuclear genome. Although one recent study presented the complete mitochondrial genomes of *Ixodiphagus* wasps (*48*), there has been no reports of intra-individual variation of the mitochondrial genes of this important wasp genus. To collect reliable molecular data on *Ixodiphagus*, it is essential to precisely characterize these intra-individual polymorphisms.

In this chapter, the geographic distribution and the genetic characteristics of *Ixodiphagus* wasps in Japan were investigated.

2. Material and Methods

2.1. Ethical statement

All animal experiments were conducted in accordance with the guidance of Institute for Laboratory Animal Research, following the Fundamental Guidelines for Proper Conduct of Animal Experiment and Related Activities in Academic Research Institutions under the jurisdiction of the Ministry of Education, Culture, Sports, Science and Technology, Japan. The procedures were approved by the Animal Experiment Committee of the Graduate School of Veterinary Medicine, Hokkaido University (Approval No. 22-0030).

2.2. Detection of *Ixodiphagus* wasps from the field collected ticks by the tick infestation on the laboratory animals

Ixodiphagus wasps were detected from nymphal ticks collected from vegetation and wild animals. A total of 1,935 questing ticks were collected by flagging at 20 sampling sites across five regions between 2021 and 2024 (Figure III - 1, Table III - 1). Ticks were also collected from dead wild animals, including tanuki (Japanese raccoon dog, *Nyctereutes viverrinus*) and badger (*Meles anakuma*). These ticks were unfed or partially fed nymphs. The collected ticks were morphologically identified based on previously described keys (*68*). The tick species included in this study were *Haemaphysalis flava*, *Haemaphysalis formosensis*, *Haemaphysalis japonica*, *Haemaphysalis longicornis*, and *Haemaphysalis megaspinosa.* All the ticks were infested on the ears of female Japanese white rabbits (Slc: JW/CSK; Japan SLC, Shizuoka, Japan) using cotton bags to cover the left and right ears separately. Multiple species from the same sampling site or animal were infested in the same ear bag. The replete ticks were kept in Petri dishes under constant dark conditions at 25℃ and 90% relative humidity until they molted or died due to drying, mold, or wasp emergence. Wasp samples were kept in 80% ethanol at -20℃ upon their emergence from ticks until being examined under a stereoscopic microscope and DNA was extracted.

Emerged wasp samples used for molecular analysis were investigated morphologically by comparing them with those reported previously (*48*, *136*, *147–154*). Morphological characters were photographed with a digital microscope VHX-7000 (KEYENCE Inc., Osaka, Japan) using a focus stacking function.

2.3. Morphological and molecular identification of host ticks

Tick carcasses (“mummies”) after wasp emergence were subjected to morphological and molecular species identification. Morphological identification was performed based on the previously described keys (*68*). Thereafter, the third and fourth legs on one side of the mummies were cut for DNA extraction with HotSHOT protocol (*155*). The collected legs were placed into 10 µl of 25 mM NaOH (pH12.0) and incubated for 30 minutes followed by neutralization with 10 µl of neutralizing

Figure III - 1: Sampling regions of the ticks used for experimental infestation on rabbits.

Table III - 1: Details of the experimental tick challenges on rabbits.

Infestation ID[*1]	Tick species[*2]					Region	Prefecture	GPS	Sampling year	Sampling month	Tick source	Number of infested nymphs	Number of ticks parasitized by wasps (%)	Mean number of wasps per single tick (Number of wasps per each tick)
	Hfla	Hfor	Hjap	Hlon	Hmeg									
1	+	+			+	Shikoku	Kochi	33.46, 133.33	2021	Dec.	Vegetation	48	1 (2.1)	4 (4)
2				+		Kyushu	Fukuoka	33.37, 130.80	2022	Mar.	Vegetation	120	0	
3	+	+		+		Kyushu	Fukuoka	33.29, 130.60	2022	Mar.	Vegetation	140	0	
4	+	+				Kyushu	Fukuoka	33.50, 130.30	2022	Mar.	Vegetation	80	0	
5			+		+	Hokkaido	Hokkaido	43.38, 144.14	2022	Sep.	Vegetation	7	0	
6	+		+	+	+	Hokkaido	Hokkaido	42.11, 143.00	2022	Sep.	Vegetation	145	0	
7	+			+		Hokuriku	Ishikawa	37.49, 137.18	2023	Mar.	Vegetation	340	7 (2.1)	7 (ND[*4])
8			+		+	Hokkaido	Hokkaido	42.11, 143.00	2023	May	Vegetation	180	0	
9					+	Hokkaido	Hokkaido	42.44, 142.48	2023	Oct.	Vegetation	160	0	
10	+					Shikoku	Kochi	33.47, 133.33	2023	Dec.	Vegetation	100	0	
11	+					Shikoku	Kochi	33.44, 133.30	2023	Dec.	Vegetation	103	0	
12	+	+				Shikoku	Kochi	33.48, 133.36	2023	Dec.	Vegetation	120	0	
13					+	Hokkaido	Hokkaido	42.11, 143.00	2024	Apr.	Vegetation	240	0	
14	+	+				Chugoku	Shimane	35.58, 133.13	2024	Mar.	Badger[*3]	36	3 (8.3)	10 (20,5,5)
15	+			+		Chugoku	Shimane	35.52, 133.04	2024	Mar.	Tanuki[*3]	114	4 (3.5)	5 (2, 4, 5, 7)
										Total		**1,933**	**15**	

[*1] Infestation ID represents individual tick infestations conducted on a single ear of each rabbit.
[*2] Infested ticks were identified morphologically but not counted individually. Abbreviations for tick species: Hfla, *Haemaphysalis flava*; Hfor, *Haemaphysalis formosensis*; Hhys, *Haemaphysalis hystricis*; Hlon, *Haemaphysalis longicornis*; Hmeg, *Haemaphysalis megaspinosa*.
[*3] Ticks collected from animals were infested on laboratory rabbits to allow them to fully engorge.
[*4] The number of wasps per each tick was not counted due to the emergence from multiple ticks in the same enclosure.

buffer containing 100 mM Tris-HCl and 0.5 mM EDTA (pH8.0). PCR was performed using a primer set (mt-rrs-1 and mt-rrs-2, Table III - 2) targeting the mitochondrial ribosomal RNA gene with conditions indicated in Table III - 2. PCR products were purified using the ExoSAP-IT Express PCR Cleanup Reagent (Thermo Fisher Scientific, Tokyo, Japan) or the NucleoSpin® Gel and PCR Clean-up kit (Macherey-Nagel, Düren, Germany). Sanger sequencing was performed with the ABI PRISM 3130xl Genetic Analyzer (Applied Biosystems, Foster City, CA, USA) using BigDye Terminator v3.1 Cycle Sequencing Kit (Applied Biosystems). The observed sequences were compared with a previously constructed sequence database (*156*).

2.4. DNA extraction from wasps

DNA was extracted from representative wasp samples using the NucleoSpin DNA Insect Kit (Macherey-Nagel). Individual samples were cut at the head-thorax and thorax-abdomen joints to extract DNA efficiently. The samples were incubated overnight at 55℃ in the mixture of 10 µl of Proteinase K, 100 µl of Buffer BE, and 40 µl of Buffer MG, followed by extraction according to the manufacturer's protocol. The exoskeletons after DNA extraction were kept in 80% ethanol at -20℃ for future investigation.

2.5. Shotgun sequencing and data analysis

Shotgun sequencing was performed with a representative wasp sample (sample code: WS03-03, Table III - 3). An Illumina sequencing library was prepared using the IDT for Illumina DNA/RNA UD Indexes (Illumina, Hayward, CA, USA) in combination with the Illumina DNA Prep kit (Illumina). The library was analyzed with the NextSeq 1000 sequence system using NextSeq™ 1000/2000 P1 XLEAP-SBS™ Reagent Kit (600 Cycles) (Illumina). Base-calling and trimming were performed with the Dynamic Read Analysis for GENomics (DRAGEN™) (Illumina). The FASTQ files were deposited in the DNA Data Bank of Japan (DDBJ) Sequence Read Archive (*https://www.ddbj.nig.ac.jp/index.html*) under an accession number of PRJDB18816. The obtained reads were error-corrected and normalized by the BBNorm function, followed by mapping to a reference *COI* gene sequence of *Ixodiphagus hookeri* (JQ315225) using the Geneious Prime build 2022-11-28 (*157*). Polymorphic sites were identified by the Geneious SNP/Variation function with a minimum variant frequency of 0.01.

2.6. Molecular detection of *Ixodiphagus* wasps in questing ticks

Molecular detection of *Ixodiphagus* wasps was conducted on the questing *H. flava* nymphs collected in Chugoku region (Figure III - 1, Table III - 1). Two hundred and three ticks were collected by flagging vegetation at nine sampling sites in April and June of 2024 (Table III - 4). The samples were rinsed once with 70% ethanol then twice with molecular-grade water before homogenization using the

Table III - 2: Primers and amplification protocols for tick identification and *Ixodiphagus* wasp *COI* gene characterization.

Primer name	Target organism (Target gene)	Purpose	Primer sequence (5' → 3')	PCR kit	Cycling conditions	Reference
mt-rrs-1	Ixodid tick	Species	CTGCTCAATGATTTTTTAAATTGCTGTGG	Tks Gflex	94℃ for 1 min and 45 cycles of 98℃ for	(*158*)
mt-rrs-2	(16S rRNA)	identification	CCGGTCTGAACTCAGATCAAGTA	(Takara Bio Inc.)	10 sec, 60℃ for 15 sec, 68℃ for 30 sec	
347F-H	*Ixodiphagus* sp.	Detection and	TTGATTCAGGAACKGGRACTGGA	KOD-Plus-Neo	94℃ for 2 min and 40 cycles of 98℃ for	This study
942R-H	(*COI*)	direct sequencing	TACTCCTGTTGGTACAGCAATA	(TOYOBO)	10 sec, 60℃ for 30 sec, 68℃ for 30 sec	
In-Fusion_347F-H	*Ixodiphagus* sp.	In-Fusion cloning	AAAACGACGGCCAGTTTGATTCAGGGACTGGGACTG	Takara Ex Premier	94℃ for 1 min and 40 cycles of 98℃ for	This study
In-Fusion_942R-H	(*COI*)		GACCATGATTACGCCTACTCCTGTTGGTACAGC	(Takara Bio Inc.)	10 sec, 55℃ for 15 sec, 68℃ for 30 sec	
M13 Primer M4	pUC19 vector	Amplifying insertion	GTTTTCCCAGTCACGAC	EmeraldAmp MAX PCR Master MIX	30 cycles of 98℃ for 10 sec, 55℃ for 30	Takara Bio
M13 Primer RV	(*COI*)	sequencing	CAGGAAACAGCTATGAC	(Takara Bio Inc.)	sec, 72℃ for 1.5 min	Inc.

Table III - 3: Information of the representative samples used for the verification of intra-individual polymorphisms in the *COI* gene.

Sample code	Infestation ID*[1]	Prefecture	Tick source	Sex
WS01-01	1	Kochi	Vegetation	F
WS03-03	7	Ishikawa	Vegetation	F
WS08-02	14	Shimane	Tanuki	M
WS09-01	15	Shimane	Badger	F
WN072	NA*[2]	Shimane	Vegetation	NA*[2]
WN203	NA*[2]	Shimane	Vegetation	NA*[2]

F, female. M, male.

*[1] Infestation ID corresponds to the Infestation ID in Table III – 1.

*[2] NA, not applicable.

Table III - 4: Sampling site information and results of molecular detection of wasps among questing nymphal *Haemaphysalis flava*.

Site ID	Sampling year	Sampling month	GPS	Number of examined ticks	Number of PCR positive ticks (%)
S03	2024	Apr.	35.37, 133.52	37	3 (8.1)
S04	2024	Apr.	35.34, 133.59	8	0
S05	2024	Apr.	35.29, 133.56	18	0
S06	2024	Apr.	35.15, 133.28	38	0
IZM02	2024	Jun.	35.42, 132.69	1	0
IZM05	2024	Jun.	35.43, 132.80	1	0
IZM08	2024	Jun.	35.24, 132.67	35	2 (5.7)
IZM09	2024	Jun.	35.29, 132.79	57	1 (1.8)
IZM10	2024	Jun.	35.38, 132.89	8	0
Total				203	6 (3.0)

Micro Smash MS-100R (TOMY, Tokyo, Japan) for two minutes at 2,500 rpm. DNA was extracted from the individual tick samples with DNAzol (Invitrogen, Carlsbad, CA) following the manufacturer's protocols. The extracted DNA was used as a template for PCR with a newly designed primer set, 347F-H and 942R-H (Table III - 2), which target a partial *COI* sequence of *Ixodiphagus.* These primers were designed on the conserved regions between the observed sequence in the sample used for the shotgun sequencing (sample code: WS03-03) and the reference sequence of *I. hookeri* (JQ315225). Mixed bases were incorporated at the variable sites to account for the intra-individual polymorphisms.

2.7. Direct sequencing of *COI* PCR amplicons

A total of six samples were selected as a representative sample set for *COI* gene sequence characterization (Table III - 3). The set included DNA from four adult wasps (sample codes: WS01-01, WS03-03, WS08-02, and WS09-01), collected from different sampling regions and tick hosts, and two questing ticks positive for wasps by PCR (sample codes: WN072 and WN203). The least damaged four wasps were chosen to facilitate future morphological investigation. DNA from each sample was used for PCR with the designed primer set as mentioned above (347F-H and 942R-H) under the conditions detailed in Table III - 2. The resulting PCR products were subjected to direct Sanger sequencing as described above. Electropherograms obtained were aligned using the software Geneious and manually examined to detect any ambiguities with multiple peaks within a 551-bp region between primer binding sites.

2.8. Cloning and sequencing of *COI* gene fragments

Cloning of the *COI* gene fragments was performed on the same set of DNA as direct sequencing analysis. Inserted *COI* gene fragments were generated using a high-fidelity PCR enzyme and modified primer set (In-Fusion_347F-H and In-Fusion_942R-H, Table III - 2), targeting the same region as the direct sequencing, as indicated in Table III - 2. The fragments were ligated with the PCR-linearized pUC19 vector (Takara Bio Inc., Shiga, Japan) using the In-Fusion HD Cloning Kit (Takara Bio Inc.). Competent *Escherichia coli* DH5α cells (Nippon Gene, Tokyo, Japan) were transformed with the ligation products and pre-incubated at 37℃ for an hour. The transformed cells were subsequently inoculated onto LB agar plates containing ampicillin and X-gal, and incubated overnight at 37℃. Individual colonies were selected to amplify the insert sequences using the EmeraldAmp MAX PCR Master MIX (Takara Bio Inc.) with a primer set (M13 Primer M4 and M13 Primer RV, Table III - 2). A total of 10 clones from each sample were sequenced by Sanger sequencing as mentioned above. The obtained clone sequences were aligned and trimmed using Geneious software. The sequences were translated with invertebrate mitochondrial genetic code. Putative NUMTs were determined based on two criteria: (1) the presence of insertion or deletion causing a frameshift, (2) the presence of

substitution resulting in a stop codon in the coding region. Clones determined as putative NUMTs were excluded from further analysis. The remaining nucleotide sequences were re-aligned and subsequently used to construct a median-joining haplotype network using the PopART v1.7 (*67*, *159*). The obtained sequences were deposited in the DDBJ under the accession numbers LC849322 – LC843959 (Table III - 5).

3. Results

3.1. Detection of wasps in engorged ticks

Out of the 1,933 *Haemaphysalis* nymphs experimentally infested on rabbits, adult wasps were obtained from a total of 15 engorged ticks collected from four regions (Figure III - 2, Table III - 1). All tick species parasitized by the wasps were identified as *H. flava* both molecularly and morphologically. Among the questing ticks infested on rabbits, 2% (1/48 from Shikoku and 7/340 from Hokuriku) of the ticks were found to be parasitized by the wasps. Four wasps emerged from a single tick in Shikoku, while an average of seven wasps emerged from seven ticks in Hokuriku (Table III - 1). Among the ticks collected from wild animals and subsequently infested on rabbits, 8% (4/36) and 3.5% (4/114) of the ticks collected from badgers and tanukis, respectively, were found to be parasitized by the wasps. The mean number of wasps that emerged from a single tick was 10 from badgers and five from tanuki (Table III - 1).

3.2. Morphological characterization of the wasps

The four samples (sample codes: females - WS01-01, WS03-03, and WS09-01; male - WS08-02, Table III - 3) used for sequencing analysis were morphologically examined (Figure III - 2).

For females, the 16 described species of *Ixodiphagus* wasps can be broadly classified based on the characteristics of the torulus and the scape of the antennae. In the three samples in this study (sample codes: WS01-01, WS03-03, and WS09-01), the torulus were above the ventral margin of compound eyes, and the scape were relatively wide and short. These characteristics correspond to the eight species of *Ixodiphagus*, including *I. hookeri*, *Ixodiphagus sagarensis*, *Ixodiphagus tadystes*, *Ixodiphagus brunneus*, *Ixodiphagus mysorensis*, *Ixodiphagus godens*, *Ixodiphagus taiaroensis*, and *Ixodiphagus theilerae*. However, the samples in this study were different from those eight species by the following characteristics: (i) the axillae were hardly raised and lacked distinct posterior ridges; (ii) the fore wings were relatively large, one to three lines of the setae were below the submarginal vein proximally, the basal cell had a naked area, and the linea calva closed with one to two rows of setae posteriorly. In *I. taiaroensis* and *I. theilerae*, the fore wings are small (brachypterous). In *I. godens*, the axillae were clearly raised with distinct posterior ridges. In the fore wings of *I. hookeri*, *I. sagarensis*, *I. tadystes*, *I. mysorensis*, and *I. brunneus*, the basal cell mostly covered with setae, and the linea calva are open.

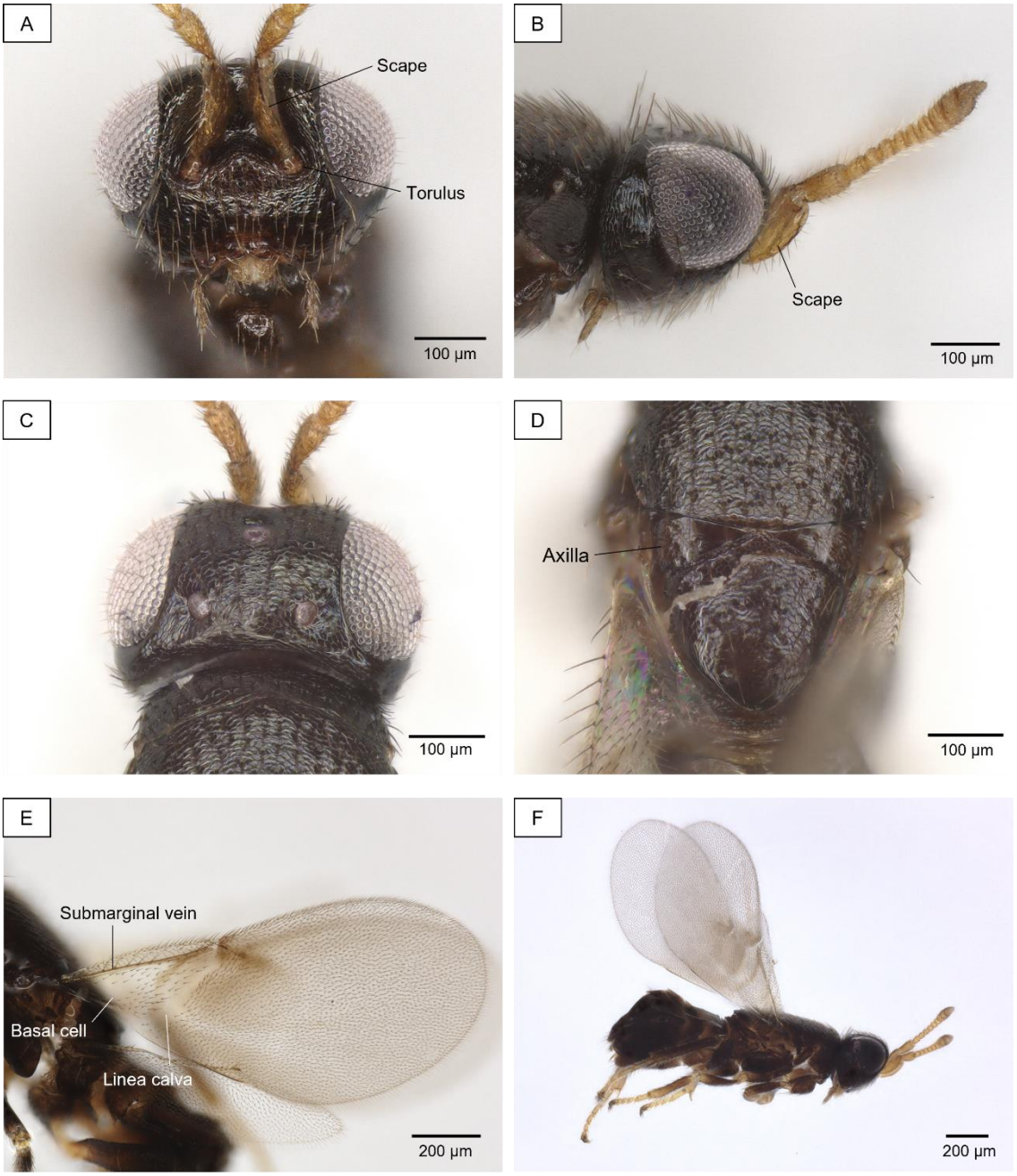

Figure III - 2: An *Ixodiphagus* wasp emerged from *Haemaphysalis flava* (sample code: WS03-03).

Head A) frontal, B) lateral, and C) dorsal views. D) Mesosoma dorsal view. E) Fore wing. F) Habitus.

For males, the information on morphological characteristics is available for eight species of *Ixodiphagus*, including *I. hookeri, I. sagarensis, I. mysorensis, I. taiaroensis, I. theilerae, Ixodiphagus texanus, Ixodiphagus hirtus,* and *Ixodiphagus biroi*. The sample in this study (sample code: WS08-02) was different from those eight species based on the morphological features of axillae and fore wings as observed in females. Therefore, the samples obtained from this study could not be identified to the species level and were considered as novel species.

3.3. Detection of wasp DNA in the questing ticks

The parasitism rates of wasps were molecularly assessed among questing *H. flava* nymphs collected at nine experimental sites in Chugoku (Figure III - 1). Three sites tested positive for wasp parasitism, with rates of 8.1% (3/37), 1.8% (1/57), and 5.7% (2/35) (Table III - 4).

3.4. Detection of polymorphisms on mitochondrial *COI* gene by shotgun sequencing

A total of 4,025,830 raw reads were obtained from a wasp sample (sample code: WS03-03) using the NextSeq platform. After trimming, error-correction, and normalizing of the raw reads, a total of 593,736 reads were kept for the downstream analysis. By mapping the reads to a reference *COI* gene sequence of I. *hookeri* (JQ315225), putative *COI* sequence of the sample WS03-03 was constructed using 1,969 reads with a mean coverage of × 143.4. In the 979-bp region of the putative *COI* gene, 38 intra-individual polymorphic sites including 23 transitions and 15 transversions were observed (Figure III - 3).

3.5. Verification of intra-individual polymorphisms by sanger sequencing

The intra-individual polymorphisms in the *COI* gene were verified through two Sanger sequencing approaches, direct sequencing of *COI* PCR amplicons, and sequencing of the inserted *COI* fragments by in-fusion cloning. For this purpose, a set of six representative DNA samples (four wasps and two ticks, Table III - 3) were analyzed. The direct sequencing of *COI* PCR amplicons yielded double peaks in the electropherograms in all six samples and a total of 17 double-peak sites were observed across the amplified region (Figure III - 4). For the in-fusion cloning sequencing, ten different clones were randomly selected per sample and sequenced to generate a final data set of 60 sequences of 474 bp in length. The sequence alignment identified a total of 38 different haplotypes from six samples (Figure III - 5, Table III - 5). The most frequent haplotype, MH1, was found in all samples and was presumed to be a putative wild type for the subsequent analysis. Four haplotypes (MH35, MH36, MH37, and MH38) and one haplotype (MH20) had a 10-bp insertion and single nucleotide deletion, respectively, causing frameshift and premature termination, while two haplotypes (MH18 and MH28) had a nucleotide substitution causing nonsense mutation. These seven haplotypes were considered putative NUMTs and were excluded from the subsequent analysis. Among the remaining 31 haplotypes, a total

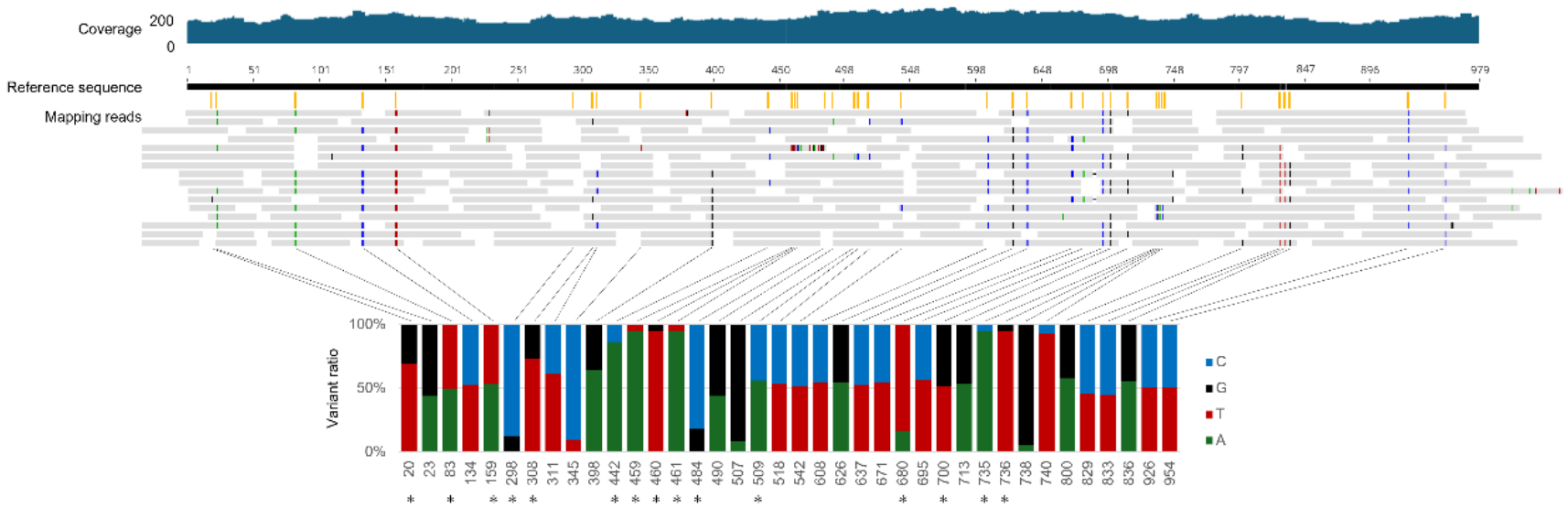

Figure III - 3: Polymorphisms in the partial *COI* gene detected by mapping of shotgun sequencing reads against a reference sequence of *Ixodiphagus hookeri*.

The Illumina sequence reads obtained from a wasp (sample code: WS03-03) were mapped against a reference *Ixodiphagus hookeri COI* gene (JQ315225). The upper panel shows the coverage of mapping reads. The middle panel shows the reference sequence and the mapped reads. Yellow bars indicate polymorphic sites. Disagreements to the consensus sequence are highlighted by representative colors in the mapped reads. The lower panel shows the ratio of observed variants at polymorphism sites. The numbers represent the polymorphic site regions corresponding to the reference sequence. The asterisks represent transversions.

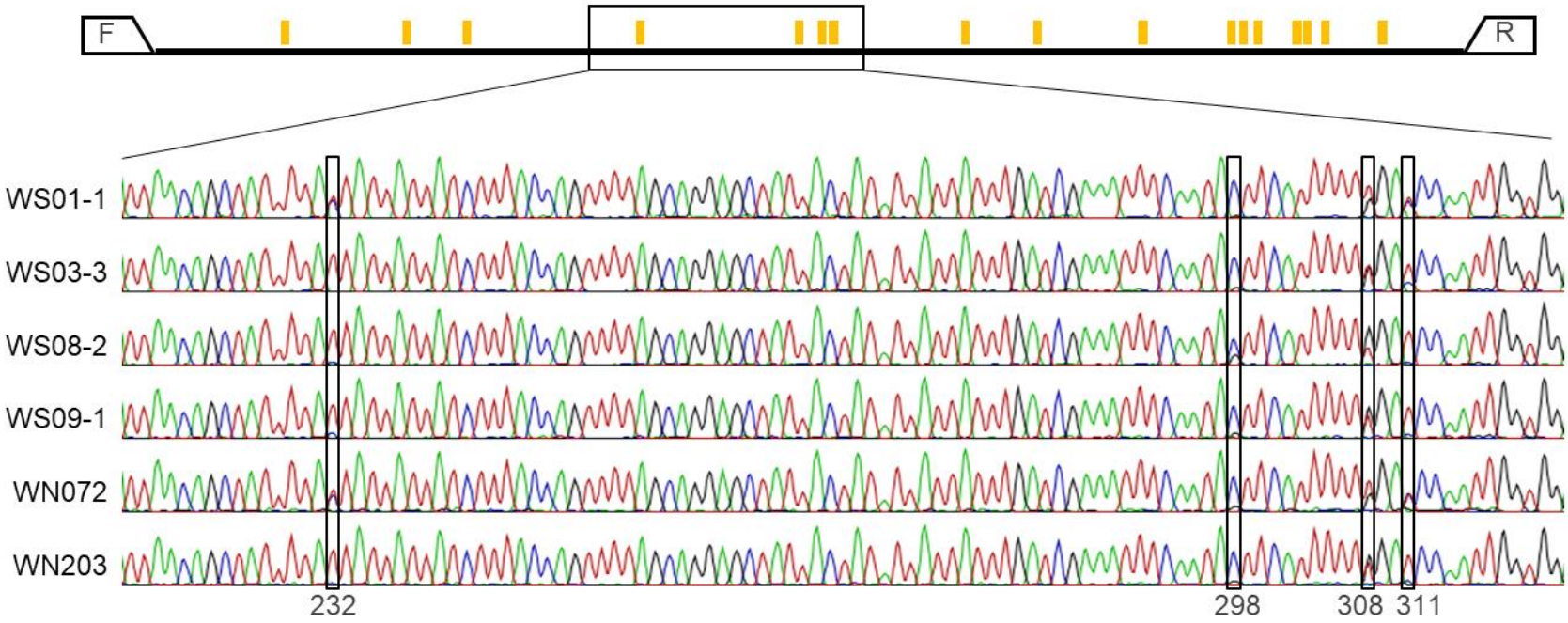

Figure III - 4: Electropherograms obtained by the direct sequencing of *Ixodiphagus COI* PCR amplicons.

The upper panel indicates the position of double-peak sites (yellow bars) in partial *COI* PCR amplicons. Trapezoids indicate primer binding regions (F, 347F-H; R, 942R-H). The alignments on the lower panel indicate ambiguities on the electropherograms. The numbers below represent the corresponding positions to the *Ixodiphagus hookeri* partial *COI* sequence (JQ315225).

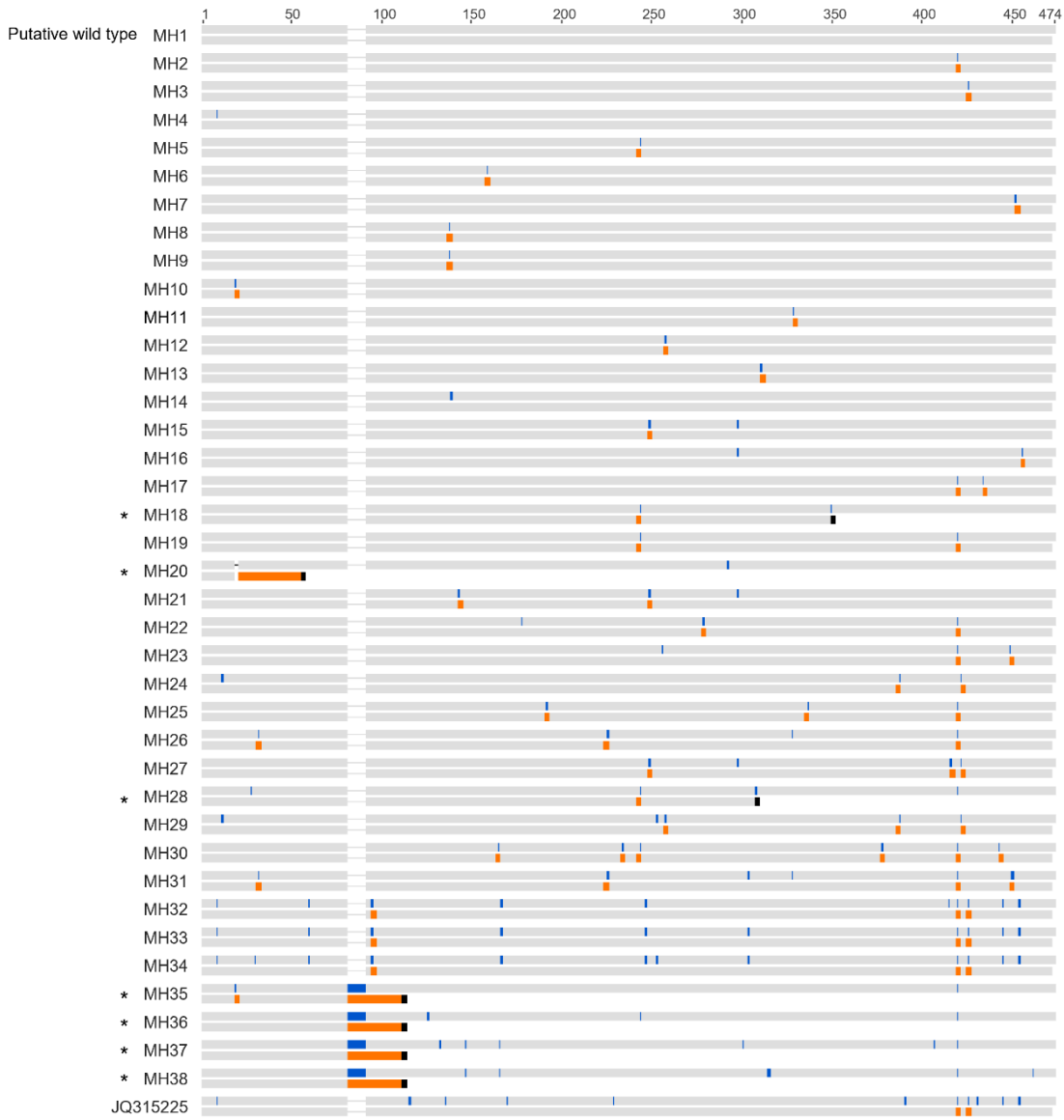

Figure III - 5: Alignment of the 38 *COI* haplotype sequences obtained in the present study.
For each haplotype, the nucleotide sequence is shown in the first row, and the translated amino-acid sequence is shown in the second row. Nucleotide and amino-acid differences from the putative wild-type (MH1) sequence are highlighted in blue and orange, respectively. Stop codons are indicated in black. Asterisks denote putative NUMTs.

Table III - 5: Observed haplotypes of *COI* gene by in-fusion cloning.

Mitochondrial haplotype	Sample code						Nucleotide polymorphism			Amino-acid polymorphism			Accession ID
	WS01-01	WS03-03	WS08-02	WS09-01	WN072	WN203	Deletion	Insertion	Substitution	Missense	Nonsense	Frameshift	
MH1	2	2	2	2	1	3							LC843922
MH2	1	1	0	0	0	0	-	-	+	+	-	-	LC843923
MH3	1	0	0	0	0	0	-	-	+	+	-	-	LC843924
MH4	1	0	0	0	0	0	-	-	+	-	-	-	LC843925
MH5	0	3	0	0	0	1	-	-	+	+	-	-	LC843926
MH6	0	0	1	0	0	0	-	-	+	+	-	-	LC843927
MH7	0	0	1	0	1	0	-	-	+	+	-	-	LC843928
MH8	0	0	1	0	0	0	-	-	+	+	-	-	LC843929
MH9	0	0	1	0	0	0	-	-	+	+	-	-	LC843930
MH10	0	0	0	1	0	0	-	-	+	+	-	-	LC843931
MH11	0	0	0	1	0	0	-	-	+	+	-	-	LC843932
MH12	0	0	0	1	0	0	-	-	+	+	-	-	LC843933
MH13	0	0	0	1	0	0	-	-	+	+	-	-	LC843934
MH14	0	0	0	0	0	2	-	-	+	-	-	-	LC843935
MH15	0	1	0	0	0	0	-	-	+	+	-	-	LC843936
MH16	0	0	1	0	1	0	-	-	+	+	-	-	LC843937
MH17	0	0	0	0	2	0	-	-	+	+	-	-	LC843938
MH18	0	0	0	0	1	0	-	-	+	+	+	-	LC843953
MH19	0	0	0	0	0	1	-	-	+	+	-	-	LC843939
MH20	0	1	0	0	0	0	+	-	+	+	+	+	LC843954
MH21	0	0	1	0	0	0	-	-	+	+	-	-	LC843940

Table III – 5 continued

MH22	0	0	0	1	0	0	-	-	+	+	-	-	LC843941
MH23	0	0	0	1	0	0	-	-	+	+	-	-	LC843942
MH24	1	0	0	1	0	0	-	-	+	+	-	-	LC843943
MH25	0	0	0	0	1	0	-	-	+	+	-	-	LC843944
MH26	0	1	0	0	0	0	-	-	+	+	-	-	LC843945
MH27	0	1	0	0	0	0	-	-	+	+	-	-	LC843946
MH28	0	0	1	0	0	0	-	-	+	+	+	-	LC843955
MH29	1	0	0	0	0	0	-	-	+	+	-	-	LC843947
MH30	0	0	0	0	1	0	-	-	+	+	-	-	LC843948
MH31	0	0	0	1	0	0	-	-	+	+	-	-	LC843949
MH32	1	0	0	0	0	0	-	-	+	+	-	-	LC843950
MH33	0	0	1	0	2	0	-	-	+	+	-	-	LC843951
MH34	0	0	0	0	0	1	-	-	+	+	-	-	LC843952
MH35	0	0	0	0	0	1	-	+	+	+	+	+	LC843956
MH36	1	0	0	0	0	0	-	+	+	+	+	+	LC843957
MH37	1	0	0	0	0	0	-	+	+	+	+	+	LC843958
MH38	0	0	0	0	0	1	-	+	+	+	+	+	LC843959

of 46 single nucleotide polymorphic sites (SNPs) were observed, including 24 transitions, 20 transversions, and two multiple variations (Table III - 6). Of those SNPs, 16 were synonymous, while 30 led to non-synonymous amino-acid changes compared to the putative wild type.

The three sequencing methods - shotgun sequencing, direct sequencing, and cloning - were compared based on the SNPs within the 474-bp overlapping region of the COI gene of a wasp sample (sample code: WS03-03, Figure III - 6). Shotgun sequencing detected the highest number of polymorphic sites (16 sites) followed by direct sequencing (12 sites) and cloning (nine sites). Two polymorphic sites were identified as shared among all three methods, whereas 12 sites were shared between shotgun sequencing and direct sequencing methods. Four polymorphic sites were unique to shotgun sequencing, and seven sites were unique to cloning.

3.6. Haplotype network analysis of wasp *COI* gene

A haplotype network was constructed based on 474-bp partial *COI* gene sequences, consisting of 31 haplotypes obtained from six representative samples (Table III - 3) and one reference sequence of *I. hookeri* from France (JQ315225). The haplotypes did not form any distinct clustering based on the sequence origin (Figure III - 7). The presumed wild type, MH1, along with 4 other haplotypes, MH2, MH3, MH4, and MH5, were closely linked and positioned as central haplotypes in the network. Other haplotypes radiated with one to 11 nucleotide differences from these central haplotypes. None of the haplotypes were identical to the reference *I. hookeri* haplotype.

4. Discussion

This study presents the first documented record of *Ixodiphagus* wasps in Japan since 1980 (*136*). This is also the first confirmed record of this wasp parasitizing *H. flava.* The representative specimens showed significant morphological differences from the described species, including *I. sagarensis* which was previously recorded in Japan. This observation indicates that these *Ixodiphagus* wasps are novel species. The detection of *Ixodiphagus* wasps across three geographically distinct regions – Hokuriku, Chugoku, and Shikoku – indicates a broad distribution of these parasitoid wasps in Japan. In addition, given the wide distribution of *H. flava* throughout East Asia (*68, 160, 161*), it is likely that the *Ixodiphagus* wasps detected in this study may also occur outside of Japan. Since *H. flava* is a significant vector with public health implications (*3, 162, 163*), the presence of these parasitic wasps may represent a valuable tool for the control of ticks and tick-borne diseases in the region. Further taxonomic studies are needed to classify these wasps.

Ixodiphagus and other Encyrtid wasps are known to parasitize multiple species (*130*, *134*, *164*, *165*). This suggests that the species detected from *H. flava* might also parasitize other tick species. However, in this study, wasps emerged solely from *H. flava*, despite the inclusion of four other *Haemaphysalis* species in the infestation experiments using rabbits (Table III - 1). This specificity may indicate that the wasp development was successful only in *H. flava*. *H. flava* has a broad host range including mammals and birds (*68*, *166*). Therefore, it is possible that this species might have allowed wasps to develop properly even with unusual blood sources, such as laboratory rabbits in this study. This could

Table III - 6: Observed polymorphisms of nucleotides and amino-acids in *COI* genes by in-fusion cloning.

Position	Nucleotide polymorphism* (Wild Type/ Variant 1 / Variant 2)	Polymorphism type	Variant frequency	Amino-acid polymorphism
9	T/A	Transversion	27/4	Synonymous
12	T/C	Transition	29/2	Synonymous
19	A/T	Transversion	30/1	Non-synonymous
30	A/G	Transition	30/1	Synonymous
32	A/G	Transition	29/2	Non-synonymous
60	T/C	Transition	28/3	Synonymous
85	A/T	Transversion	28/3	Non-synonymous
128	C/A/T	Transversion/Transition	29/1/1	Non-synonymous
129	T/C	Transition	30/1	Synonymous
133	G/A	Transition	30/1	Non-synonymous
149	C/A	Transversion	30/1	Non-synonymous
155	T/C	Transition	30/1	Non-synonymous
157	T/C	Transition	28/3	Synonymous
168	T/C	Transition	30/1	Synonymous
182	C/A	Transversion	30/1	Non-synonymous
216	T/A	Transversion	29/2	Non-synonymous
224	C/G	Transversion	30/1	Non-synonymous
234	T/G	Transversion	28/3	Non-synonymous
237	T/C	Transition	28/3	Synonymous
239	C/G	Transversion	28/3	Non-synonymous
243	T/C	Transition	29/2	Synonymous
246	T/A	Transversion	30/1	Synonymous
248	G/A	Transition	29/2	Non-synonymous
269	A/T	Transversion	30/1	Non-synonymous
288	T/C	Transition	27/4	Synonymous
294	T/C	Transition	28/3	Synonymous

Table III – 6 continued

301	G/A	Transition	30/1	Non-synonymous
318	T/C	Transition	29/2	Synonymous
319	C/A	Transversion	30/1	Non-synonymous
327	T/A	Transversion	30/1	Non-synonymous
368	A/C	Transversion	30/1	Non-synonymous
378	T/A	Transversion	29/2	Non-synonymous
405	A/G	Transition	30/1	Synonymous
406	T/A	Transversion	30/1	Non-synonymous
410	G/C	Transversion	19/12	Non-synonymous
412	A/T/G	Transversion/Transition	28/2/1	Non-synonymous
416	A/G	Transition	27/4	Non-synonymous
424	G/A	Transition	30/1	Non-synonymous
433	G/A	Transition	30/1	Non-synonymous
435	C/A	Transversion	28/3	Synonymous
439	G/T	Transversion	30/1	Non-synonymous
440	C/T	Transition	30/1	Non-synonymous
441	T/G	Transversion	30/1	Non-synonymous
442	C/T	Transition	30/1	Non-synonymous
444	C/T	Transition	28/3	Synonymous
446	A/G	Transition	30/1	Non-synonymous

*Polymorphic sites detected only in observed haplotypes with stop codons were excluded.

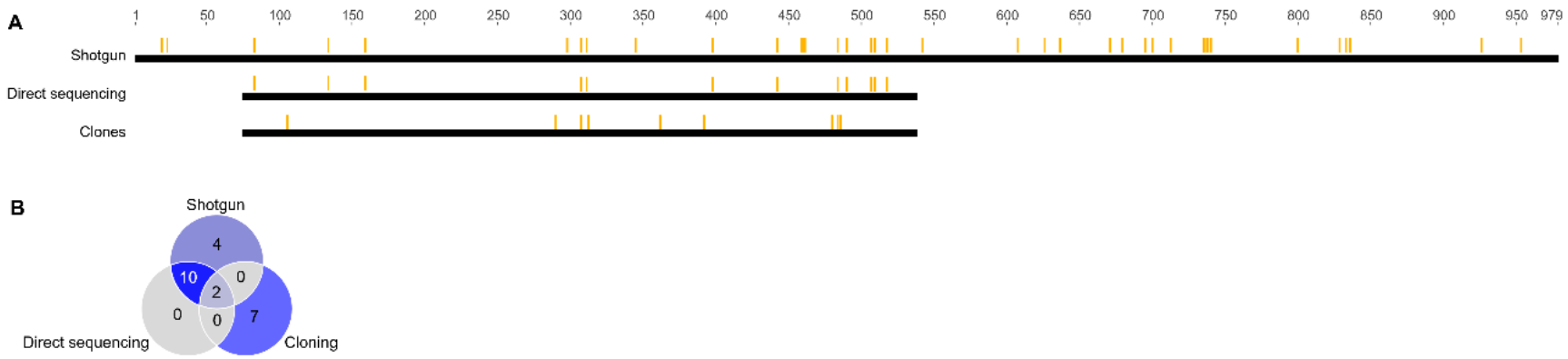

Figure III - 6: Comparison of intra-individual polymorphisms in the partial *COI* gene of a wasp sample (sample code: WS03-03) using three different sequencing approaches.

A) Regions of SNPs detected by each method. B) Number of common SNPs in the preserved 474 bp region across the three methods.

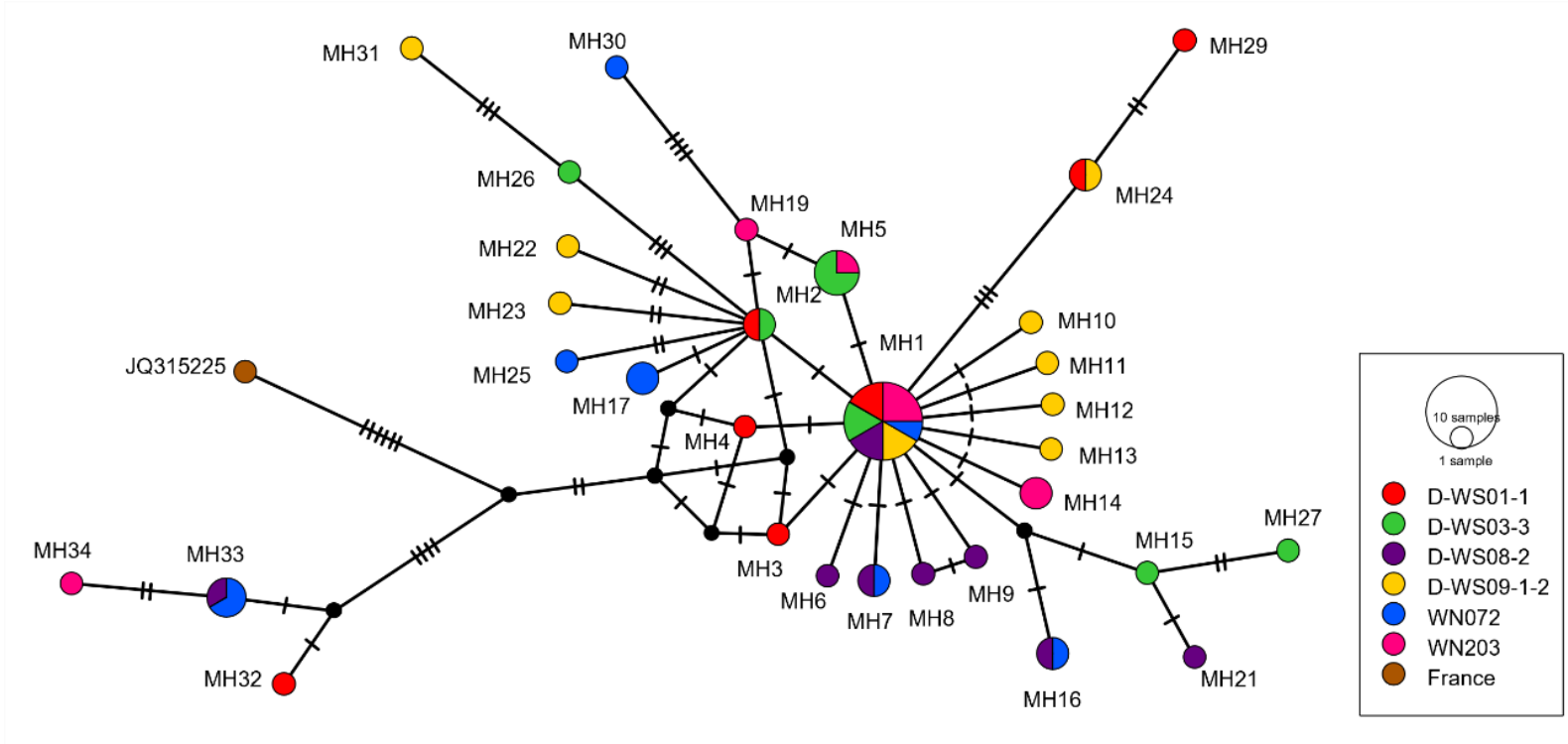

Figure III - 7: Median-joining haplotype network of the *Ixodiphagus* wasp partial *COI* gene sequences.

A haplotype network was constructed based on 474-bp partial *COI* gene sequences, consisting of 31 haplotypes obtained from six representative samples (Table III - 3) and one reference sequence of *I. hookeri* from France (JQ315225). Circle represents unique haplotypes, size of circle corresponds to the frequency of its haplotype, color represents wasp or tick sample, and lines on the branches correspond to number of mutations between haplotypes.

be determined by investigating other field-collected *Haemaphysalis* species by *Ixodiphagus*-specific PCR. Another hypothesis is that the detected wasps were host-specific to *H. flava*. In a trial conducted in Kenya, a reduction in *Amblyomma variegatum* infestations was observed, while the number of *Rhipicephalus appendiculatus* remained unchanged after releasing *Ixodiphagus* wasps (*167*). This outcome underscores the potential of *Ixodiphagus* wasps in species-specific tick management. Investigation of the host range of *Ixodiphagus* wasp species will support future applications in biological control.

Intra-individual polymorphisms in the mitochondrial *COI* gene were observed in all the tested wasps. There was no association of the observed *COI* haplotypes with geographic origins of the wasps or animal species from which the tick hosts were collected (Table III - 3). This suggests that NUMTs and/or heteroplasmic mitochondrial genomes are common across populations and generations of the *Ixodiphagus* wasps. While NUMTs and heteroplasmic mitochondrial genomes are relatively common in other Hymenoptera species (*143–146*, *168*), mechanisms underlying these genetic features remain poorly understood. Inconsistencies in the polymorphic sites were observed among three sequencing methods (Figure III - 6). This could be caused by several factors. Shotgun sequencing was likely the least biased, but the continuities between short reads were not detectable. In direct sequencing, minor mutations may be masked due to manual observation of double peaks in electropherograms. In cloning sequencing, the observation of haplotypes could have been biased due to harmful insertion sequences for competent cells which could be poorly detected after cloning. To obtain genuine mitochondrial sequences, other methods such as long-read sequencing, cDNA sequencing, mitochondrial DNA purification during DNA extraction, or limiting dilution could be employed (*168*). Careful approaches are needed in the molecular investigation of *Ixodiphagus* wasps.

The present study has several technical limitations. The infestation experiments using rabbits may have underestimated the infestation rate of wasps in *H. flava*. Questing ticks were collected mostly from vegetation by flagging and then challenged on rabbits. Since *Ixodiphagus* wasps are known to locate feeding ticks by following host vertebrate odor plumes (*169*, *170*), the ticks tested may not have had sufficient exposure to the wasps. In addition, the emergence rate might be lower than the parasitism rate, as wasps have previously been observed to fail to emerge inside ticks, as found in dissections (*171*). In the molecular detection of wasps from questing ticks, several factors may have influenced the results. The amount of wasp DNA in the questing ticks could be low due to its dormant state as wasp eggs (*135*), reducing detection sensitivity. Additionally, the seasonality of wasps may have affected both the infestation and molecular detection experiments (*134*). Further studies are needed to investigate the relationship between *Ixodiphagus* wasps and Ixodid ticks.

The distribution, host range, and molecular information presented in this study are just a small fragment of the true diversity of *Ixodiphagus*. Information on the *Ixodiphagus* wasps has mostly been gained through incidental observations. There are only a few documentations to catalog *Ixodiphagus*

species in certain regions (*152*). Integrated approaches with morphological and molecular techniques are needed to classify this group with active sampling from host ticks. Furthermore, to apply these wasps for biological tick management in the future, investigations into host range and general biological factors under laboratory conditions are necessary. Comprehensive approaches including these investigations will contribute to elucidating the diversity of *Ixodiphagus* wasps.

5. Summary

Biological control with natural enemies represents a sustainable tool for managing pests. However, there is a substantial lack of knowledge about the natural enemies of ticks. Wasps of the genus *Ixodiphagus* (Encyrtidae) are currently the only known tick-specific parasitoids. While these wasps have been sporadically recorded worldwide, their presence in Eastern Asia is poorly documented. In this study, the occurrence of *Ixodiphagus* wasps was investigated in Japan by infesting field-collected ticks on rabbits under laboratory conditions. Ticks were collected from the Hokuriku, Chugoku, and Shikoku regions. Out of 1,933 *Haemaphysalis* ticks infested on rabbits, adult wasps emerged from 15 engorged ticks. All the ticks from which wasps emerged were morphologically and molecularly identified as *Haemaphysalis flava*. Additionally, wasp DNA was detected in unfed *H. flava* nymphs using a newly designed *Ixodiphagus*-specific PCR assay. Among nine experimental sites in the Chugoku region, *Ixodiphagus* wasps were detected at three sites, with parasitism rates ranging from 1.8% to 8.1%. Finally, the mitochondrial *COI* gene was characterized using shotgun sequencing, direct sequencing, and in-fusion cloning approaches. Multiple intra-individual polymorphisms were observed in all the tested samples. Further studies are needed to investigate the relationship between *Ixodiphagus* wasps and Ixodid ticks. An increased understanding of these parasitoid wasps could contribute to future biological control measures against ticks.

GENERAL CONCLUSION

Ixodid ticks are significant vectors of pathogens affecting humans and animals. While research on tick control has primarily focused on characterizing pathogenic microbes, ticks carry both pathogenic and nonpathogenic organisms. Some of these nonpathogenic organisms play beneficial roles for ticks, while others are commensal or pathogenic to ticks. Research into the eukaryotic communities in ticks has been limited due to lack of interest and technical challenges. To support future biological control strategies and understanding of tick biology, a comprehensive investigation of the tick eukaryotic microbiome was performed in this dissertation.

Chapter I introduces and evaluates novel methods to analyze the eukaryotic microbiome in ticks using high-throughput sequencing. The methods were designed to selectively amplify microeukaryote genes in tick-derived DNA while suppressing the amplification of host tick DNA. Two types of artificial nucleic acids, PNAs and LNAs, were assessed. Additionally, a PCR approach using UNonMet was evaluated. Using a set of tick DNA samples, these methods demonstrated significantly increased proportions of microeukaryotic reads. Furthermore, these methods recovered greater alpha diversity compared to conventional approaches, which predominantly yielded tick-derived sequences. The UNonMet method was particularly effective in detecting fungi and Alveolata, while the PNA-based method captured a broader range of taxa, including fungi, Alveolata, Archaeplastida, Rhizaria, Chloroplastida, and unclassified eukaryotes. Consequently, the PNA-based method is suited for broad-spectrum eukaryotic analyses, whereas UNonMet is better for targeted studies of fungi and Alveolata.

Chapter II identifies potentially important eukaryotic taxa in ticks based on the sequencing data generated with the PNA-based methods developed in Chapter I. This chapter focused on identifying key eukaryotic taxa important for host tick and microbial network. The criteria for identifying important taxa were, high relative abundance, taxonomically close to arthropod-pathogenic groups, or determination as keystone taxa in microbial network. Samples were collected from four tick species across four regions. The bacterial and eukaryotic microbiomes from this sample set revealed several key findings. First, ASVs classified as Bivalvulida or Eugregarinorida were detected as the abundant taxa. Second, ASVs classified as Nematozoa and Hypocreales were close groups as entomopathogenic organisms. Finally, the keystone taxa in the cross-domain network in the ticks were determined. As a result, *Bromeliothrix* (Ciliophora) in *Haemaphysalis flava*, and *Kurtzmanomyces* (Basidiomycota), unclassified Brachybasidiaceae (Basidiomycota), and *Pestalotiopsis* (Sordariomycetes: Ascomycota) in *Haemaphysalis longicornis*, were determined as keystone taxa. These findings propose valuable hypothesis, which needs to be clarified with specific techniques, including phylogeny, morphology, isolation, and culture.

Chapter III investigates the occurrence of the insect enemy of ticks in Japan by experimental infestation of ticks on laboratory animals. *Ixodiphagus* spp. are the only known tick-specific parasitoids, though records of their presence in Eastern Asia are sparse. In this study, ticks collected from the Hokuriku, Chugoku, and Shikoku regions were fed on rabbits in the lab, yielding adult wasps. Out of 1,933 *Haemaphysalis* ticks exposed to rabbits, adult wasps emerged from 15 engorged *Haemaphysalis flava*. Additionally, the mitochondrial *COI* gene was characterized using shotgun sequencing, direct sequencing, and in-fusion cloning methods. Across the six samples analyzed, notable intra-individual polymorphisms were detected, suggesting genetic diversity within this parasitoid species.

Through the three chapters, the predominant eukaryotes carried by ticks were catalogued. The developed technique to detect eukaryotes microbiome in ticks is applicable to various tick species in the future. The microbiome findings have limitations to be explained, so these findings need to be clarified with more specific approaches in the future. The parasitoid wasps of ticks were detected throughout Japan, which suggests the wide distribution of this species. In addition, the characterization detected massive intra-individual polymorphisms on the wasp mitochondrial gene. This finding is valuable for future species classification and biological study. The eukaryotic communities in ticks were yet barely investigated, so multiple approaches will elucidate their role in ticks.

ACKNOWLEDGMENTS

I wish to express my deepest gratitude to my supervisors, Professor Nariaki Nonaka and Professor Ryo Nakao, for their invaluable guidance, unwavering support, and constructive critiques throughout the course of my research. Their exceptional commitment to academic rigor and meticulous attention to detail have been instrumental in shaping the quality and direction of this dissertation. I am equally indebted to the members of my dissertation committee, Professor Kazuhiko Ohashi and Professor Junya Yamagishi, for their insightful feedback and thoughtful recommendations, which have significantly enhanced the depth and scope of this work.

I am profoundly grateful to the faculty and staff of the Graduate School of Infectious Diseases and the Research Center for Zoonosis Control at Hokkaido University for providing the resources and support necessary to facilitate this research. I also extend my appreciation to my colleagues and peers for their intellectual camaraderie and engaging discussions, which have enriched my academic journey and inspired me throughout the process.

I extend my heartfelt appreciation to my partner, Sam, for his steadfast encouragement and unwavering confidence in my abilities. His support has been an enduring source of strength during the more challenging moments of this journey.

I am equally indebted to my family and friends for their enduring emotional support, without which this achievement would not have been possible. I deeply value their encouragement and look forward to celebrating this milestone together.

Finally, I wish to express my sincere gratitude to the technical staff, Ms. Aiko Ohnuma and Ms. Yukari Horio, for their expertise in managing laboratory equipment and their consistent assistance throughout my experiments. Their professionalism and dedication have been critical to the successful completion of this project.

REFERENCES

1. M. R. Talactac, K. Yoshii, E. P. Hernandez, K. Kusakisako, R. L. Galay, K. Fujisaki, M. Mochizuki, T. Tanaka, Vector competence of *Haemaphysalis longicornis* ticks for a Japanese isolate of the Thogoto virus. *Sci. Rep.* **8**, 9300 (2018).

2. H. M. Stanley, S. L. Ford, A. N. Snellgrove, K. Hartzer, E. B. Smith, I. Krapiunaya, M. Levin, The ability of the invasive Asian longhorned tick *Haemaphysalis longicornis* (Acari: Ixodidae) to acquire and transmit *Rickettsia rickettsii* (Rickettsiales: Rickettsiaceae), the agent of Rocky Mountain spotted fever, under laboratory conditions. *J. Med. Entomol.* **57**, 1635–1639 (2020).

3. L.-Z. Fang, X. Xiao, S.-C. Lei, J.-W. Liu, X.-J. Yu, *Haemaphysalis flava* ticks as a competent vector of severe fever with thrombocytopenia syndrome virus. *Ticks Tick Borne Dis.* **14**, 102100 (2023).

4. S. Madison-Antenucci, L. D. Kramer, L. L. Gebhardt, E. Kauffman, Emerging tick-borne diseases. *Clin. Microbiol. Rev.* **33** (2020).

5. C. A. Lippi, S. J. Ryan, A. L. White, H. D. Gaff, C. J. Carlson, Trends and opportunities in tick-borne disease geography. *J. Med. Entomol.* **58**, 2021–2029 (2021).

6. D. O. Agwunobi, Z. Yu, J. Liu, A retrospective review on ixodid tick resistance against synthetic acaricides: implications and perspectives for future resistance prevention and mitigation. *Pestic. Biochem. Physiol.* **173**, 104776 (2021).

7. W. D. Dzemo, O. Thekisoe, P. Vudriko, Development of acaricide resistance in tick populations of cattle: A systematic review and meta-analysis. *Heliyon* **8**, e08718 (2022).

8. K. C. Stafford III, S. C. Williams, G. Molaei, Integrated pest management in controlling ticks and tick-associated diseases. *J. Integr. Pest Manag.* **8**, 28 (2017).

9. A. Kapranas, A. Tena, Encyrtid parasitoids of soft scale insects: biology, behavior, and their use in biological control. *Annu. Rev. Entomol.* **60**, 195–211 (2015).

10. M. Kenis, B. P. Hurley, A. E. Hajek, M. J. W. Cock, Classical biological control of insect pests of trees: facts and figures. *Biol. Invasions* **19**, 3401–3417 (2017).

11. E. Conti, G. Avila, B. Barratt, F. Cingolani, S. Colazza, S. Guarino, K. Hoelmer, R. A. Laumann, L. Maistrello, G. Martel, E. Peri, C. Rodriguez-Saona, G. Rondoni, M. Rostás, P. F. Roversi, R. F. H. Sforza, L. Tavella, E. Wajnberg, Biological control of invasive stink bugs: review of global state and future prospects. *Entomol. Exp. Appl.* **169**, 28–51 (2021).

12. Y. Gottlieb, I. Lalzar, L. Klasson, Distinctive genome reduction rates revealed by genomic analyses of two *Coxiella*-like endosymbionts in ticks. *Genome Biol. Evol.* **7**, 1779–1796 (2015).

13. D. J. Hunter, J. L. Torkelson, J. Bodnar, B. Mortazavi, T. Laurent, J. Deason, K. Thephavongsa, J. Zhong, The *Rickettsia* Endosymbiont of *Ixodes pacificus* contains all the genes of De Novo folate biosynthesis. *PLoS One* **10**, e0144552 (2015).

14. S. Narasimhan, N. Rajeevan, L. Liu, Y. O. Zhao, J. Heisig, J. Pan, R. Eppler-Epstein, K. Deponte, D. Fish, E. Fikrig, Gut microbiota of the tick vector *Ixodes scapularis* modulate colonization of the Lyme disease spirochete. *Cell Host Microbe* **15**, 58–71 (2014).

15. T. Hosokawa, R. Koga, Y. Kikuchi, X.-Y. Meng, T. Fukatsu, *Wolbachia* as a bacteriocyte-associated nutritional mutualist. *Proc. Natl. Acad. Sci. U. S. A.* **107**, 769–774 (2010).

16. E. Machado-Ferreira, V. F. Vizzoni, E. Balsemão-Pires, L. Moerbeck, G. S. Gazeta, J. Piesman, C. M. Voloch, C. A. G. Soares, *Coxiella* symbionts are widespread into hard ticks. *Parasitol. Res.* **115**, 4691–4699 (2016).

17. R. V. M. Rio, G. M. Attardo, B. L. Weiss, Grandeur alliances: Symbiont metabolic integration and obligate arthropod hematophagy. *Trends Parasitol.* **32**, 739–749 (2016).

18. J. H.-O. Pettersson, M. Shi, J. Bohlin, V. Eldholm, O. B. Brynildsrud, K. M. Paulsen, Å. Andreassen, E. C. Holmes, Characterizing the virome of *Ixodes ricinus* ticks from northern Europe. *Sci. Rep.* **7**, 10870 (2017).

19. E. Harvey, K. Rose, J.-S. Eden, N. Lo, T. Abeyasuriya, M. Shi, S. L. Doggett, E. C. Holmes, Extensive diversity of RNA viruses in Australian ticks. *J. Virol.* **93** (2019).

20. S. Thapa, Y. Zhang, M. S. Allen, Effects of temperature on bacterial microbiome composition in *Ixodes scapularis* ticks. *Microbiologyopen* **8**, e00719 (2019).

21. L. Li, J. Fröhlich, P. Pfeiffer, H. König, Termite gut symbiotic archaezoa are becoming living metabolic fossils. *Eukaryot. Cell* **2**, 1091–1098 (2003).

22. T. Inoue, S. Moriya, M. Ohkuma, T. Kudo, Molecular cloning and characterization of a cellulase gene from a symbiotic protist of the lower termite, *Coptotermes formosanus*. *Gene* **349**, 67–75 (2005).

23. M. Ohkuma, Symbioses of flagellates and prokaryotes in the gut of lower termites. *Trends Microbiol.* **16**, 345–352 (2008).

24. Y. Matsuura, M. Moriyama, P. Łukasik, D. Vanderpool, M. Tanahashi, X.-Y. Meng, J. P. McCutcheon, T. Fukatsu, Recurrent symbiont recruitment from fungal parasites in cicadas. *Proc. Natl. Acad. Sci. U. S. A.* **115**, E5970–E5979 (2018).

25. O. M. M. Thekisoe, T. Honda, H. Fujita, B. Battsetseg, T. Hatta, K. Fujisaki, C. Sugimoto, N. Inoue, A trypanosome species isolated from naturally infected *Haemaphysalis hystricis* ticks in Kagoshima Prefecture, Japan. *Parasitology* **134**, 967–974 (2007).

26. A. R. Tuininga, J. L. Miller, S. U. Morath, T. J. Daniels, R. C. Falco, M. Marchese, S. Sahabi, D. Rosa, K. C. Stafford 3rd, Isolation of entomopathogenic fungi from soils and *Ixodes scapularis* (Acari: Ixodidae) ticks: prevalence and methods. *J. Med. Entomol.* **46**, 557–565 (2009).

27. J. M. Austen, U. M. Ryan, J. A. Friend, W. G. F. Ditcham, S. A. Reid, Vector of *Trypanosoma copemani* identified as *Ixodes* sp. *Parasitology* **138**, 866–872 (2011).

28. P. J. Greengarten, A. R. Tuininga, S. U. Morath, R. C. Falco, H. Norelus, T. J. Daniels, Occurrence of soil- and tick-borne fungi and related virulence tests for pathogenicity to *Ixodes scapularis* (Acari: Ixodidae). *J. Med. Entomol.* **48**, 337–344 (2011).

29. D. Otranto, E. Brianti, M. S. Latrofa, G. Annoscia, S. Weigl, R. P. Lia, G. Gaglio, E. Napoli, S. Giannetto, E. Papadopoulos, G. Mirò, F. Dantas-Torres, O. Bain, On a *Cercopithifilaria* sp. transmitted by *Rhipicephalus sanguineus*: a neglected, but widespread filarioid of dogs. *Parasit. Vectors* **5**, 1 (2012).

30. C. L. Yuan, P. J. Keeling, P. J. Krause, A. Horak, S. Bent, L. Rollend, X. G. Hua, *Colpodella* spp.-like parasite infection in woman, China. *Emerg. Infect. Dis.* **18**, 125–127 (2012).

31. K. A. Jimale, M. A. Bezerra-Santos, J. A. Mendoza-Roldan, M. S. Latrofa, G. Baneth, D. Otranto, Molecular detection of *Colpodella* sp. and other tick-borne pathogens in ticks of ruminants, Italy. *Acta Trop.* **257**, 107306 (2024).

32. A. M. Soliman, H. Y. A. H. Mahmoud, T. Hifumi, T. Tanaka, Discovery of *Colpodella* spp. in ticks (*Hyalomma dromedarii*) infesting camels in southern Egypt. *Ticks Tick Borne Dis.* **15**, 102352 (2024).

33. L. Luu, K. J. Bown, A. M. Palomar, M. Kazimírová, L. Bell-Sakyi, Isolation and partial characterisation of a novel *Trypanosoma* from the tick *Ixodes ricinus*. *Ticks Tick Borne Dis.* **11**, 101501 (2020).

34. F. Binetruy, O. Duron, Molecular detection of *Cercopithifilaria*, *Cruorifilaria* and *Dipetalonema*-like filarial nematodes in ticks of French Guiana. *Parasite* **30**, 24 (2023).

35. J. Oliver, Tick reproduction: Sperm development and cytogenetics. *Physiology of ticks*, 245–275 (1982).

36. M. Samish, I. Glazer, Entomopathogenic nematodes for the biocontrol of ticks. *Trends Parasitol.* **17**, 368–371 (2001).

37. É. K. K. Fernandes, V. R. E. P. Bittencourt, D. W. Roberts, Perspectives on the potential of entomopathogenic fungi in biological control of ticks. *Exp. Parasitol.* **130**, 300–305 (2012).

38. J. Alcalá-Gómez, G. Alcalá-Gómez, K. G. Balleza-Díaz Barriga, G. de J. Vite-Méndez, M. Reyes-Hernández, *Beauveria bassiana* native strains affect the reproductive index of *Rhipicephalus microplus* ticks. *Exp. Appl. Acarol.* **93**, 485–496 (2024).

39. M. Samish, E. Alekseev, Arthropods as predators of ticks (Ixodoidea). *J. Med. Entomol.* **38**, 1–11 (2001).

40. M. Samish, H. Ginsberg, I. Glazer, Biological control of ticks. *Parasitology* **129**, S389–S403 (2004).

41. F. J. F. Van Veen, C. B. Müller, J. K. Pell, H. C. J. Godfray, Food web structure of three guilds of natural enemies: predators, parasitoids and pathogens of aphids. *J. Anim. Ecol.* **77**, 191–200 (2008).

42. K. Okabe, S. Makino, T. Shimada, T. Furukawa, H. Iijima, Y. Watari, Tick predation by the pseudoscorpion *Megachernes ryugadensis* (Pseudoscorpiones: Chernetidae), associated with small mammals in Japan. *J. Acarol. Soc. Japan* **27**, 1–11 (2018).

43. A. T. Showler, W. L. A. Osbrink, V. Abrigo, P. L. Phillips, Relationships of salinity, relative humidity, mud flat fiddler crabs, ants, and sea ox-eye Daisy with ixodid distribution and egg survival on the South Texas coastal plains. *Environ. Entomol.* **48**, 733–746 (2019).

44. M. Fei, R. Gols, J. A. Harvey, The biology and ecology of parasitoid wasps of predatory arthropods. *Annu. Rev. Entomol.* **68**, 109–128 (2023).

45. D. D. Vinogradov, A. S. Smagin, O. A. Belova, S. M. Tsurikov, G. G. Karganova, A. V. Tiunov, Identification of soil-dwelling predators of tick nymphs (Acari: Ixodidae) by stable isotope labeling. *J. Med. Entomol.* **61**, 512–516 (2024).

46. S. Kar, D. Sirin, G. Akyildiz, Z. Sakaci, S. Talay, Y. Camlitepe, Predation of ant species Lasius alienus on tick eggs: impacts of egg wax coating and tick species. *Sci. Rep.* **12**, 1–11 (2022).

47. E. N. Mwangi, O. O. Dipeolu, R. M. Newson, G. P. Kaaya, S. M. Hassan, Predators, parasitoids and pathogens of ticks: A review. *Biocontrol Sci. Technol.* **1**, 147–156 (1991).

48. M. M. Giannotta, I. Smith, M. Michie, K. Blasdell, M. Dunn, J. Nicholls, A. C. G. Heath, J. Rodriguez, A. W. Gofton, Molecular characterisation of Australasian *Ixodiphagus* (Hymenoptera; Encyrtidae; Encyrtinae) reveals unexpected diversity and a potential novel host switch. *Int. J. Parasitol.*, doi: 10.1016/j.ijpara.2024.09.001 (2024).

49. J. Xie, I. Vilchez, M. Mateos, Spiroplasma bacteria enhance survival of *Drosophila hydei* attacked by the parasitic wasp *Leptopilina heterotoma*. *PLoS One* **5**, e12149 (2010).

50. J. Xie, S. Butler, G. Sanchez, M. Mateos, Male killing Spiroplasma protects *Drosophila melanogaster* against two parasitoid wasps. *Heredity (Edinb.)* **112**, 399–408 (2014).

51. Y. Qiu, R. Nakao, A. Ohnuma, F. Kawamori, C. Sugimoto, Microbial population analysis of the salivary glands of ticks; a possible strategy for the surveillance of bacterial pathogens. *PLoS One* **9**, e103961 (2014).

52. A. Swei, J. Y. Kwan, Tick microbiome and pathogen acquisition altered by host blood meal. *ISME J.* **11**, 813–816 (2017).

53. T. L. Greay, A. W. Gofton, A. Paparini, U. M. Ryan, C. L. Oskam, P. J. Irwin, Recent insights into the tick microbiome gained through next-generation sequencing. *Parasit. Vectors* **11**, 12 (2018).

54. D. S. Lundberg, S. Yourstone, P. Mieczkowski, C. D. Jones, J. L. Dangl, Practical innovations for high-throughput amplicon sequencing. *Nat. Methods* **10**, 999–1002 (2013).

55. M.-C. Arrieta, A. Arévalo, L. Stiemsma, P. Dimitriu, M. E. Chico, S. Loor, M. Vaca, R. C. T. Boutin, E. Morien, M. Jin, S. E. Turvey, J. Walter, L. W. Parfrey, P. J. Cooper, B. Finlay, Associations between infant fungal and bacterial dysbiosis and childhood atopic wheeze in a nonindustrialized setting. *J. Allergy Clin. Immunol.* **142**, 424–434 (2017).

56. E. Belda, B. Coulibaly, A. Fofana, A. H. Beavogui, S. F. Traore, D. M. Gohl, K. D. Vernick, M. M. Riehle, Preferential suppression of *Anopheles gambiae* host sequences allows detection of the mosquito eukaryotic microbiome. *Sci. Rep.* **7**, 3241 (2017).

57. A. M. Reigel, S. M. Owens, M. E. Hellberg, Reducing host DNA contamination in 16S rRNA gene surveys of anthozoan microbiomes using PNA clamps. *Coral Reefs* **39**, 1817–1827 (2020).

58. S. J. Taerum, B. Steven, D. J. Gage, L. R. Triplett, Validation of a PNA clamping method for reducing host DNA amplification and increasing eukaryotic diversity in rhizosphere microbiome studies. *Phytobiomes J.* **4**, 291–302 (2020).

59. C. Briones, M. Moreno, Applications of peptide nucleic acids (PNAs) and locked nucleic acids (LNAs) in biosensor development. *Anal. Bioanal. Chem.* **402**, 3071–3089 (2012).

60. M. Ikenaga, M. Tabuchi, T. Kawauchi, M. Sakai, Application of locked nucleic acid (LNA) primer and PCR clamping by LNA oligonucleotide to enhance the amplification of internal transcribed spacer (ITS) regions in investigating the community structures of plant-associated fungi. *Microbes Environ.* **31**, 339–348 (2016).

61. R. B. Carnegie, G. R. Meyer, J. Blackbourn, N. Cochennec-Laureau, F. C. J. Berthe, S. M. Bower, Molecular detection of the oyster parasite *Mikrocytos mackini*, and a preliminary phylogenetic analysis. *Dis. Aquat. Organ.* **54**, 219–227 (2003).

62. S. M. Bower, R. B. Carnegie, B. Goh, S. R. Jones, G. J. Lowe, M. W. Mak, Preferential PCR amplification of parasitic protistan small subunit rDNA from metazoan tissues. *J. Eukaryot. Microbiol.* **51**, 325–332 (2004).

63. A. M. Comeau, W. K. W. Li, J.-É. Tremblay, E. C. Carmack, C. Lovejoy, Arctic Ocean microbial community structure before and after the 2007 record sea ice minimum. *PLoS One* **6**, e27492 (2011).

64. J. Del Campo, M. J. Pons, M. Herranz, K. C. Wakeman, J. Del Valle, M. J. A. Vermeij, B. S. Leander, P. J. Keeling, Validation of a universal set of primers to study animal-associated microeukaryotic communities. *Environ. Microbiol.* **21**, 3855–3861 (2019).

65. S. Kumar, G. Stecher, K. Tamura, MEGA7: Molecular evolutionary genetics analysis version 7.0 for bigger datasets. *Mol. Biol. Evol.* **33**, 1870–1874 (2016).

66. D. A. Filatov, proseq: A software for preparation and evolutionary analysis of DNA sequence data sets. *Mol. Ecol. Notes* **2**, 621–624 (2002).

67. H. J. Bandelt, P. Forster, A. Röhl, Median-joining networks for inferring intraspecific phylogenies. *Mol. Biol. Evol.* **16**, 37–48 (1999).

68. N. Yamaguti, V. J. Tipton, H. L. Keegan, S. Toshioka, Ticks of Japan, Korea, and the Ryukyu Islands. *Brigham Young University Science Bulletin, Biological Series* **15**, 1 (1971).

69. T. Stoeck, D. Bass, M. Nebel, R. Christen, M. D. M. Jones, H.-W. Breiner, T. A. Richards, Multiple marker parallel tag environmental DNA sequencing reveals a highly complex eukaryotic community in marine anoxic water. *Mol. Ecol.* **19**, 21–31 (2010).

70. E. Bolyen, J. R. Rideout, M. R. Dillon, N. A. Bokulich, C. C. Abnet, G. A. Al-Ghalith, H. Alexander, E. J. Alm, M. Arumugam, F. Asnicar, Y. Bai, J. E. Bisanz, K. Bittinger, A. Brejnrod, C. J. Brislawn, C. T. Brown, B. J. Callahan, A. M. Caraballo-Rodríguez, J. Chase, E. K. Cope, R. Da Silva, C. Diener, P. C. Dorrestein, G. M. Douglas, D. M. Durall, C. Duvallet, C. F. Edwardson, M. Ernst, M. Estaki, J. Fouquier, J. M. Gauglitz, S. M. Gibbons, D. L. Gibson, A.

Gonzalez, K. Gorlick, J. Guo, B. Hillmann, S. Holmes, H. Holste, C. Huttenhower, G. A. Huttley, S. Janssen, A. K. Jarmusch, L. Jiang, B. D. Kaehler, K. B. Kang, C. R. Keefe, P. Keim, S. T. Kelley, D. Knights, I. Koester, T. Kosciolek, J. Kreps, M. G. I. Langille, J. Lee, R. Ley, Y.-X. Liu, E. Loftfield, C. Lozupone, M. Maher, C. Marotz, B. D. Martin, D. McDonald, L. J. McIver, A. V. Melnik, J. L. Metcalf, S. C. Morgan, J. T. Morton, A. T. Naimey, J. A. Navas-Molina, L. F. Nothias, S. B. Orchanian, T. Pearson, S. L. Peoples, D. Petras, M. L. Preuss, E. Pruesse, L. B. Rasmussen, A. Rivers, M. S. Robeson 2nd, P. Rosenthal, N. Segata, M. Shaffer, A. Shiffer, R. Sinha, S. J. Song, J. R. Spear, A. D. Swafford, L. R. Thompson, P. J. Torres, P. Trinh, A. Tripathi, P. J. Turnbaugh, S. Ul-Hasan, J. J. J. van der Hooft, F. Vargas, Y. Vázquez-Baeza, E. Vogtmann, M. von Hippel, W. Walters, Y. Wan, M. Wang, J. Warren, K. C. Weber, C. H. D. Williamson, A. D. Willis, Z. Z. Xu, J. R. Zaneveld, Y. Zhang, Q. Zhu, R. Knight, J. G. Caporaso, Reproducible, interactive, scalable and extensible microbiome data science using QIIME 2. *Nat. Biotechnol.* **37**, 852–857 (2019).

71. B. J. Callahan, P. J. McMurdie, M. J. Rosen, A. W. Han, A. J. A. Johnson, S. P. Holmes, DADA2: High-resolution sample inference from Illumina amplicon data. *Nat. Methods* **13**, 581–583 (2016).

72. N. M. Davis, D. M. Proctor, S. P. Holmes, D. A. Relman, B. J. Callahan, Simple statistical identification and removal of contaminant sequences in marker-gene and metagenomics data. *Microbiome* **6**, 226 (2018).

73. J. E. Bisanz, *Qiime2R: Importing QIIME2 Artifacts and Associated Data into R Sessions* (2018; *https://github.com/jbisanz/qiime2R*).

74. P. J. McMurdie, S. Holmes, phyloseq: an R package for reproducible interactive analysis and graphics of microbiome census data. *PLoS One* **8**, e61217 (2013).

75. D. Bates, M. Mächler, B. Bolker, S. Walker, Fitting linear mixed-effects models Using lme4. *J. Stat. Softw.* **67**, 1–48 (2015).

76. N. Segata, J. Izard, L. Waldron, D. Gevers, L. Miropolsky, W. S. Garrett, C. Huttenhower, Metagenomic biomarker discovery and explanation. *Genome Biol* **12**, R60 (2011).

77. A. E. Mann, F. Mazel, M. A. Lemay, E. Morien, V. Billy, M. Kowalewski, A. Di Fiore, A. Link, T. L. Goldberg, S. Tecot, A. L. Baden, A. Gomez, M. L. Sauther, F. P. Cuozzo, G. A. O. Rice, N. J. Dominy, R. Stumpf, R. J. Lewis, L. Swedell, K. Amato, L. Wegener Parfrey, Biodiversity of protists and nematodes in the wild nonhuman primate gut. *ISME J.* **14**, 609–622 (2020).

78. K. Hadziavdic, K. Lekang, A. Lanzen, I. Jonassen, E. M. Thompson, C. Troedsson, Characterization of the 18S rRNA gene for designing universal eukaryote specific primers. *PLoS One* **9**, e87624 (2014).

79. A. Djurhuus, C. J. Closek, R. P. Kelly, K. J. Pitz, R. P. Michisaki, H. A. Starks, K. R. Walz, E. A. Andruszkiewicz, E. Olesin, K. Hubbard, E. Montes, D. Otis, F. E. Muller-Karger, F. P. Chavez, A. B. Boehm, M. Breitbart, Environmental DNA reveals seasonal shifts and potential interactions in a marine community. *Nat. Commun.* **11**, 254 (2020).

80. L. Morin, A. Goubet, C. Madigou, J.-J. Pernelle, K. Palmier, K. Labadie, A. Lemainque, O. Michot, L. Astoul, P. Barbier, J.-L. Almayrac, A. Sghir, Colonization kinetics and implantation follow-up of the sewage microbiome in an urban wastewater treatment plant. *Sci. Rep.* **10**, 11634 (2020).

81. V. V. Phelan, W.-T. Liu, K. Pogliano, P. C. Dorrestein, Microbial metabolic exchange--the chemotype-to-phenotype link. *Nat. Chem. Biol.* **8**, 26–35 (2011).

82. K. Z. Coyte, J. Schluter, K. R. Foster, The ecology of the microbiome: Networks, competition, and stability. *Science* **350**, 663–666 (2015).

83. V. Horrocks, O. G. King, A. Y. G. Yip, I. M. Marques, J. A. K. McDonald, Role of the gut microbiota in nutrient competition and protection against intestinal pathogen colonization. *Microbiology* **169** (2023).

84. M. Kratou, A. Maitre, L. Abuin-Denis, E. Piloto-Sardiñas, I. Corona-Guerrero, A. L. Cano-Argüelles, A. Wu-Chuang, T. Bamgbose, C. Almazan, J. Mosqueda, D. Obregón, L. Mateos-Hernández, M. B. Said, A. Cabezas-Cruz, Disruption of bacterial interactions and community

assembly in *Babesia*-infected *Haemaphysalis longicornis* following antibiotic treatment. *BMC Microbiol.* **24**, 322 (2024).

85. A. Maitre, A. Wu-Chuang, L. Mateos-Hernández, A. Foucault-Simonin, S. Moutailler, J.-C. Paoli, A. Falchi, A. A. Díaz-Sánchez, P. Banović, D. Obregón, A. Cabezas-Cruz, *Rickettsia helvetica* infection is associated with microbiome modulation in *Ixodes ricinus* collected from humans in Serbia. *Sci. Rep.* **12**, 11464 (2022).

86. L. Tipton, C. L. Müller, Z. D. Kurtz, L. Huang, E. Kleerup, A. Morris, R. Bonneau, E. Ghedin, Fungi stabilize connectivity in the lung and skin microbial ecosystems. *Microbiome* **6**, 12 (2018).

87. M. S. Matchado, M. Lauber, S. Reitmeier, T. Kacprowski, J. Baumbach, D. Haller, M. List, Network analysis methods for studying microbial communities: A mini review. *Comput. Struct. Biotechnol. J.* **19**, 2687–2698 (2021).

88. B. Ma, Y. Wang, S. Ye, S. Liu, E. Stirling, J. A. Gilbert, K. Faust, R. Knight, J. K. Jansson, C. Cardona, L. Röttjers, J. Xu, Earth microbial co-occurrence network reveals interconnection pattern across microbiomes. *Microbiome* **8**, 82 (2020).

89. B. D. Jameson, S. A. Murdock, Q. Ji, C. J. Stevens, D. S. Grundle, S. Kim Juniper, Network analysis of 16S rRNA sequences suggests microbial keystone taxa contribute to marine N_2O cycling. *Commun. Biol.* **6**, 212 (2023).

90. S. Banerjee, K. Schlaeppi, M. G. A. van der Heijden, Keystone taxa as drivers of microbiome structure and functioning. *Nat. Rev. Microbiol.* **16**, 567–576 (2018).

91. X. Lin, B. Qiao, R. Chang, Y. Li, W. Zheng, Z. He, Y. Tian, Characterization of two keystone taxa, sulfur-oxidizing, and nitrate-reducing bacteria, by tracking their role transitions in the benzo[a]pyrene degradative microbiome. *Microbiome* **11**, 139 (2023).

92. B. Cibichakravarthy, N. Shaked, E. Kapri, Y. Gottlieb, Endosymbiont-derived metabolites are essential for tick host reproductive fitness. *mSphere* **9**, e0069323 (2024).

93. O. Duron, O. Morel, V. Noël, M. Buysse, F. Binetruy, R. Lancelot, E. Loire, C. Ménard, O. Bouchez, F. Vavre, L. Vial, Tick-bacteria mutualism depends on B vitamin synthesis pathways. *Curr. Biol.* **28**, 1896-1902.e5 (2018).

94. C. A. Gall, K. E. Reif, G. A. Scoles, K. L. Mason, M. Mousel, S. M. Noh, K. A. Brayton, The bacterial microbiome of *Dermacentor andersoni* ticks influences pathogen susceptibility. *ISME J.* **10**, 1846–1855 (2016).

95. B. Guo, L. Zhang, H. Sun, M. Gao, N. Yu, Q. Zhang, A. Mou, Y. Liu, Microbial co-occurrence network topological properties link with reactor parameters and reveal importance of low-abundance genera. *NPJ Biofilms Microbiomes* **8**, 3 (2022).

96. L. Abuin-Denis, E. Piloto-Sardiñas, A. Maître, A. Wu-Chuang, L. Mateos-Hernández, D. Obregon, B. Corona-González, A. C. Fogaça, V. Palinauskas, J. Aželytė, A. Rodríguez-Mallon, A. Cabezas-Cruz, Exploring the impact of *Anaplasma phagocytophilum* on colonization resistance of *Ixodes scapularis* microbiota using network node manipulation. *Curr. Res. Parasitol. Vector Borne Dis.* **5**, 100177 (2024).

97. A. Klindworth, E. Pruesse, T. Schweer, J. Peplies, C. Quast, M. Horn, F. O. Glöckner, Evaluation of general 16S ribosomal RNA gene PCR primers for classical and next-generation sequencing-based diversity studies. *Nucleic Acids Res.* **41**, e1 (2013).

98. D. P. Herlemann, M. Labrenz, K. Jürgens, S. Bertilsson, J. J. Waniek, A. F. Andersson, Transitions in bacterial communities along the 2000 km salinity gradient of the Baltic Sea. *ISME J.* **5**, 1571–1579 (2011).

99. T. G. Martijn, *Fantaxtic - Nested Bar Plots for Phyloseq Data* (2022; *https://github.com/gmteunisse/Fantaxtic*).

100. J. Oksanen, G. Simpson, F. Blanchet, R. Kindt, P. Legendre, P. Minchin, S. P. O'Hara R, M. Stevens, E. Szoecs, H. Wagner, M. Barbour, M. Bedward, B. Bolker, D. Borcard, T. Borman,

G. Carvalho, M. Chirico, M. De Caceres, S. Durand, H. Evangelista, R. FitzJohn, M. Friendly, B. Furneaux, G. Hannigan, M. Hill, L. Lahti, D. McGlinn, M. Ouellette, C. E. Ribeiro, T. Smith, A. Stier, C. Ter Braak, J. Weedon, *Vegan: An R Package for Community Ecologists* (2024; *https://vegandevs.github.io/vegan/*).

101. Z. D. Kurtz, C. L. Müller, E. R. Miraldi, D. R. Littman, M. J. Blaser, R. A. Bonneau, Sparse and compositionally robust inference of microbial ecological networks. *PLoS Comput. Biol.* **11**, e1004226 (2015).

102. D. Berry, S. Widder, Deciphering microbial interactions and detecting keystone species with co-occurrence networks. *Front. Microbiol.* **5**, 219 (2014).

103. G. Csárdi, T. Nepusz, K. Müller, S. Horvát, V. Traag, F. Zanini, D. Noom, *Igraph for R: R Interface of the Igraph Library for Graph Theory and Network Analysis* (Zenodo, 2023; *https://zenodo.org/records/10369053*).

104. P. Shannon, A. Markiel, O. Ozier, N. S. Baliga, J. T. Wang, D. Ramage, N. Amin, B. Schwikowski, T. Ideker, Cytoscape: a software environment for integrated models of biomolecular interaction networks. *Genome Res.* **13**, 2498–2504 (2003).

105. J. F. Zhang, F. Li, H. Y. Zhong, J. M. Chen, *Nilaparvata lugens* (Hemiptera: Delphacidae) midgut microbial community responses to exposure to *Metarhizium flavoviride* (Sordariomycetes: Hypocreales). *J. Entomol. Sci.* **57**, 587–602 (2022).

106. T. Pröschold, T. Darienko, P. C. Silva, W. Reisser, L. Krienitz, The systematics of Zoochlorella revisited employing an integrative approach. *Environ. Microbiol.* **13**, 350–364 (2011).

107. A. Tartar, The non-photosynthetic algae *Helicosporidium* spp.: Emergence of a novel group of insect pathogens. *Insects* **4**, 375–391 (2013).

108. M. Ma, Y. Gong, Q. Hu, Identification and feeding characteristics of the mixotrophic flagellate *Poterioochromonas malhamensis*, a microalgal predator isolated from outdoor massive Chlorella culture. *Algal Res.* **29**, 142–153 (2018).

109. S. S. N. Maharachchikumbura, L.-D. Guo, E. Chukeatirote, A. H. Bahkali, K. D. Hyde, Pestalotiopsis—morphology, phylogeny, biochemistry and diversity. *Fungal Divers.* **50**, 167–187 (2011).

110. P. C. Beaver, W. Burgdorfer, A microfilaria of exceptional size from the ixodid tick, *Ixodes dammini*, from Shelter Island, New York. *J. Parasitol.* **70**, 963–966 (1984).

111. T. C. Henning, J. M. Orr, J. D. Smith, J. R. Arias, J. L. Rasgon, D. E. Norris, Discovery of filarial nematode DNA in *Amblyomma americanum* in Northern Virginia. *Ticks Tick Borne Dis.* **7**, 315–318 (2016).

112. S. H. Pourseyed, M. Tavassoli, I. Bernousi, K. Mardani, *Metarhizium anisopliae* (Ascomycota: Hypocreales): an effective alternative to chemical acaricides against different developmental stages of fowl tick *Argas persicus* (Acari: Argasidae). *Vet. Parasitol.* **172**, 305–310 (2010).

113. N. Pedrini, Molecular interactions between entomopathogenic fungi (Hypocreales) and their insect host: Perspectives from stressful cuticle and hemolymph battlefields and the potential of dual RNA sequencing for future studies. *Fungal Biol.* **122**, 538–545 (2018).

114. C. Szekely, S. D. Atkinson, K. Molnar, L. Egyed, A. Gubanyi, G. Cech, A synopsis of records of myxozoan parasites (Cnidaria: Myxozoa) from shrews, with additional data on Soricimyxum fegati from common shrew *Sorex araneus* in Hungary and pygmy shrew Sorex minutus in Slovakia. *Folia Parasitol. (Praha)* **63** (2016).

115. S. D. Atkinson, J. L. Bartholomew, T. Lotan, Myxozoans: Ancient metazoan parasites find a home in phylum Cnidaria. *Zoology (Jena)* **129**, 66–68 (2018).

116. A. S. Holzer, P. Bartošová-Sojková, A. Born-Torrijos, A. Lövy, A. Hartigan, I. Fiala, The joint evolution of the Myxozoa and their alternate hosts: A cnidarian recipe for success and vast biodiversity. *Mol. Ecol.* **27**, 1651–1666 (2018).

117. S. Rueckert, E. L. Betts, A. D. Tsaousis, The symbiotic spectrum: Where do the gregarines fit? *Trends Parasitol.* **35**, 687–694 (2019).

118. F. Bollatti, A. Ceballos, Effect of gregarines (Apicomplexa: Sporozoa) on survival and weight loss of *Victorwithius similis* (Arachnida: Pseudoscorpiones). *J. Invertebr. Pathol.* **117**, 13–18 (2014).

119. E. M. McCray Jr, R. W. Fay, H. F. Schoof, The bionomics of *Lankesteria culicis* and *Aedes aegypti*. *J. Invertebr. Pathol.* **16**, 42–53 (1970).

120. L. Lantova, M. Svobodova, P. Volf, Effects of *Psychodiella sergenti* (Apicomplexa, Eugregarinorida) on its natural host *Phlebotomus sergenti* (Diptera, Psychodidae). *J. Med. Entomol.* **48**, 985–990 (2011).

121. J. Soghigian, L. R. Valsdottir, T. P. Livdahl, A parasite's modification of host behavior reduces predation on its host. *Ecol. Evol.* **7**, 1453–1461 (2017).

122. T. Cavalier-Smith, E. E. Chad, Sarcomonad ribosomal RNA sequences, rhizopod phylogeny, and the origin of euglyphid amoebae. *Arch. Protistenkunde* **147**, 227–236 (1997).

123. F. Ekelund, N. Daugbjerg, L. Fredslund, Phylogeny of Heteromita, Cercomonas and Thaumatomonas based on SSU rDNA sequences, including the description of *Neocercomonas jutlandica* sp. nov., gen. nov. *Eur. J. Protistol.* **40**, 119–135 (2004).

124. F. Trielli, M. G. Chessa, A. Amaroli, M. Ognibene, M. U. Delmonte Corrado, Effects of organophosphate compounds on a soil protist, *Colpoda inflata* (Ciliophora, Colpodidae). *Chemosphere* **65**, 1731–1737 (2006).

125. A. Hoffmann, V. Fingerle, M. Noll, Analysis of tick surface decontamination methods. *Microorganisms* **8**, 987 (2020).

126. A. Meyer-König, M. Zahler, R. Gothe, Studies on survival and water balance of unfed adult *Dermacentor marginatus* and *D. reticulatus* ticks (Acari: Ixodidae). *Exp. Appl. Acarol.* **25**, 993–1004 (2001).

127. L. P. Maldonado-Ruiz, Y. Park, L. Zurek, Liquid water intake of the lone star tick, *Amblyomma americanum*: Implications for tick survival and management. *Sci. Rep.* **10**, 6000 (2020).

128. E. Lejal, J. Chiquet, J. Aubert, S. Robin, A. Estrada-Peña, O. Rue, C. Midoux, M. Mariadassou, X. Bailly, A. Cougoul, P. Gasqui, J. F. Cosson, K. Chalvet-Monfray, M. Vayssier-Taussat, T. Pollet, Temporal patterns in *Ixodes ricinus* microbial communities: an insight into tick-borne microbe interactions. *Microbiome* **9**, 153 (2021).

129. P. Barbera, A. M. Kozlov, L. Czech, B. Morel, D. Darriba, T. Flouri, A. Stamatakis, EPA-ng: Massively parallel evolutionary placement of genetic sequences. *Syst. Biol.* **68**, 365–369 (2019).

130. A. Bistline-East, R. Pandey, M. Kececi, M. S. Hoddle, Host range testing of *Diaphorencyrtus aligarhensis* (Hymenoptera: Encyrtidae) for use in classical biological control of *Diaphorina citri* (Hemiptera: Liviidae) in California. *J. Econ. Entomol.* **108**, 940–950 (2015).

131. G. Japoshvili, Y. Higashiura, S. Kamitani, A review of Japanese Encyrtidae (Hymenoptera), with descriptions of new species, new records and comments on the types described by Japanese authors. *Acta Entomol. Mus. Natl. Pragae* **56**, 345–401 (2016).

132. G. R. Burke, B. J. Sharanowski, Parasitoid wasps. *Curr. Biol.* **34**, R483–R488 (2024).

133. A. H. Bokonon-Ganta, P. Neuenschwander, Impact of the Biological Control Agent *Gyranusoidea tebygi* Noyes (Hymenoptera: Encyrtidae) on the Mango Mealybug, *Rastrococcus*

invadens Williams (Homoptera: Pseudococcidae), in Benin. *Biocontrol Sci. Technol.* **5**, 95–108 (1995).

134. F. Larrousse, A. G. King, S. B. Wolbach, The Overwintering in Massachusetts of Ixodiphagus caucurtei. *Science* **67**, 351–353 (1928).

135. R. Hu, K. E. Hyland, J. O. J. H., A review on the use of *Ixodiphagus* wasps (Hymenoptera: Encyrtidae) as natural enemies for the control of ticks (Acari: Ixodidae). *Saalburg. Jahrb.*, 19–27 (1998).

136. T. Tachikawa, Disovery of a tick parasite, *Hunterellus sagarensis* Geevarghese from Japan (Hymenoptera: Chalcidoidea - Encyrtidae). *Trans. Shikoku Ent. Soc.* **15**, 119–120 (1980).

137. R. A. N. Ramos, L. O. de Macedo, M. A. Bezerra-Santos, G. A. de Carvalho, G. G. Verocai, D. Otranto, The role of parasitoid wasps, *ixodiphagus* spp. (Hymenoptera: Encyrtidae), in tick control. *Pathogens* **12** (2023).

138. J. M. Jasso-Martínez, B. F. Santos, A. Zaldívar-Riverón, J. L. Fernández-Triana, B. J. Sharanowski, R. Richter, J. R. Dettman, B. B. Blaimer, S. G. Brady, R. R. Kula, Phylogenomics of braconid wasps (Hymenoptera, Braconidae) sheds light on classification and the evolution of parasitoid life history traits. *Mol. Phylogenet. Evol.* **173**, 107452 (2022).

139. B. B. Blaimer, B. F. Santos, A. Cruaud, M. W. Gates, R. R. Kula, I. Mikó, J.-Y. Rasplus, D. R. Smith, E. J. Talamas, S. G. Brady, M. L. Buffington, Key innovations and the diversification of Hymenoptera. *Nat. Commun.* **14**, 1212 (2023).

140. S. Kurata, S. Mano, N. Nakahama, S. K. Hirota, Y. Suyama, M. Ito, Development of mitochondrial DNA cytochrome c oxidase subunit I primer sets to construct DNA barcoding library using next-generation sequencing. *Biodivers. Data J.* **12**, e117014 (2024).

141. R. Desalle, B. Schierwater, H. Hadrys, MtDNA: The small workhorse of evolutionary studies. *Front. Biosci.* **22**, 873–887 (2017).

142. C. M. French, L. D. Bertola, A. C. Carnaval, E. P. Economo, J. M. Kass, D. J. Lohman, K. A. Marske, R. Meier, I. Overcast, A. J. Rominger, P. P. A. Staniczenko, M. J. Hickerson, Global determinants of insect mitochondrial genetic diversity. *Nat. Commun.* **14**, 5276 (2023).

143. K. N. Magnacca, M. J. F. Brown, Mitochondrial heteroplasmy and DNA barcoding in Hawaiian *Hylaeus* (Nesoprosopis) bees (Hymenoptera: Colletidae). *BMC Evol. Biol.* **10**, 174 (2010).

144. P. C. Ricardo, E. Françoso, M. C. Arias, Mitochondrial DNA intra-individual variation in a bumblebee species: A challenge for evolutionary studies and molecular identification. *Mitochondrion* **53**, 243–254 (2020).

145. O. K. Davies, J. B. Dorey, M. I. Stevens, M. G. Gardner, T. M. Bradford, M. P. Schwarz, Unparalleled mitochondrial heteroplasmy and *Wolbachia* co-infection in the non-model bee, *Amphylaeus morosus*. *Curr Res Insect Sci* **2**, 100036 (2022).

146. E. Françoso, A. R. Zuntini, P. C. Ricardo, P. K. F. Santos, N. de Souza Araujo, J. P. N. Silva, L. T. Gonçalves, R. Brito, R. Gloag, B. A. Taylor, B. A. Harpur, B. P. Oldroyd, M. J. F. Brown, M. C. Arias, Rapid evolution, rearrangements and whole mitogenome duplication in the Australian stingless bees Tetragonula (Hymenoptera: Apidae): A steppingstone towards understanding mitochondrial function and evolution. *Int. J. Biol. Macromol.* **242**, 124568 (2023).

147. J. Erdős, Chalcidoidea nova in collectione Birói (Hymenoptera). *Annales Historico-Naturales Musei Nationalis Hungarici (Series Nova)* **7**, 181–194 (1955).

148. O. G. H. Fiedler, A new African tick parasite, *Hunterellus theilerae* sp. n. *Onderstepoort J. Vet. Res.* **26** (1953).

149. A. C. G. Heath, R. P. Cane, A new species of *Ixodiphagus* (Hymenoptera: Chalcidoidea: Encyrtidae) parasitizing seabird ticks in New Zealand. *N. Z. J. Zool.* **37**, 147–155 (2010).

150. M. Hayat, S. I. Kazmi, On some Encyrtidae (Hymenoptera: Chalcidoidea) from Namdapha Tiger Reserve in Arunachal Pradesh, India. *Zootaxa* **2830**, 1–19 (2011).

151. M. Nikol'skaya, A new Species of Parasite of Ixodid Ticks *Ixodiphagus hirtus* Nik., sp. n. (Hymenoptera, Chalcidoidea). *Parazitologicheski Sbornik* **12** (1950).

152. J. S. Noyes, Encyrtidae of Costa Rica (Hymenoptera: Chalcidoidea), 3. (2010).

153. M. S. Quaraishi, Morphology of Two Chalcidoid Parasites of Ticks, *Hunterellus hookeri* Howard, 1908, and *Ixodiphagus texanus* Howard, 1907. *Am. Midl. Nat.* **59**, 489–504 (1958).

154. M. Hayat, K. Veenakumari, Description of four new species of brachypterous Encyrtidae (Hymenoptera: Chalcidoidea) from India. *Zootaxa* **3990**, 259–271 (2015).

155. G. E. Truett, P. Heeger, R. L. Mynatt, A. A. Truett, J. A. Walker, M. L. Warman, Preparation of PCR-quality mouse genomic DNA with hot sodium hydroxide and tris (HotSHOT). *Biotechniques* **29**, 52, 54 (2000).

156. A. Takano, H. Fujita, T. Kadosaka, M. Takahashi, T. Yamauchi, F. Ishiguro, N. Takada, Y. Yano, Y. Oikawa, T. Honda, M. Gokuden, T. Tsunoda, M. Tsurumi, S. Ando, M. Andoh, K. Sato, H. Kawabata, Construction of a DNA database for ticks collected in Japan: application of molecular identification based on the mitochondrial 16S rDNA gene. *Medical Entomology* **65**, 13–21 (2014).

157. M. Kearse, R. Moir, A. Wilson, S. Stones-Havas, M. Cheung, S. Sturrock, S. Buxton, A. Cooper, S. Markowitz, C. Duran, T. Thierer, B. Ashton, P. Meintjes, A. Drummond, Geneious Basic: an integrated and extendable desktop software platform for the organization and analysis of sequence data. *Bioinformatics* **28**, 1647–1649 (2012).

158. Y. Ushijima, J. H. Oliver Jr, J. E. Keirans, M. Tsurumi, H. Kawabata, H. Watanabe, M. Fukunaga, Mitochondrial sequence variation in Carlos capensis (Neumann), a parasite of seabirds, collected on Torishima Island in Japan. *J. Parasitol.* **89**, 196–198 (2003).

159. J. W. Leigh, D. Bryant, Popart: Full‐feature software for haplotype network construction. *Methods Ecol. Evol.* **6**, 1110–1116 (2015).

160. G. Zhang, D. Zheng, Y. Tian, S. Li, A dataset of distribution and diversity of ticks in China. *Sci. Data* **6**, 105 (2019).

161. H. K. St John, P. Masuoka, J. Jiang, R. Takhampunya, T. A. Klein, H.-C. Kim, S.-T. Chong, J.-W. Song, Y.-J. Kim, C. M. Farris, A. L. Richards, Geographic distribution and modeling of ticks in the Republic of Korea and the application of tick models towards understanding the distribution of associated pathogenic agents. *Ticks Tick Borne Dis.* **12**, 101686 (2021).

162. P.-E. Fournier, H. Fujita, N. Takada, D. Raoult, Genetic identification of rickettsiae isolated from ticks in Japan. *J. Clin. Microbiol.* **40**, 2176–2181 (2002).

163. K. Yoshii, J. Y. Song, S.-B. Park, J. Yang, H.-J. Schmitt, Tick-borne encephalitis in Japan, Republic of Korea and China. *Emerg. Microbes Infect.* **6**, e82 (2017).

164. J. L. Bowman, "Host suitability and laboratory biology of *Ixodiphagus texanus* Howard," thesis, Oklahoma State University (1979).

165. C. J. Geden, R. D. Moon, Host ranges of gregarious muscoid fly parasitoids: *Muscidifurax raptorellus* (Hymenoptera: Pteromalidae), *Tachinaephagus zealandicus* (Hymenoptera: Encyrtidae), and *Trichopria nigra* (Hymenoptera: Diapriidae). *Environ. Entomol.* **38**, 700–707 (2009).

166. T. Yamauchi, A bibliographical survey of host-parasite relationships between birds and ticks from Japan. *Hoshizaki Green Foundation* **5**, 271–308 (2001).

167. E. N. Mwangi, S. M. Hassan, G. P. Kaaya, S. Essuman, The impact of *Ixodiphagus hookeri*, a tick parasitoid, on *Amblyomma variegatum* (Acari: Ixodidae) in a field trial in Kenya. *Exp. Appl. Acarol.* **21**, 117–126 (1997).

168. S. Calvignac, L. Konecny, F. Malard, C. J. Douady, Preventing the pollution of mitochondrial datasets with nuclear mitochondrial paralogs (numts). *Mitochondrion* **11**, 246–254 (2011).

169. C. B. Philip, Occurrence of a colony of the tick parasite *Hunterellus hookeri* Howard in west Africa. *Public Health Rep.* **46**, 2168–2172 (1931).

170. N. López-López, J. C. Rojas, L. Cruz-López, E. A. Malo, Behavioral responses of *Ixodiphagus hookeri* (Hymenoptera; Encyrtidae) to *Rhipicephalus sanguineus* nymphs (Ixodida: Ixodidae) and dog hair volatiles. *Fla. Entomol.* **107** (2024).

171. L. Dominguez A., T. F. Martins, N. Kadoch, S. Bermúdez C., First report of *Amblyomma varium* (Ixodida: Ixodidae) as hosts of *Ixodiphagus* sp. (Hymenoptera: Encyrtidae). *Syst. Appl. Acarol.* **28**, 2171–2176 (2023).

Japanese Abstract（日本語要旨）

マダニは公衆衛生や家畜衛生に深刻な影響を及ぼす病原体の重要な媒介者である。一方で、マダニは病原体だけではなく、非病原性微生物も多く保有する。これらの非病原性生物には、マダニに栄養素の供給を行う共生細菌や、マダニにとって無害あるいは有害な細菌が含まれる。また、非病原性生物を含むマダニの細菌叢が、病原体の伝播や定着の効率に影響を与えることも報告されている。マダニが保有する真核生物としては、原虫、線虫、真菌などが知られている。しかし、病原体であるアピコンプレックス門の原虫を除き、それらの生態や機能などはほとんど知られていない。真核生物群集に関する研究が限定的である主な理由として、関心の低さと技術的な課題が挙げられる。そこで本研究では、マダニが保有する真核生物群を包括的に調査し、その生態や役割を明らかにすることを目的とした。

第一章では、マダニの真核微生物叢を解析するための新しい方法を考案し、それらの有効性を評価した。これらの方法は、宿主マダニ DNA の増幅を抑制し、同時にマダニ抽出 DNA 中の微小真核生物 DNA を選択的に増幅するように設計した。ペプチド核酸（PNA）と架橋核酸（LNA）の 2 種類の人工核酸を、マダニ DNA 特異的な PCR 増幅ブロッカーとして評価した。さらに、非後生生物を標的とするプライマー（UNonMet）を用いた PCR 法も検討した。これらの方法を用いて、マダニ抽出 DNA からアンプリコンライブラリーを作製し、次世代シーケンサーを用いた配列解析を行なった。その結果、従来のアプローチと比較して、考案した方法により、保有真核生物由来の配列の割合が有意に増加し、アルファ多様性も向上した。PNA を用いた方法は、真菌類、Alveolata、Archaeplastida、Rhizaria、Chloroplastida、未分類の真核生物など、より幅広い分類群を捕捉し、真核生物を網羅的に解析するのに適していると考えられた。一方、UNonMet は真菌類と Alveolata (Apicomplexa 門を含む)の検出に効率的であり、これらの特定の分類群を対象とした研究に適していると考えられた。

第二章では、第一章で開発した PNA を用いた方法により、マダニが保有する潜在的に重要な真核生物分類群を同定した。本章の目的は、宿主マダニおよびその微生物ネットワークにとって重要な役割を果たす分類群を明らかにすることである。相対的存在量が多い分類群、節足動物病原性微生物が属する分類群、さらに微生物ネットワークのキーストーンとなる分類群を、重要分類群として検出した。日本国内の 4 地域から採集した 4 種のマダニを対象として、細菌叢と真核生物叢の両方についてアンプリコンシーケンシングを行った。まず、相対的存在量が多い分類群として、未分類の Bivalvulida（刺胞動物門）および Eugregarinorida（アピコンプレクサ門）が検出された。次に、昆虫病原性生物が属する分類群として、Nematozoa と Hypocreales が確認された。さらに、マダニにおけるクロスドメインネットワークを構築し、キーストーン分類群を推定した。その結果、キチマダニでは Bromeliothrix (繊毛虫綱)、フタトゲチマダニでは *Kurtzmanomyces*（担子菌門）、未分類の Brachybasidiaceae

（担子菌門）、および *Pestalotiopsis*（子嚢菌門）がキーストーン分類群として特定された。これらの結果は、今後の研究に向けた重要な仮説を提供するものであり、それら分類群の具体的な機能解明が必要である。

第三章では、マダニへ産卵し寄生することが報告されている寄生蜂の検出と、その遺伝的特徴を調査した。マダニの天敵としては、一般的な捕食者であるアリ、甲虫、カニムシ、クモ等が知られている。一方、マダニ特異的な天敵昆虫は、*Ixodiphagus* 属寄生蜂のみが知られている。*Ixodiphagus* 属寄生蜂は、マダニ体内に産卵し、マダニの吸血開始後に発育を始め、最終的に宿主を殺して成虫として脱出する。本研究では、北海道、北陸、中国、四国、九州地方で採集したマダニを対象に、実験室でウサギに吸血させることで、寄生蜂成虫を得た。吸血実験に供した 1,933 匹のマダニのうち、北陸、中国、四国地方由来のキチマダニ合計 15 匹から寄生蜂が出現した。形態学的特徴により、記載された種からは異なることが示唆された。さらに、ショットガンシーケンス、ダイレクトシーケンス、In-Fusion クローニング法を用いて、寄生蜂のミトコンドリア *COI* 遺伝子の特徴を調査した。配列解析に使用した 6 つのサンプル全てから、顕著な個体内遺伝的多型が検出された。この発見により、*Ixodiphagus* 属寄生蜂の分類学的および生態学的理解の発展が期待できる。

三つの章を通して、マダニが保有する真核生物群がカタログ化された。開発されたマダニの真核生物叢解析技術は、様々なマダニ種に応用可能である。また、検出された分類群や寄生蜂を対象とした更なる研究が、マダニの生態の解明や生物学的防除法開発に寄与すると期待される。